Pilbara Ports Authority (**PPA**) is the proponent for the Dampier Cargo Wharf Extension and Landside Redevelopment Project at the Port of Dampier, WA (**Project**).

PPA is planning to construct and operate a southern wharf extension to the Dampier Cargo Wharf. The Project incorporates the development of a new (adjoining) southern section of wharf and associated mooring dolphin, wharf connecting structure, dredged berth pocket and vessel manoeuvring area.

As part of PPA's referral of the Project to the Commonwealth Department of Climate Change, Energy, the Environment and Water under the *Environmental Protection and Biodiversity Conservation Act 1999* (Cth), PPA welcomes public comment on the preliminary documentation for the Project.

Disclaimer and Non-Reliance

By accessing the information provided and any associated digital files in connection with the information provided (**Information**), you acknowledge and agree the following:

(a) Pilbara Ports Authority (**PPA**) and the author of the Information (**Author**) make no statements, representations or warranties about the accuracy, currency or completeness of the Information.

(b) You will make your own assessment of the Information to satisfy yourself as to the suitability of such Information for your own purposes and you will not rely on the Information. Any reliance by you on any Information, or any use of any Information, is solely at your own risk.

(c) PPA and the Author do not accept any responsibility for any interpretation, opinion or conclusion that you may form as a result of examining the Information and PPA and the Author are not liable, and you covenant not to make any claim or commence or pursue any proceedings against PPA or the Author, for any loss of any kind arising from an error, inaccuracy, incompleteness or similar defect in the Information.

(d) PPA and the Author specifically note that where any of the Information, including but not limited to any data, plans or drawings, uses or relies on positioning technology to determine the coordinates of infrastructure on a PPA site, you must conduct your own investigations, checks and verifications on the accuracy of the infrastructure positioning and any coordinates for the physical location of any infrastructure.

(e) You must not disclose the Information to any other party without obtaining the prior written consent of PPA.

Dampier Cargo Wharf Extension and Landside Redevelopment Project

Dredge Plume Modelling Assessment

CLIENT: Pilbara Ports Authority

STATUS: Rev 1

REPORT NUMBER: 21MET-0026 / R210292

ISSUE DATE: 1 April 2022

WA MARINE PTY LTD | ABN 84 168 014 819 | www.o2marine.com.au

WA Marine Pty Ltd t/as O2 Metocean
ACN 168 014 819
Originating Office – Western Australia
11 Mews Road FREMANTLE WA 6160
T 1300 739 447 | info@o2marine.com.au

Version Register

Version	Status	Author	Reviewer	Change from Previous Version	Authorised for Release (signed and dated)
Rev A	Draft	J.O-C.	A.Z.	N/A	DRAFT NOT AUTHORISED FOR RELEASE
RevB	Draft	J.O-C.	A.Z. R.M.	Model results reprocessed with updated light attenuation parameterisation	DRAFT NOT AUTHORISD FOR RELEASE
Rev 1	Final	J.O-C.	A.Z.	Editorial changes.	S.M.

Transmission Register

Controlled copies of this document are issued to the persons/companies listed below. Any copy of this report held by persons not listed in this register is deemed uncontrolled. Updated versions of this report if issued will be released to all parties listed below via the email address listed.

Name	Email Address
Dave Pozzari	dave.pozzari@pilbaraports.com.au

Contents

Figures

Tables

1. Executive summary

The objective of this study (***The Study***) was to evaluate the probable and possible environmental impact of dredging and dredge spoil disposal plumes associated with the Pilbara Port Authority's (PPA) Dampier Cargo Wharf Extension Project (***The Project***). The assessment presented herein includes both backactor and cutter-suction scenarios, and three separate spoil disposal locations (6 scenarios total). The framework (legislation, guidelines, recommendations) for the environmental impact assessment follows the EP act and associated guidance. The purpose of this document is to present background, methodology, and results of ***The Study***, and a discussion of the results with respect to the regulatory framework. The report also highlights the key areas of uncertainty and makes recommendations for monitoring such that these uncertainties may be reduced in future works.

2. Introduction

2.1. Objective and scope of this plume modelling study

The objective of ***this study*** was to evaluate the probable and possible environmental impact of dredging and dredge spoil disposal plumes associated with ***the Project*** The framework (legislation, guidelines, recommendations) for the environmental impact assessment (EIA) follows the ***Environmental Protection Act 1986*** (EP act) and associated guidance (***see Section 3.6***).

The specific scope of ***The Study*** was to:

1. Adapt an existing hydrodynamic and wave model of the Pilbara region to be suitable for the objectives of ***The Study*** Adaptation includes incorporation PPA supplied bathymetry, and revalidation using oceanographic observations provided by PPA;
2. Review past geotechnical studies of the dredge area to characterise the sediments that may be mobilised in the marine environment by dredging of dredge spoil disposal;
3. Undertake a literature review to estimate the probable rates of sediment spill associated with any credible dredge scenario;
4. Select the most appropriate methodology for numerical modelling of such sediment;
5. Undertake numerical sediment plume modelling for the credible scenarios, and;
6. Liaise with benthic habitat specialists to confirm the most appropriate threshold values for environmental impact assessment (following Western Australian EPA's guidance for EIA of dredge plume modelling, 2021);
7. Interpret the modelling results in accordance with these thresholds.

Through liaison with benthic habitat specialists (point 6 above), it was confirmed that the most appropriate thresholds were the values default guideline values for coral with a non-conservative conversion factor of 1.5 (i.e. SSC thresholds multiplied by a factor of 1.5, DLI thresholds reduced by a factor of 1.5). The justification for this non-conservative conversion factor relates to the turbidity and light tolerance of the local species

compared to the much more sensitive acropora species for which the guideline was derived. Further comment on this is beyond the scope of this package.

Excluded from the scope are:

1. Review of background/environmental water quality;
2. Assessment of benthic habitats and the most appropriate thresholds for EIA;
3. Actual assessment of cumulative impacts on benthic habitats;

These assessments can be found in the following reports:

- Marine Water Quality Baseline Report (O2 Marine 2022a), provided in Appendix A of Referral Supporting Document).
- Benthic Communities and Habitat Cumulative Assessment Report (O2 Marine 2022b), provided in Appendix C of Referral Supporting Document.

The purpose of this document is to present background, methodology, and results of ***The Study*** and a discussion of the results with respect to the regulatory framework.

2.2. The Dampier Cargo Wharf Extension and Landside Redevelopment Project

PPA as the proponent for the Project is proposing to develop and operate a land-backed wharf extension to the Dampier Cargo Wharf (DCW) at the Port of Dampier (***the Port***). The ultimate scope of the Project incorporates the development of a new (adjoining) southern section of wharf and associated mooring dolphin, wharf connecting structure, dredged berth pocket and vessel manoeuvring area. The Project's Development Envelope (DE), Project Footprint, and other key physical elements are presented in Figure 1. The project Dredging Footprint and existing bathymetry are presented in Figure 2.

2.2.1. Key Project Characteristics

The Project will comprise of the following physical elements:

- Land-backed wharf and wharf face
- Berth pocket to design depth of -13.2 m Chart Datum (CD)
- Vessel manoeuvring area to design depth of -11 m CD

The proposal includes the following key construction elements:

- Construction of DCW Extension: Key construction elements are proposed to include pile driving works, construction of rock revetment and installation to form the wharf deck and associated mooring dolphin.
- Capital Dredging: Up to 380,000 m^3 of capital dredging will be undertaken to establish a new berth pocket and associated manoeuvring basin to design depths (plus an allowance for up to 1m of over-dredging to achieve these depths), respectively. Dredging will be undertaken using a backactor dredge or a cutter suction dredge.
- Drilling and blasting: Up to 100,000m^3 of granophyre rock material to the south and east of the Project dredging area will be broken up using drilling and blasting techniques.
- Disposal of material: Dredge spoil, including blasted rock material to be placed at established spoil grounds located in Port waters including Spoil Ground 2B, Spoil Ground A/B and East Lewis Island (ELI) Spoil Ground. There are three potential spoil grounds (Figure 3).

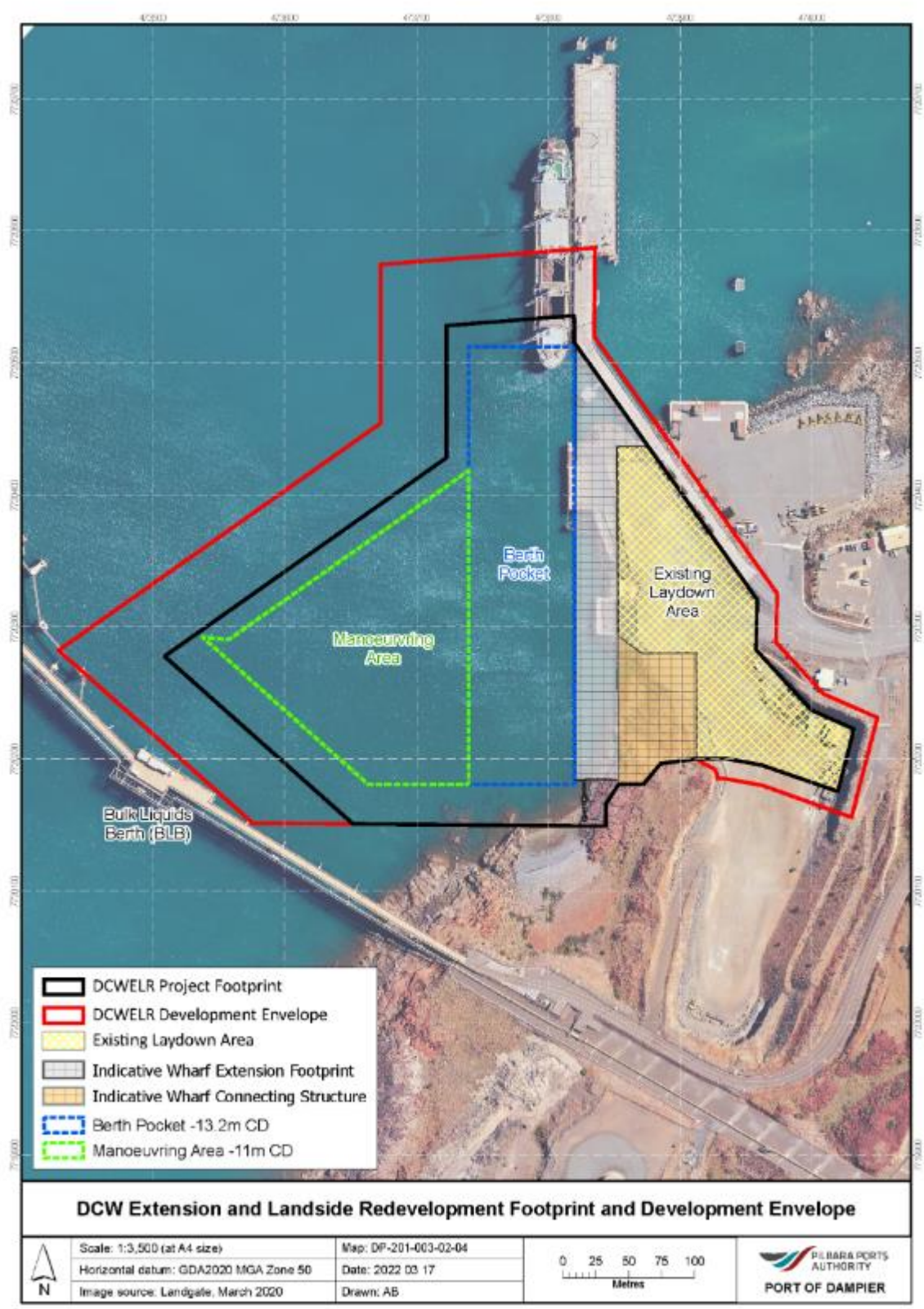

Figure 1 Project Development Envelope and Project Footprint

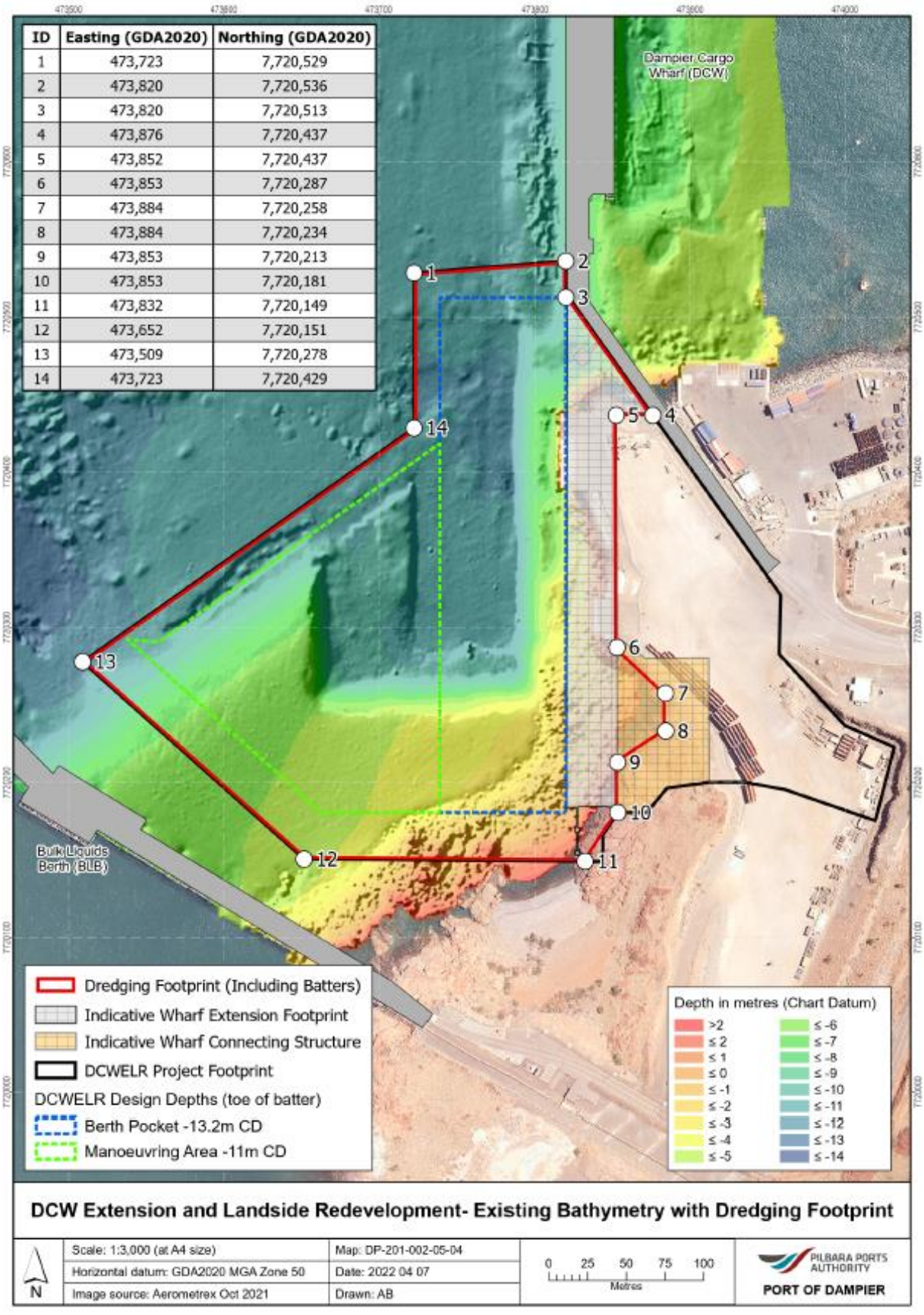

Figure 2 Project Dredging Footprint and existing bathymetry.

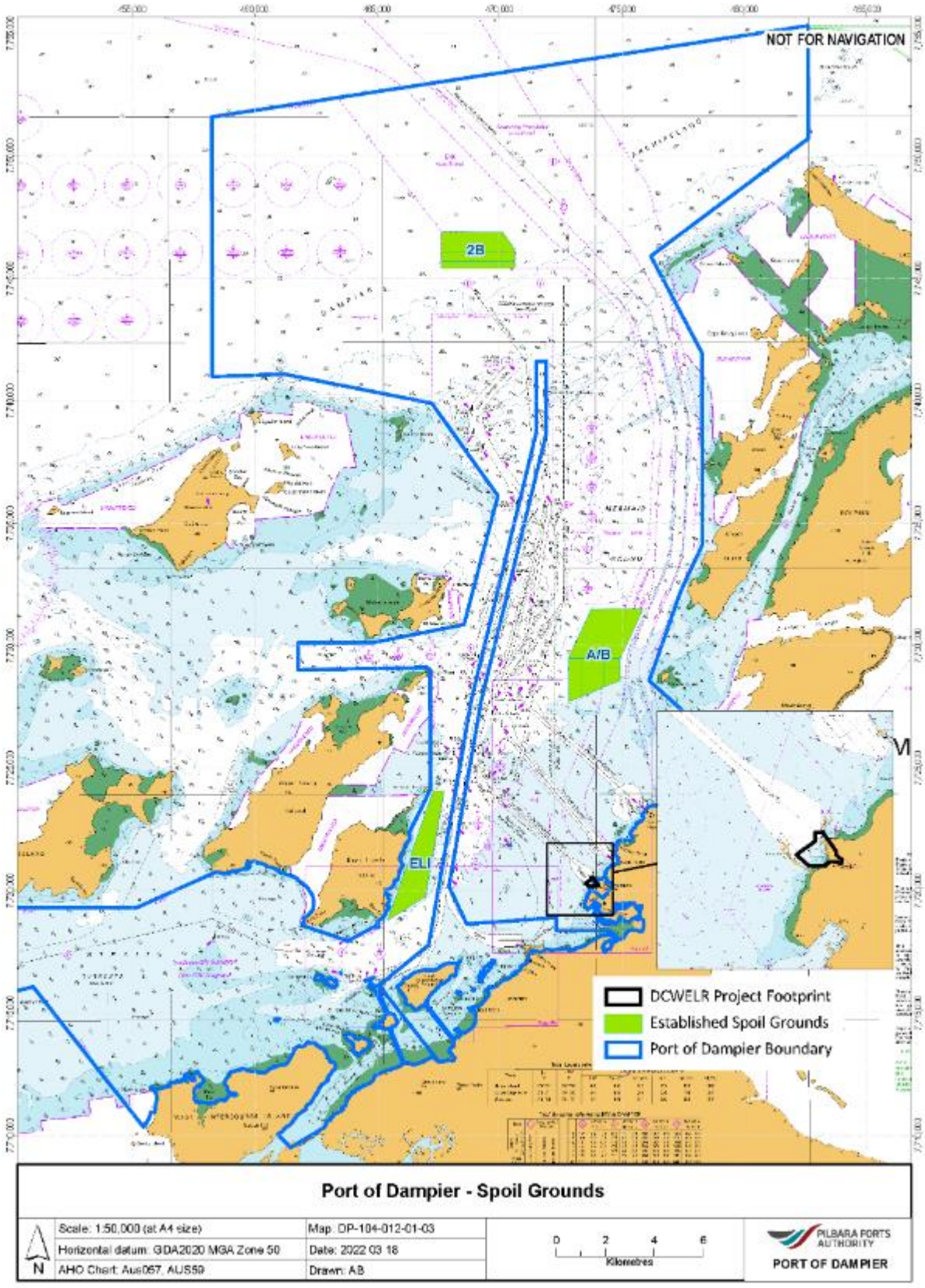

Figure 3 Map of the Dampier Archipelago showing the Project Footprint and the three potential spoil grounds ELI (East Lewis Island); A/B and 2B.

2.2.2. Project significance

The Port services major industries located in the port and the nearby Burrup Strategic Industrial Area (Burrup SIA) and is an important logistics hub for the offshore oil and gas industry, downstream gas processing and mining operations in the central Pilbara.

Major exports from the Port are iron ore, salt, Liquid Natural Gas (LNG), condensate and anhydrous ammonia. PPA operates two multi-user facilities in the Port; namely the Dampier Bulk Liquids Berth (DBLB) to support bulk liquid imports and exports (including diesel fuel and anhydrous ammonia), and the DCW providing for general cargo and offshore supply vessels (Figure 1). Additional facilities managed by others within the vicinity of the DCW and DBLB are also shown in Figure 1.

There is currently no multi-user bulk solid export cargo capacity in the Port. The need for a new multi-user facility has been recognised by PPA, to support new and existing trades and proposed industrial developments in the Burrup SIA.

The Project will create a new multi-user wharf that will align with and extend directly south from the DCW, enabling larger vessels to access this terminal and support new trades and products being handled at the Port. The Project will be connected to the Burrup SIA by the existing Burrup Services Corridor (BSC), a dedicated infrastructure corridor designed to accommodate pipelines and conveyors which facilitate the export of a range of liquid and solid product(s).

2.2.3. Project Location

The Port is located approximately 1,540 kilometres (by road) north of Perth, WA and 260 kilometres (by road) west of Port Hedland. The Port is located on the western side of the Burrup Peninsula on the Pilbara coastline, approximately 20 km west of Karratha (Figure 4).

The Port consists of ten port terminals with separate navigational channels, which facilitate the export of iron ore, salt, gas products and the transfer of general cargo, break-bulk and bulk liquid fuels (Figure 5). PPA is responsible for managing Port waters and vessel traffic operating within the Port.

Port waters extend out into Mermaid Sound and the Indian Ocean beyond the limits of State Waters and incorporates the waters surrounding the Burrup Peninsula and some waters of the Dampier Archipelago (Figure 3).

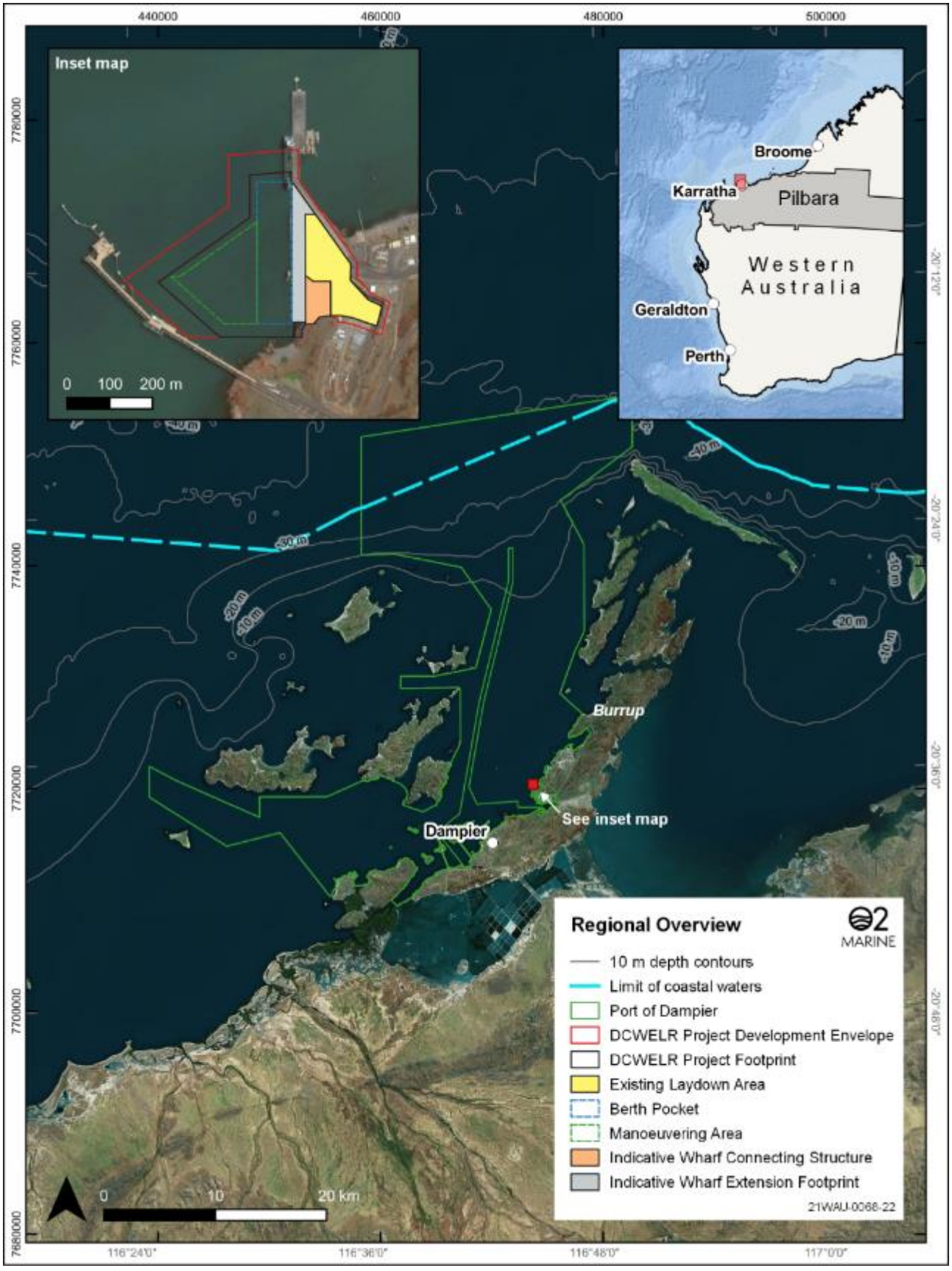

Figure 4 Project location and regional overview

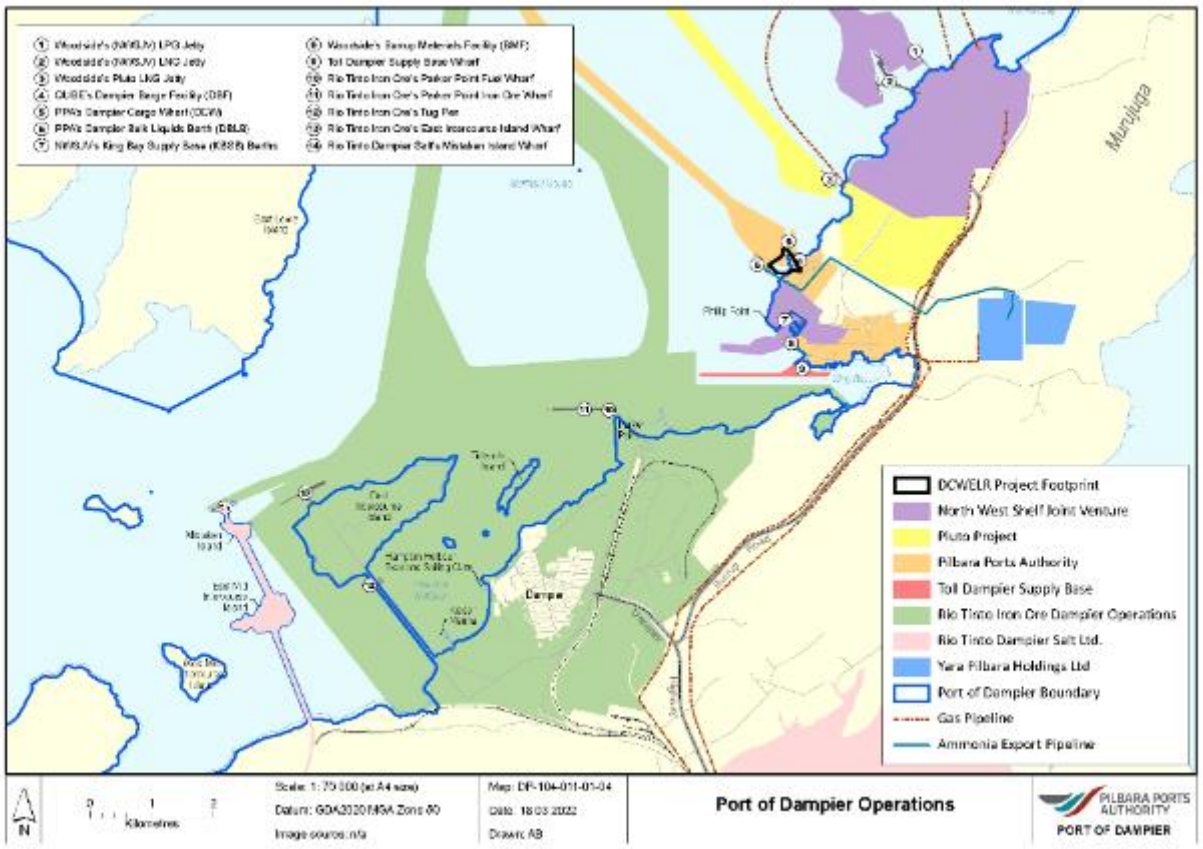

Figure 5 Location of the Project and other Port operations

2.2.4. Details of the proposed dredge programme

Dredging is intended for the last quarter of 2022 or first quarter of 2023. Dredging with both Backactor and cutter-suction (CSD) dredgers is being considered at this early stage. In both instances dredge spoil will be placed into barges and transport to ocean disposal sites. Similar dredge rates are expected in both instances, and so the high-level details (timing, duration, number of disposals) of both programmes are expected to be similar, however the nature and method of sediment mobilisation will differ appreciably between the two scenarios. Key parameters of the proposed dredging are given in Table 1.

Table 1 Dredge and disposal program for backactor and cutter suction dredging.

Parameter	Value	Notes
Dredge Volume	144,700 m^3	Actual in-situ volume of overburden that must be removed (excluding granophyre rock) to reach target dredge depth. Note that the actual amount to be modelled will be greater than this as contingency for dredging past target depth.
Dredge equipment	Backactor dredger ***OR*** Cutter suction dredger (CSD)	Both Backactor and CSD will be simulated.
Dredge rate	150 m^3/hour	Hourly dredge rate for the total material according to the dredge plan shown in this table. The same rate is assumed for Backactor and CSD.
Dredge schedule	7 days a week; 24 hours a day	Continuous operation expected
Dredge hours per day	14 hours per day	While operations are expected to be 24/7, shift changes and other downtime are likely to result in 14 hours of effective dredging during any 24-hour period.
Duration of dredging	98 days	Anticipated duration of the dredge operation (for overburden material removal only). Anticipated for Q2 2022.
Disposal method	Sea dumping by ~1000 m^3 barges filled at site	Sea dumping is anticipated for both Backactor and CSD
Disposal frequency	8 hours	Estimated based on typical loading times, transit times and disposal times using a ~1000 - 1500 m^3 barge. Three disposal events to occur every day. Disposals therefore contain 4 hours and 40 minutes of dredge material (14/3) minus the material spilt from the hopper barge.
Dredge disposal location	Three possible locations: ELI Spoil Ground, 2B, and A/B	All options will be simulated for both Backactor and CSD. For locations see Figure 3

3. Background

This section presents background information used to derive the methodology (Section 4) of ***The Study*** and that is necessary to appreciate the significance of the results and discussion.

3.1. Physical environment

Figure 6 Key geographic features in the project area

3.1.1. Weather

The Pilbara is an arid region with pronounced wet and dry seasons, influenced by the Indonesian-Australian monsoon and the meridional migration of the equatorial and subtropical pressure belts. The wet season (November to April) is characterised by high temperatures, higher than average rainfall, and lower atmospheric pressures (over the land). The dry season (May to October) is characterised by warm temperatures, clear skies, limited thunderstorm activity, very low rainfall, and higher atmospheric pressures. Over 1991-2020 at the BOM's Karratha Airport station, the maximum daily temperatures averaged 32.5 °C, with the monthly average peaking at 36.3 °C in March (36.0 °C in January) and falling to 26.4 °C in July (Figure 8).

Winds are predominantly west to south-westerly during the northwest monsoon (approximately the wet season) (Figure 9) and easterly to southerly (coincident with the trade winds) during the southeast monsoon (approximately the dry season). Non-cyclonic synoptic scale winds are typically stronger in the dry season. Near the coast a diurnal land-sea breeze system is present throughout the year, intensifying in the warmer months.

The region is exposed to tropical storms and cyclones during the wet season. The Karratha to Onslow coastline is the most-cyclone prone section of the Australian coast, with one cyclone making landfall every two years on average. Cyclones affecting the Pilbara typically form in the tropical waters between the Kimberley and the Timor Sea and intensify as they propagate westward and poleward, though the tracks and intensities of

cyclones passing the Archipelago vary greatly (Figure 10). In addition to tropical storms, troughs of low pressure also bring rain, strong winds, and sharp changes in wind direction.

The annual average rainfall is only 325 mm, though this value can be exceeded in a single day during an extreme tropical storm (Figure 7). The mean monthly rainfall has a bimodal distribution with one peak in the wet season and a second peak in June. Tropical storms dominate this first peak, while frontal systems from the south can contribute to the rainfall in the middle of the year. Very little rain falls between August and October (Figure 7).

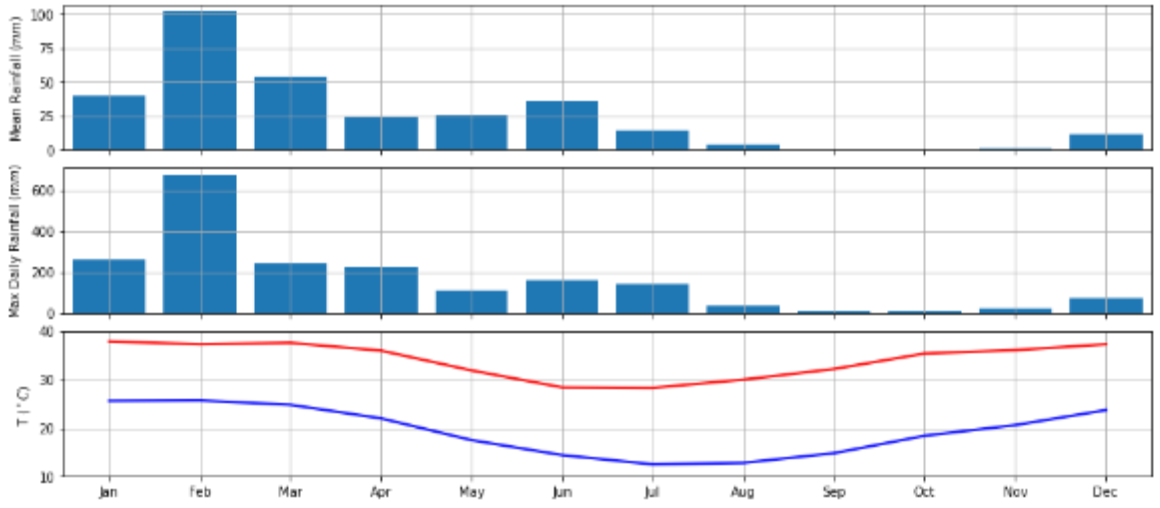

Figure 7 Climate Statistics for BOM Mardi weather station over ten years of 1991 to 2020. Top: mean monthly rainfall. Middle: maximum daily rainfall per month. Bottom: monthly mean maximum daily temperature [red] and monthly mean minimum daily temperature [blue].

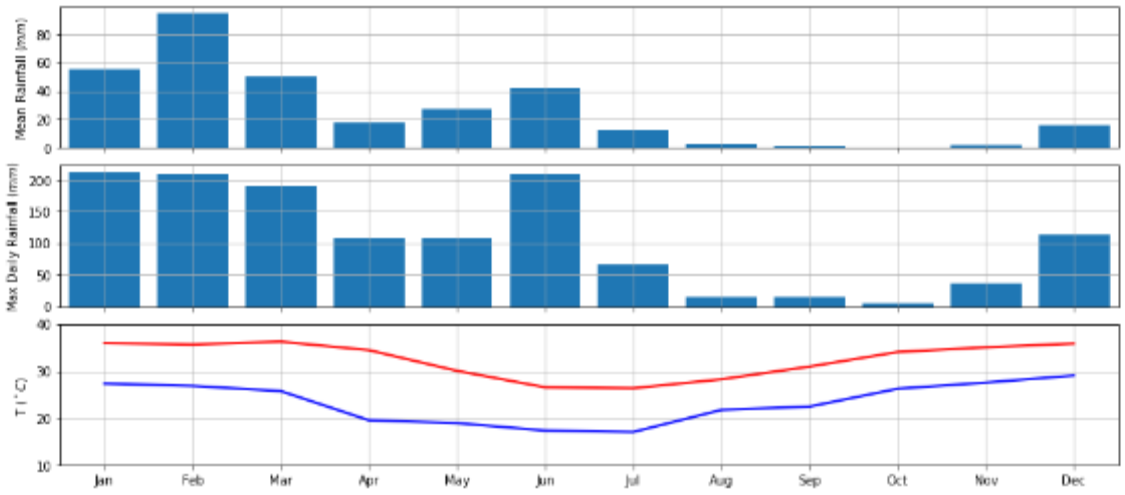

Figure 8 Climate Statistics for BOM Karratha Airport weather station over ten years of 1991 to 2020. Top: mean monthly rainfall. Middle: maximum daily rainfall per month. Bottom: monthly mean maximum daily temperature [red] and monthly mean minimum daily temperature [blue].

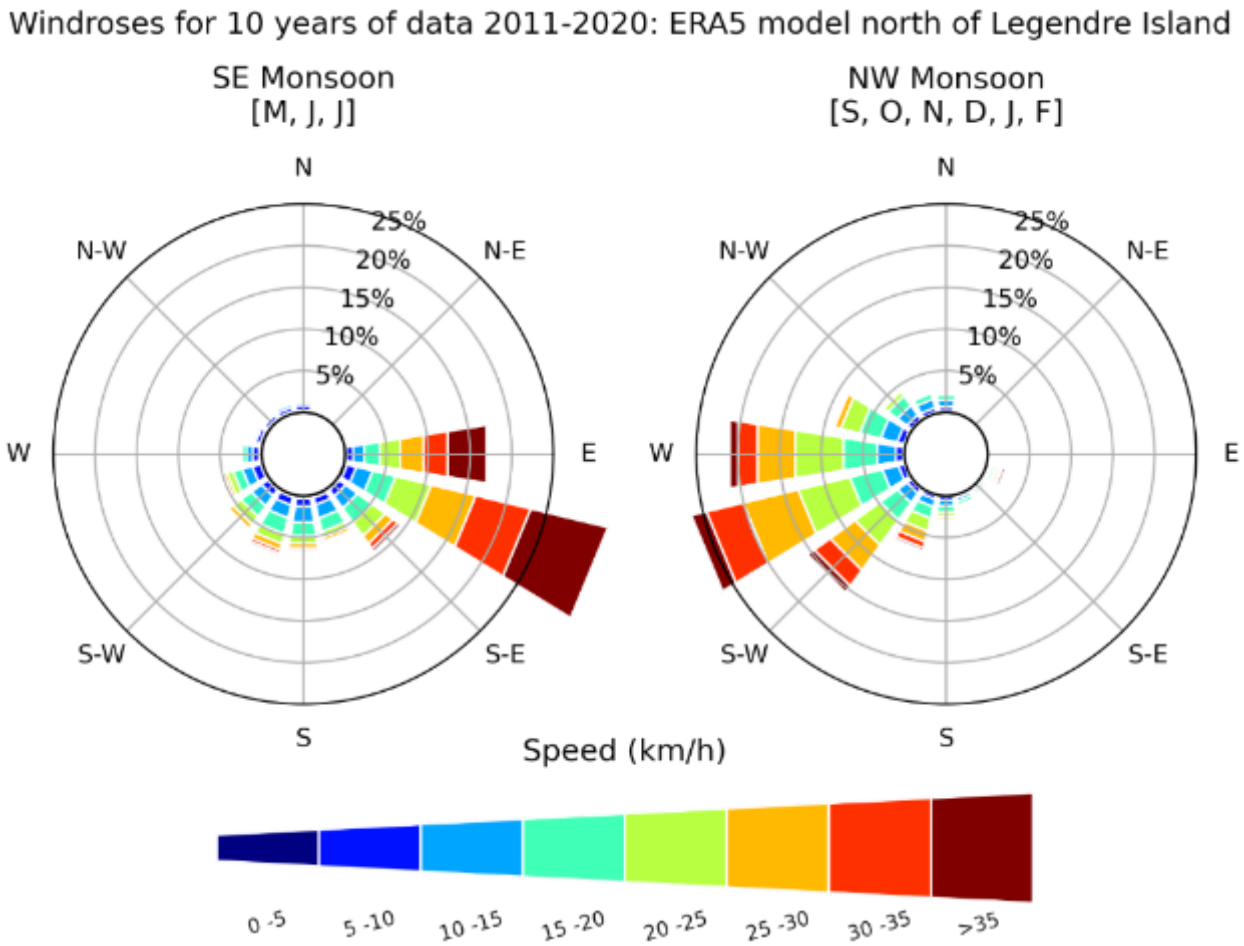

Figure 9 Wind Rose plots for SE Monsoon (left) and NW Monsoon Months (right) based on analysis of the 10 years of modelled data from near Cape Preston.

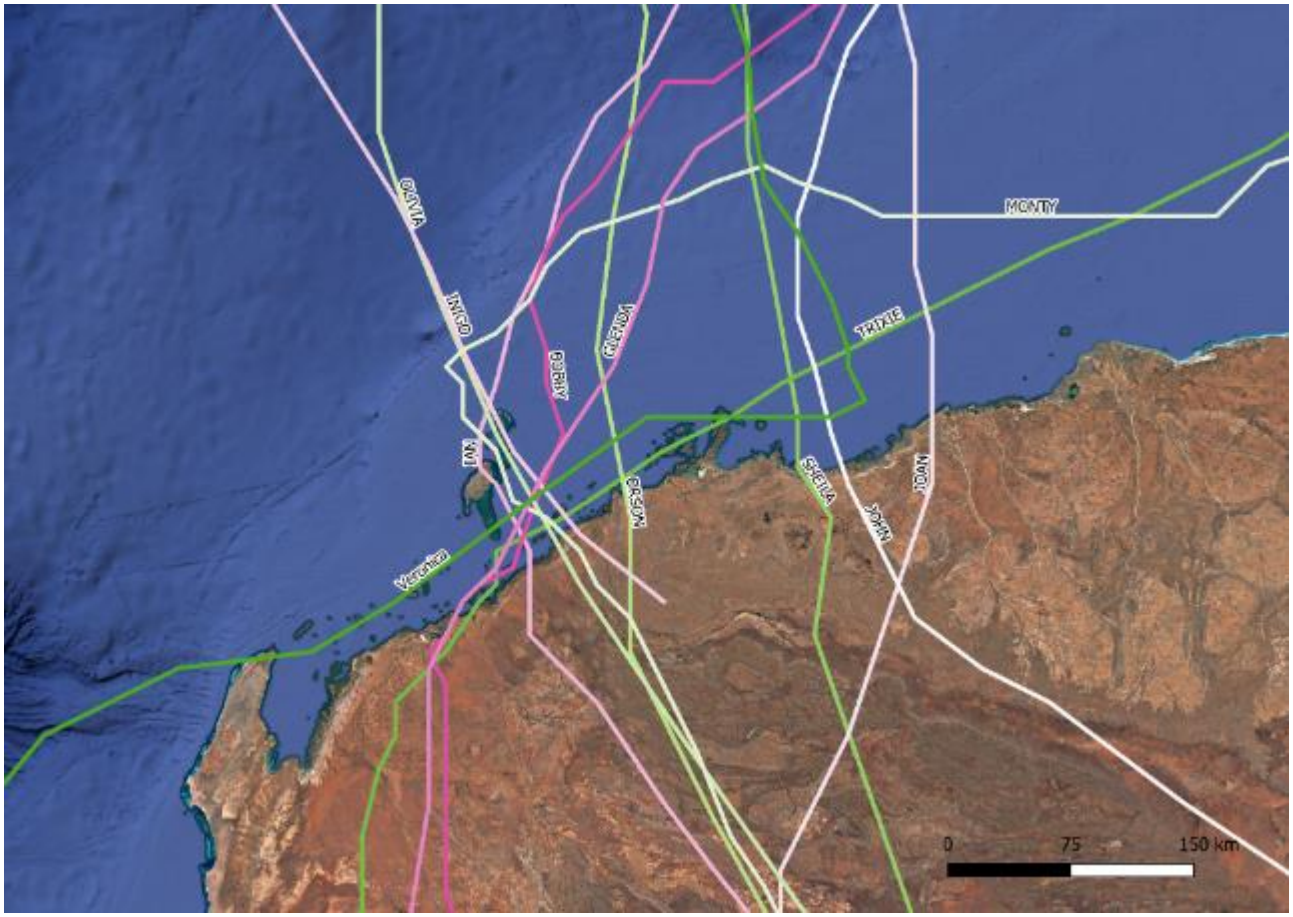

Figure 10 Tracks of notable cyclones impacting the Dampier Archipelago. Events are filtered to include only events that had a minimum pressure below 940 hPa and passing within 150 km of Karratha (though these did not need to occur concurrently). The notable recent cyclone TC Damien, which made landfall over the peninsula on February 8 2020, did not reach 940 hPa, and is thus not shown.

Drivers of climate variability

Over short timescales (i.e. decades), the main driver of interannual climate variability in Northern Australia and the Pilbara region is the El Nino Southern Oscillation (ENSO). The positive phase of ENSO, known as La Nina, is characterised by a strengthening of the trade winds over the tropical Pacific. This intensification drives more warm water over the western Pacific, leading to less stable atmospheric conditions and increased rainfall over northern and eastern Australia, warmer than average conditions over the Cape York Peninsula, and cooler than average conditions over southern Australia. The negative phase, El Nino, has approximately opposite effects. Compared to the Pacific coast, the effects of ENSO over the Pilbara coast are less dramatic, and often less consistent, though La Nina years are linked to an increase in both the number and intensity of tropical cyclones in the Pilbara, despite distance from the direct effects of the Pacifica Ocean trade winds.

The Indian Ocean Dipole (IOD) is another empirically defined oscillation which impacts interannual climate in the Indian ocean, modulating the effects of ENSO. A negative IOD reflects an intensification of the standard atmospheric circulation in the upper Indian ocean. This is associated with warmer ocean temperatures and increased atmospheric instability over northern Australia, reinforcing La Nina conditions. Conversely, a positive IOD reflects a weakening or disruption to this circulation, associated with a more stable atmospheric conditions over northern Australia, reenforcing the effects of El Nino.

The contemporary warming trend in the ocean and atmosphere (global warming) are another source of long-term climate variability, though significant effects are generally measured (and predicted) over timescales larger than the life of many engineering projects.

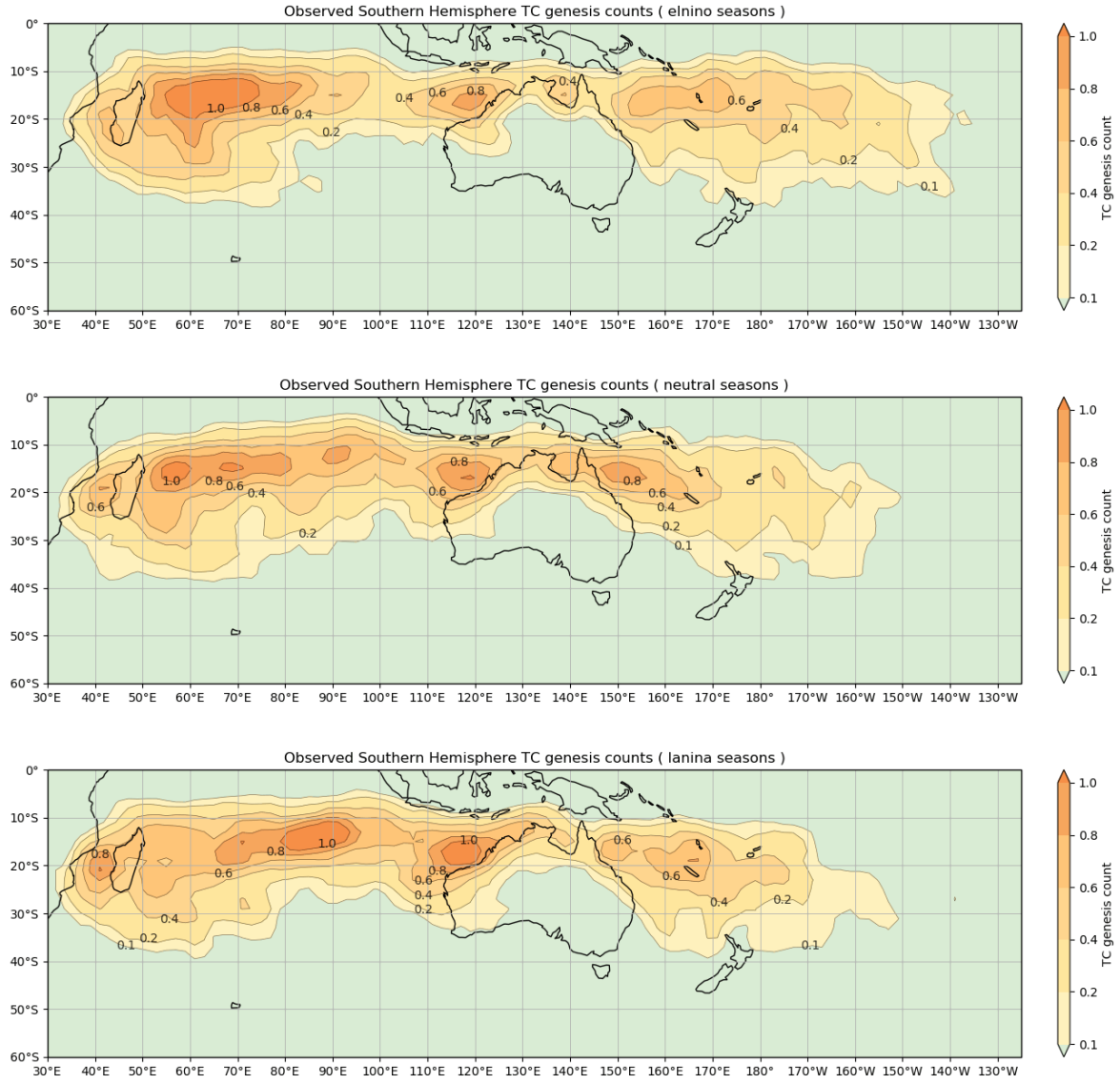

Figure 11 Tropical Cyclone genesis for El Nino (top), Neutral (middle) and La Nina (bottom) seasons (source: BOM)

3.1.2. Geomorphology

The Pilbara has a very broad continental shelf, ranging from around 100 km at the western extent to 300 km in the east. To the west (i.e. offshore from Barrow Island) the shelf breaks gradually onto the Exmouth Plateau, while in the east (i.e. offshore from the Rowley Shoals), the shelf breaks much more rapidly into deeper waters. Barrow Island, the Montebello Islands, and the shoals to the south of Barrow are significant features of the inner shelf that influence waves, tidal currents, and wind driven circulation in the region. Between North-West Cape and the Dampier Archipelago, many smaller islands lie inside the 30 m depth contour, providing further shelter for the coastline. These islands introduce heterogeneity in the ambient hydrodynamic conditions along the coast, which in turn promotes heterogeneity in marine habitat.

The mainland Pilbara coastline is characterised by extensive beaches, mud flats, mangroves and tidal creeks seaward of an ancient hard-rock terrain. Marine sediments are delivered and deposited through the action of wave and tides, while terrigenous sediments are delivered to the coast episodically through flood plains and river deltas. There are no major rivers within the Archipelago itself, however. The nearest major river, and hence source of terrigenous sediments, is the Maitland River approximately 30 km west of the project location (Figure 6). The coast within the Archipelago, west of the Burrup Peninsula, is predominantly rocky coastline or sandy beaches, with fewer mangroves and salt flats comparative to other Pilbara regions. Cyclones, and the associated extreme high-water levels, waves, and freshwater discharge are likely to be a significant driver of coastal geomorphic changes in the region (Elliot et al 2013), however Port infrastructure has also altered the natural west coast of the Burrup. This has included construction of rock causeways and trestle jetties, land reclamation and dredging.

Port of Dampier bathymetry

Excluding man-made features, Mermaid Sound is generally less than 20 m CD, deepening to 35 – 40 m CD approximately 5 km offshore of the northern entrance to Mermaid Sound, and exceeds 50 m CD by 25 km offshore. Man-made features within the Port include berth pockets, turning basins and channels, of which vary in depths between 15 m CD to 25 m CD.

3.1.3. Water levels

Water levels along the Pilbara coast are dominated by the semidiurnal lunisolar tides, with the eastern Pilbara classified as from macro-tidal, and the western Pilbara as meso-tidal (Table 2). At the proposal site the mean spring tide range exceeds 3 m and the maximum tide range is approximately 4.5 m. The presence of Barrow Island and the shallow waters to the south strongly affect the westward propagation of semidiurnal and diurnal tidal energy, introducing complex non-linear tidal flows to the west of Barrow Island.

Wind, pressure and wave-setup in the Pilbara are typically low in comparison to the tidal variability, though they can be significant under tropical cyclone forcing, particularly in partially closed water bodies (i.e. marine embayments). Appreciable inundation of coastal areas occurs under these conditions, and wave action can be highly destructive.

Table 2 Tidal Planes at Dampier, Barrow Island, Onslow and Cape Preston [datum mean sea level].

Table Heading (left) Style	Onslow [m]	Barrow Island West [m]	Barrow Island East [m]	Cape Preston [m]	Dampier [m]	Central Nikol
HAT	1.29	1.30	2.20	2.25	2.46	2.46
MHWS	0.85	0.89	1.50	1.71	1.76	1.77
MHWN	0.26	0.26	0.41	0.38	0.46	0.47
MSL	0	0	0	0	0	0
MLWN	-0.25	-0.25	-0.40	-0.38	-0.46	-0.46
MLWS	-0.84	-0.94	-1.33	-1.45	-1.48	-1.48
LAT	-1.29	-1.32	-2.21	-2.19	-2.66	-2.76

3.1.4. Ocean Currents

Instantaneous currents on the inner shelf are dominated by barotropic tides, with wind-driven currents, steric currents and continental shelf waves playing a lesser role (Godfrey and Mansbridge, 2000; Condie & Andrewartha, 2008; Ridgway and Godfrey, 2015; Sun and Branson, 2018, and the references therein). Persistent large-scale currents (e.g. the Holloway current) are typically constrained to waters depths greater than 100 m. Sub-tidal circulation is seasonally variable, and driven predominantly by winds (Condie and Andrewartha, 2008). During the wet season these low-frequency wind-driven currents typically flow towards the east, while in the dry season they typically flow towards the west.

Seaward of the Dampier Archipelago, tidal currents flow approximately east-west, parallel to the coast. Tides in these deeper waters propagate faster than they do through the Archipelago itself, and so the Archipelago has a complex flushing pattern. Rather than flushing the entire archipelago from east to west (i.e. from Mermaid Sound to Mermaid Strait following the direction of flow in the open ocean), the rising tide infiltrates through each of the numerous straits and passages see (Figure 6). This flow pattern results in a marked reduction in tidal currents between the outer port (i.e. the outer stretches of Mermaid Sound) and the inner port, where *The Project* is located.

Currents through the narrow Searipple and Flying Foam Passages can exceed 2 ms^{-1} (Pearce et al., 2003; PPA 2020), though their contribution to the total flushing is not well known. This is in part due to inadequate bathymetric resolution in past numerical studies.

3.1.5. Waves

Waves on the Pilbara shelf can be broadly classified into three primary generation mechanisms: (1) southern Indian Ocean swell, (2) locally generated wind-waves and (3) tropical cyclone waves. Indian ocean swells lose appreciable energy as they refract around Northwest Cape and onto the Northward facing Pilbara coastline. Though consistently mild, this swell climate is stronger in the dry season owing to stronger swells during winter months in the southern Indian Ocean. It is high-frequency wind waves then that dominate the non-cyclonic

wave climate. These seas vary appreciably in magnitude, period and direction along the Pilbara coastal waters, but typically have a north-westerly aspect in the wet-season, and a north-easterly aspect in the dry season. The largest waves are associated with cyclone forcing, and again vary greatly across the coast, influenced by the proximity, intensity and travel speed of the cyclone.

Most surface wave energy at the Port arrives from the north, propagating through Mermaid Sound. Ambient waves may attenuate in amplitude by 50% compared to open ocean values (Pearce et al., 2003), while extreme cyclone waves may attenuate by 75% (PPA, 2020).

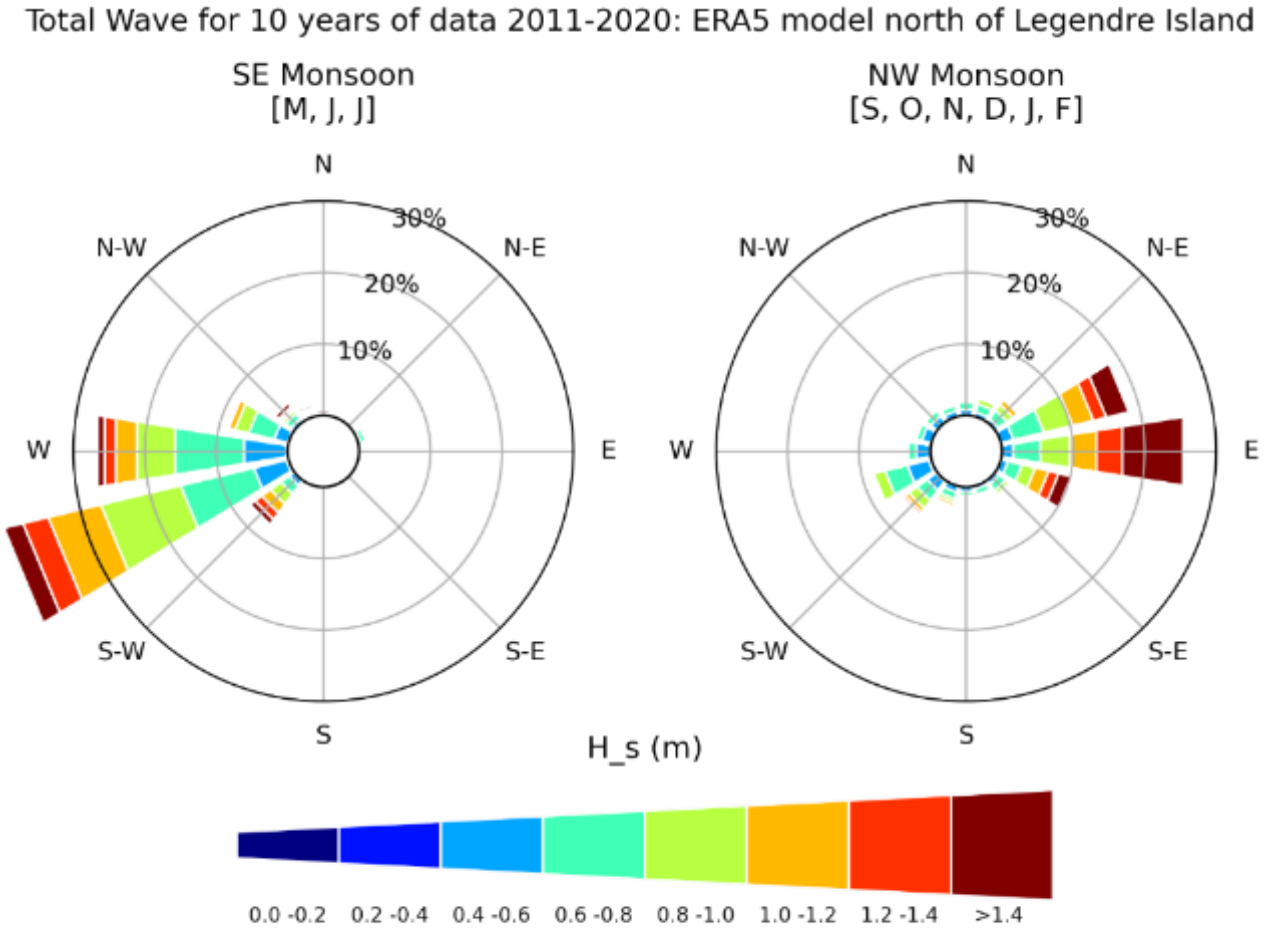

Figure 12 Wave conditions offshore of Legendre Island for the SE Monsoon (left) and NW Monsoon (right) based on 10 years of modelled data.

3.2. Geotechnical Investigations

The comprehensive geotechnical investigation of GHD (2020) was the primary source for geotechnical data used to inform this study. MScience (2022) recently performed additional surficial sediment sampling (top 1 m), however these data were not included in the present study due to the timing of the publication of results. Given that the samples were not to dredge depth, as in GHD (2020), their inclusion would likely have little impact on the findings of this study.

3.2.1. GHD, 2020

The GHD (2020) investigation involved:

1. **Geophysical survey:** conducted in the berth pocket and manoeuvring area and included sub-bottom profiling, continuous marine seismic refraction, side scan sonar and marine magnetics.
2. **Geotechnical borehole drilling:** 30 cored boreholes to depths between 2 m and 19.9 m below the seabed with laboratory tests also being conducted on selected samples.

The geotechnical investigation characterised the site as predominantly of marine sediments, calcareous gravel, coastal limestone, and beach deposits, overlaying basement rock of granophyre or granite in select borehole locations (GHD, 2020).

3.2.1.1. Geotechnical Composition within the Dredge Footprint

GHD (2020) classify the material in the proposed dredge into five categories (or strata):

1. Marine Sediment: Sand dominant brown-grey to grey, silty sand to sand with silt, fine to medium grained. A variable minor component of gravel was sometimes observed.
2. Calcareous Gravel: Uncemented to moderately cemented gravel size fragments with a variable minor to secondary component of sand and clay.
3. Coastal Limestone: comprised of variably cemented siliceous calcarenite, conglomeratic calcirudite and coral limestone.
4. Beach Deposits: Typically comprising of a mixture of gravel and cobbles of granophyre and often intersected above granophyre bedrock and often the boundary between beach deposits and bedrock was difficult to determine.
5. Granophyre bedrock

Herein we use the term '*overburden*' to refer collectively to the first four classifications – i.e. to the total dredge volume less the volume of basement rock. The existing bathymetry and anticipated bathymetry after overburden removal are shown Figure 13. This map, generated by interpolation of borehole data, is qualitatively consistent with the sub-bottom profiling conducted and presented in GHD (2020). The difference between these two is the thickness of this overburden layer. This is shown against the total dredge material thickness (i.e. including the granophyre) in Figure 14.

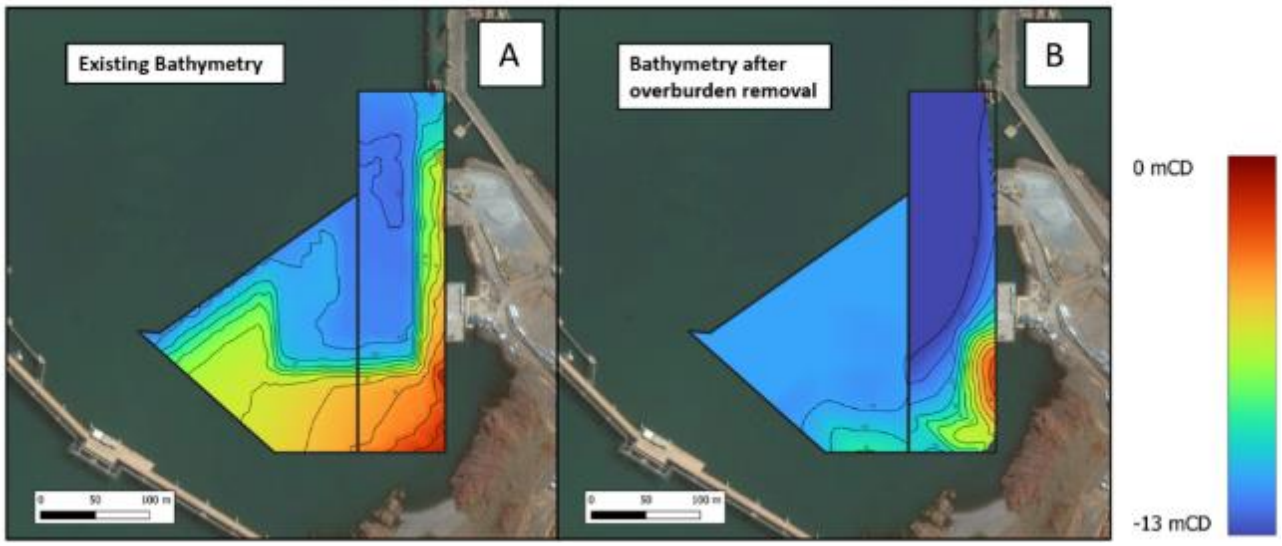

Figure 13 Existing bathymetry (left (A)) and bathymetry after overburden removal (right (B)). At any point in space, the bathymetry after overburden removal was calculated as the (absolute) minimum of the granophyre layer depth and target dredge depth (i.e. whichever is shallower). The presence of the basement rock layer in the south and south-easterly region of the dredge footprint does not allow for regular dredging activity down to the desired -13.2 m CD in the berth pocket and -11 m CD in the manoeuvring area.

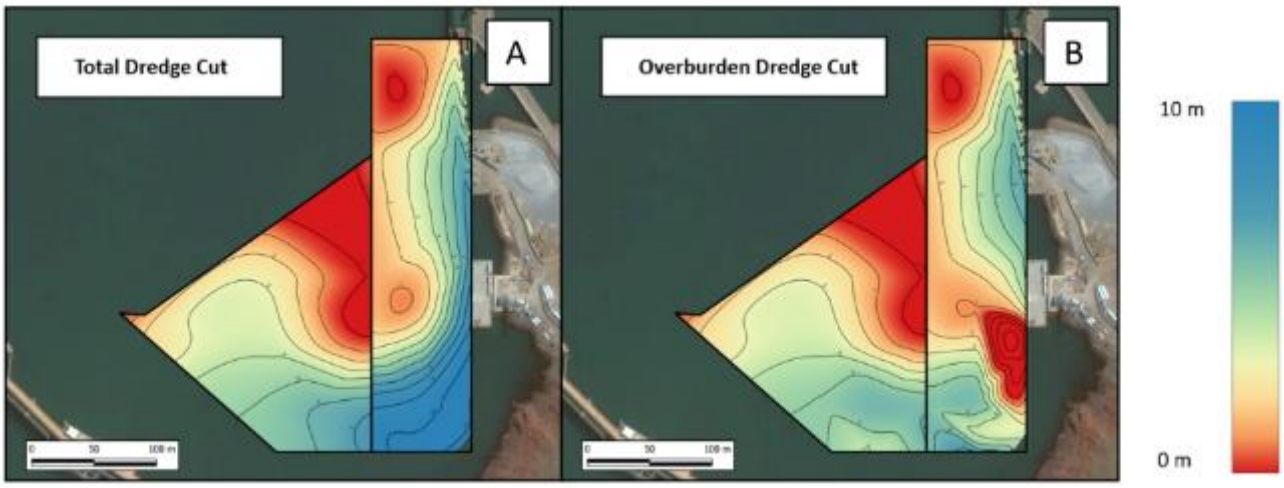

Figure 14 Total dredge material requiring removal (panel A) and volume of overburden requiring removal (panel B). Image A was derived by subtracting the dredge bathymetry from the existing bathymetry. Image B was derived by subtracting the right-hand image in Figure 11 from the existing bathymetry.

In Figure 15 we present the relative thickness of each of the four overburden classifications (marine sediments, calcareous gravel, coastal limestone and beach deposits). These were calculated by horizontally interpolating borehole data, and then vertically integrating the total thickness of each layer, and are presented as fractions of the total overburden thickness at that point (1 (0) representing 100% (0%) of the total overburden thickness). The thickness of each stratum to be removed is then the pointwise product of these maps and the total overburden thickness (i.e. Figure 14 b). The total volume of each layer in the overburden was calculated by horizontal integration of this product and is presented in Table 3 below.

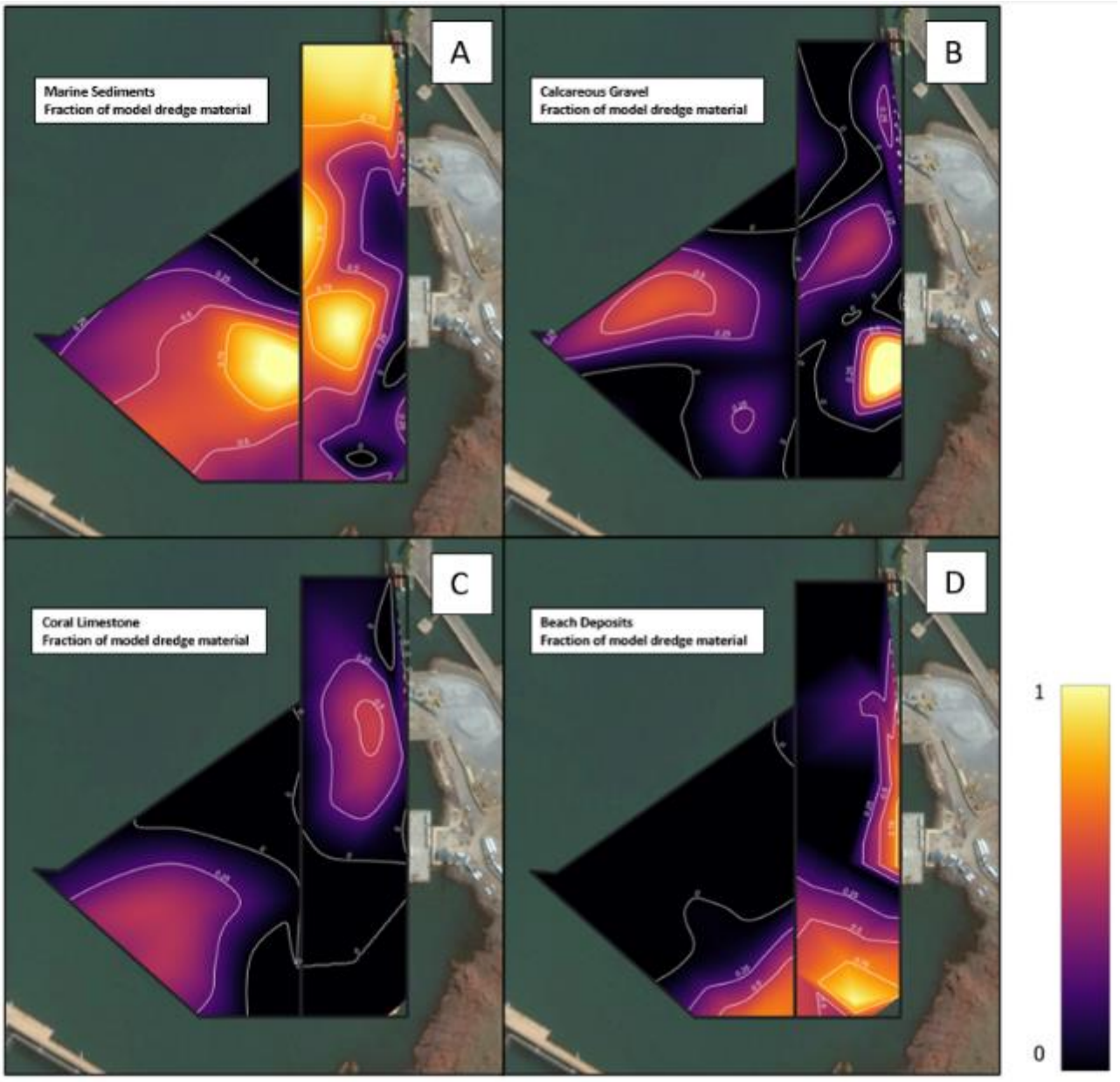

Figure 15 Fraction of marine sediment (Panel A), calcareous gravel (Panel B), coastal limestone (Panel C) and beach deposit (Panel D) within the overburden/model dredge material

Table 3 Material composition within the overburden

Material	Approximate Volume (m^3)	Percentage of Overburden Material (%)
Marine Sediments	66,788	46.2
Calcareous Gravel	19,771	13.7
Coastal Limestone	25,503	17.6
Beach Deposits	32,639	22.5
Overburden Total	144,701	100

3.2.1.2. Particle Size Distribution

GHD (2020) analysed particle size distribution (PSD) for a total of 50 sediment samples of either the marine sediment classification (36 samples) or calcareous gravel classification (14 sample). We synthesised these results by averaging over all samples for each material classification (i.e. marine sediments or calcareous gravel). Representative PSD for each classification are given in Table 4 for three sediment fractions. These sediment fractions - fines, sand and gravel – and are the original fractions of GHD (2020), and differ slightly from the fractions used in the present modelling assessment.

Table 4 Particle Size Distribution of Marine Sediment and Calcareous Gravel. These fractions are the original fractions of GHD (2020), and differ slightly from the fractions used in the present modelling assessment.

Geological Stratum	% Fines (< 75µm)	% Sand (75µm to 2.36mm)	% Gravel (> 2.36mm)
Marine Sediment	47.6	39.4	12.5
Calcareous Gravel	18.8	32.4	48.8

Hydrometer-based PSD tests, to subclassify the fines contents, were only conducted on 16 of the 50 PSD samples, all of which were marine sediment samples. We averaged these to estimate that approximately 14% of total fines within the marine sediment are classified as clay (< 2 µm) and the remaining 86% of total fines are classified as silt (2 µm-75 µm). In the absence of equivalent testing data for calcareous gravel, the distribution of silt and clay within the fines was assumed to be the same as the marine sediment.

To inform modelling, we further categorised the GHD PSD data to distinguish fine sand and coarse sand. Fine sand was defined having a particle diameter between 75 µm and 150 µm (as this was the first interval of percentage passing within the PSD's sand fraction in GHD 2020). This was done for all 50 samples and averaged for each classification (marine sediment and calcareous gravel). The results are summarised in Table 5.

Table 5 Particle Size Distribution of Marine Sediment and Calcareous Gravel. These data are derived from GHD (2020), and modified to distinguish clay, silt and fine sand.

Geological Stratum	% Clay (< 2µm)	% Silt (2 µm-75µm)	% Fine Sand (75µm-150 µm)	% Coarse Sand (150µm-2.36 mm)	% Gravel (> 2.36mm)
Marine Sediment	6.7	40.9	14.2	25.8	12.4
Calcareous Gravel	2.6	16.2	6.6	25.8	48.8

3.3. Benthic habitat

Benthic Communities and Habitat (BCH) is relevant to the present study, as sessile benthic primary producers are the primary consideration to EIA of dredge plumes. The dominant light and SSC sensitive BCH communities in the area are corals, though seagrass, macroalgae, sponges and mangroves are also found (O2 Marine 2022b and the references therein). Corals within the archipelago are predominantly in shallow coastal areas at depths below 12 m CD (Figure 16).

As mentioned in the *Objectives and Scope* section of this report (Section 2.1), the default guideline thresholds in EPA (2021) are anticipated to be highly conservative in this area, as the local coral species are adapted to

the highly turbid port waters. For such cases, EPA (2021) describes the appropriate use of conversion factors, which are used to adjust the default guideline values. These factors are derived through exercise of professional judgement on the local species. O2 Marine (2022b) recommend a conversion factor or 1.5 applied for this local environment (i.e. SSC thresholds multiplied by a factor of 1.5, DLI thresholds reduced by a factor of 1.5). The justification for this non-conservative multiplication factor relates to the turbidity and light tolerance of the local species vs. the much more sensitive acropora species for which the guideline was derived. Further comment on this is beyond the scope of this package. For further detail please see O2 Marine (2022b).

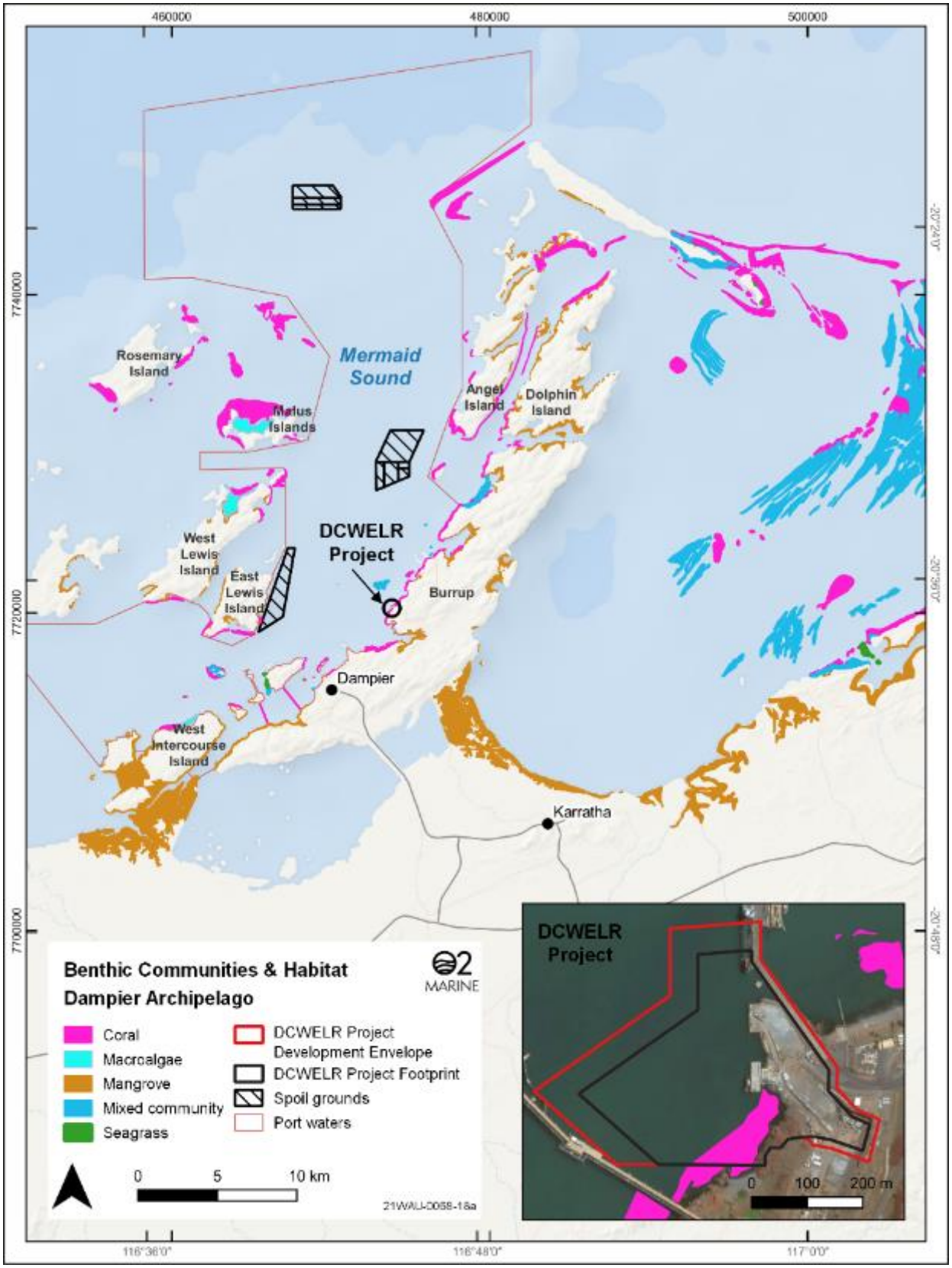

Figure 16 Significant BCH of Mermaid Sound in the Dampier Archipelago and Nickol Bay (reproduced from O2 Marine, 2022b)

3.4. Suspended solids concentration

Mean background SSC was taken from O2 Marine (2022a) as defined in Table 6 below. O2 Marine (2022a) also defines the boundary between offshore and nearshore background concentrations as being the 10 m isobath.

Table 6 Background SSC (O2 Marine 2022a)

Location	Background Concentration (SSC)
Offshore	0.6 mg/l
Nearshore	1.2 mg/l

3.5. Underwater light climate

The assessment of environmental impact from dredge plume modelling requires a relationship between suspended sediment concentration (SSC) and light attenuation. The optimal relationship is a Beer-Lambert type attenuation relation that reflects the properties of both SSC and water as a function of the wavelength of light (see Sun and Branson, 2018, and the references therein). O2 Marine (2022a) found that there was no such relationship for Dampier in the public domain, and no data to derive such a local relationship directly.

MScience (2019) present an empirical relationship between SSC and LAC – defined as the daily integral across the full PAR spectrum - that is tuned to a very narrow depth range, low SSC range, and cannot be directly used outside of October it does not account for seasonal availability of insolation, reflection and refraction at the sea surface. This relationship cannot be used for environmental impact assessment of benthic habitat in 12 m of water (O2 Marine, 2022a).

A Beer-Lambert type light attenuation coefficient (can be estimated indirectly from the MScience (2019) relationship by means of generalised linear regression. The approach requires application of a theoretical models for solar radiation, reflection, and refraction at the ocean's surface. From this approach we derived the relationship:

The subscript ***PAR*** indicates that this relationship is applied to the full PAR spectrum, and is not wavelength dependent. The slope in this equation (0.041) is comparable to the slope derived by MScience (2009) for Ashburton, which also presented

The coefficient in the above reflects the attenuation in clear (zero SSC) water. Fitting to the results of MScience (2019) we found m^{-1}. Following Smith and Baker (1981), this corresponds to attenuation of yellow light in clear ocean water. This may be reasonable for 4-5 m depths in which the MScience (2009) relation was derived, as there is an abundance of red and yellow light. It appears less reasonable to extrapolate this result down to 12 m as required in the present study, as availability these longer wavelengths of light becomes reduced. MScience (2009) report a much lower m^{-1} for PAR in deeper waters (order ten metres) than MScience (2019). Following Smith and Baker (1981), this corresponds approximately to the least attenuated 490 nm wavelengths in clear ocean water, and so seems to be small for full a weighted average over the PAR band in over 12 m depth.

We note that the more recent study of Fearns et al (2019), also near Ashburton, presented relations for Beer-Lambert type attenuation that did model wavelength dependence of the light. Given the wavelength dependent approach, the significance of results are difficult to compare to the above. While this spectral approach is more desirable than modelling attenuation of PAR, the analysis was not local to Dampier, and so O2 Marine (2022a) did not recommend adoption for the present study.

3.6. Regulatory framework for impact assessment

The EPBC Act and EP Act aim to support environmentally sustainable development while protecting environmental values, including biodiversity.

3.6.1. EPBC Act

The EPBC Act lists 'nationally significant' animals, plants, habitats and places as Matters of National Environmental Significance (MNES) and aims to ensure that potential negative impacts on them are carefully considered before changes in land use or new developments are approved. Increased turbidity through dredging has the potential to indirectly affect marine fauna species through reduced habitat quality and redistribution of prey species. Dredge plume modelling has been undertaken, in part, to inform this assessment.

3.6.2. EP Act Guidance

The ***Environmental Protection Act 1986*** (EP Act) is the primary legislation that governs environmental impact assessment (EIA) and environmental protection in Western Australia. EIA in Western Australia is conducted by the Environmental Protection Authority (EPA) which has prepared administrative procedures for the purposes of establishing the practices of EIA. Proposals likely to have a significant impact on the environment are required to be referred to the EPA under Section 38 of the EP Act.

The EPA expects proponents to present their assessment of dredging impacts in accordance with the EPA Technical Guidance for the Environmental Impact Assessment of Marine Dredging Proposals (Environmental Protection Authority, 2016). The guidance describes an impact zonation scheme (Table 7), and the appendices therein offer guideline trigger values for each of these zones of impact. While we do not reproduce the trigger values here, the approach for assessing impact to corals is laid out in (

Table 8).

While we note that the EPA Technical Guidance is not meant to be prescriptive methodology for proponents, the scope of the present study was to follow this methodically (Section 2.1). Professional judgement of the actual damage to and recovery of benthic communities is excluded from the present study (Section 2.1). So too is the choice of most relevant receptor (i.e. corals vs. seagrass; see Section 2.1).

Table 7 EPA (2021) Impact zonation scheme

Zone	EPA (2021) Description
Zone of Influence (ZoI)	The area within which changes in environmental quality associated with dredge plumes are predicted and anticipated during the dredging operations, but where these changes would not result in a detectible impact on benthic biota. This area can be very large, but at any point in time the dredge plume is likely to be restricted to a relatively small portion of the ZoI.
Zone of Moderate Impact (ZoMI)	The area within which predicted impacts on benthic organisms are sub-lethal, and/or the impacts are recoverable within a period of five years.
Zone of High Impact (ZoHI)	The area where serious damage to benthic communities is predicted or where impacts are considered irreversible. Serious damage is defined as damage that is irreversible or damage that is unlikely to be recovered for at least five years following the completion of dredging activities.

Table 8 EPA (2021) Appendix A guidelines to predict the impacts of dredging on corals

BCH category	Zone	Subcategory	Guideline description
Corals	ZOMI	Light Reduction (all corals)	Based on moving average of DLI exceeding a threshold value. Three separate averaging windows given for each of possible and probable effects, and exceedance of any of these constitutes an exceedance.
		Light Reduction and SSC combined (massive and foliose corals)	Based on moving average of both DLI and SSC exceeding a threshold value. Three separate averaging windows given for each of possible and probable effects. For a given averaging window, both the DLI and SSC thresholds must be exceeded simultaneously to be considered an exceedance. The exceedance of any averaging window constitutes an exceedance. **While no specific guidance is given, interpret SCC to mean nea rd SSC, as th threshold is based around depositio effects.*
	ZOHI	All corals	Based on moving average of DLI, SSC and Sediment Deposition exceeding a threshold value. Three separate averaging windows given for each of possible and probable effects. Unlike the guidance for the ZOMI, the guidance is not clear on whether these should be exceeded contemporaneously to be considered an exceedance, though for consistency with the ZOMI it is considered here that they are. The exceedance of any of the three averaging windows constitutes an exceedance.

			*While no specific guidance is given, we interpret SCC to mean near-bed SSC, as the threshold is based around deposition effects.

3.7. Guidance on dredge plume modelling for environmental impact assessment and source term estimation

In June of 2016, the Western Australian Marine Science Institute (WAMSI) provided an overview of various dredge plume modelling studies that had been conducted throughout Australia and set recommendations for standard practice for modelling such as clarity of model input parameters to be selected (Sun et al 2016).

In November of 2020, WAMSI published a guideline for dredge plume modelling for the purpose of environmental impact assessment (Sun et al 2020). This guideline emphasised the need for a standardised approach to estimate source terms for dredge plume modelling (in the absence of field datasets). WAMSI has encouraged the use of an approach set out by Becker et al. (2015) in estimating source terms, which has been adopted in this present study.

Source term estimation is particularly complex where soft rock (such as limestone) exists within the dredge layer, as mechanical disturbance may lead to generation of fine-grained material, and release of these fines into the marine environment. These processes are poorly understood yet require parameterisation in dredge modelling.

Mills and Kemps (2016) note that in-situ limestone dredged cutter suction (CSD) may produce particles in the range of very fine silts to small rocks. This review included a case study of CSD dredging of limestone within Western Australia in which water samples taken close to the cutter head during featured predominantly particles less than 40 µm in size. The exact PSD generated, however, is likely affected by material strength, excavation rate, as well as cutterhead geometry and power. Some of these factors are impossible to ascertain at the environmental impact assessment stage.

The fraction of sediment released into the marine environment as a plume, rather than taken up by the cutter head, may also increase for dredging of limestone compared to unconsolidated material. Empirically derived source terms from published literature provided in Sun et al. (2020) (originally sourced from Lorenz (1999)) list a band of 2% to 5% of total fines contributing to a far-field plume through use of a cutter suction dredger in a clay and sand mix. This band increases to 3% - 8% of total fines when the cutter suction dredger is used for dredging hard limestone.

4. Methods

This section outlines the model that has been adopted to simulate the dredge and disposal program previously presented in Section 2.2.4.

4.1. Hydrodynamic Model

The 3D far-field dredge plume model adopted solves the 3D incompressible Reynolds averaged Navier Stokes (RANS) equations, and transport equations for temperature and salinity. The RANS equations are closed using a 2-equation (k-epsilon) closure scheme for vertical fluxes, and a variable Smagorinsky scheme in the horizontal. Transport equations are closed by scaled eddy diffusivity. The equations are discretised in space using a cell-centred finite volume approximation, with an unstructured grid in the horizontal, and a structured sigma scheme in the vertical.

The discretisation of the RANS and transport equations was second-order accurate in space, and flux limiting schemes were used to reduce shocks. A second-order explicit time step was used for the horizontal terms and vertical convective terms, and a second-order implicit time step for the vertical diffusive terms. Pressure was baroclinic and hydrostatic, with density calculated by a non-linear equation of state.

Figure 17 below presents the numerical mesh generated for this project. The model domain is within the extent of larger scale Pilbara models run and validated previously by O2, and the setup and validation leverages on previous experience with these models. The open boundaries were forced with TPXO9 predicted tides and hindcast waves from ECMWF's ERA5. Surface stress was too derived from ECMWF's ERA5 hindcast winds. PPA survey data was used for bathymetry in port area, which covers most of Mermaid Sound and Mermaid Strait. This was supplemented by the Lebrec et al. (2021) satellite derived bathymetry product, which extends to around the 30 m (MSL) isobath. Beyond this we used the Geosciences Australia 250 m gridded bathymetry product (see Figure 18 for extents of these datasets). As the scope of this study involved the adaptation of an existing Pilbara coastal model, rather than creation of an entirely new model, a full model setup and validation is not presented here. More information on the model setup and some sample wave and current validation plots within the Dampier Archipelago are given in Appendix A.

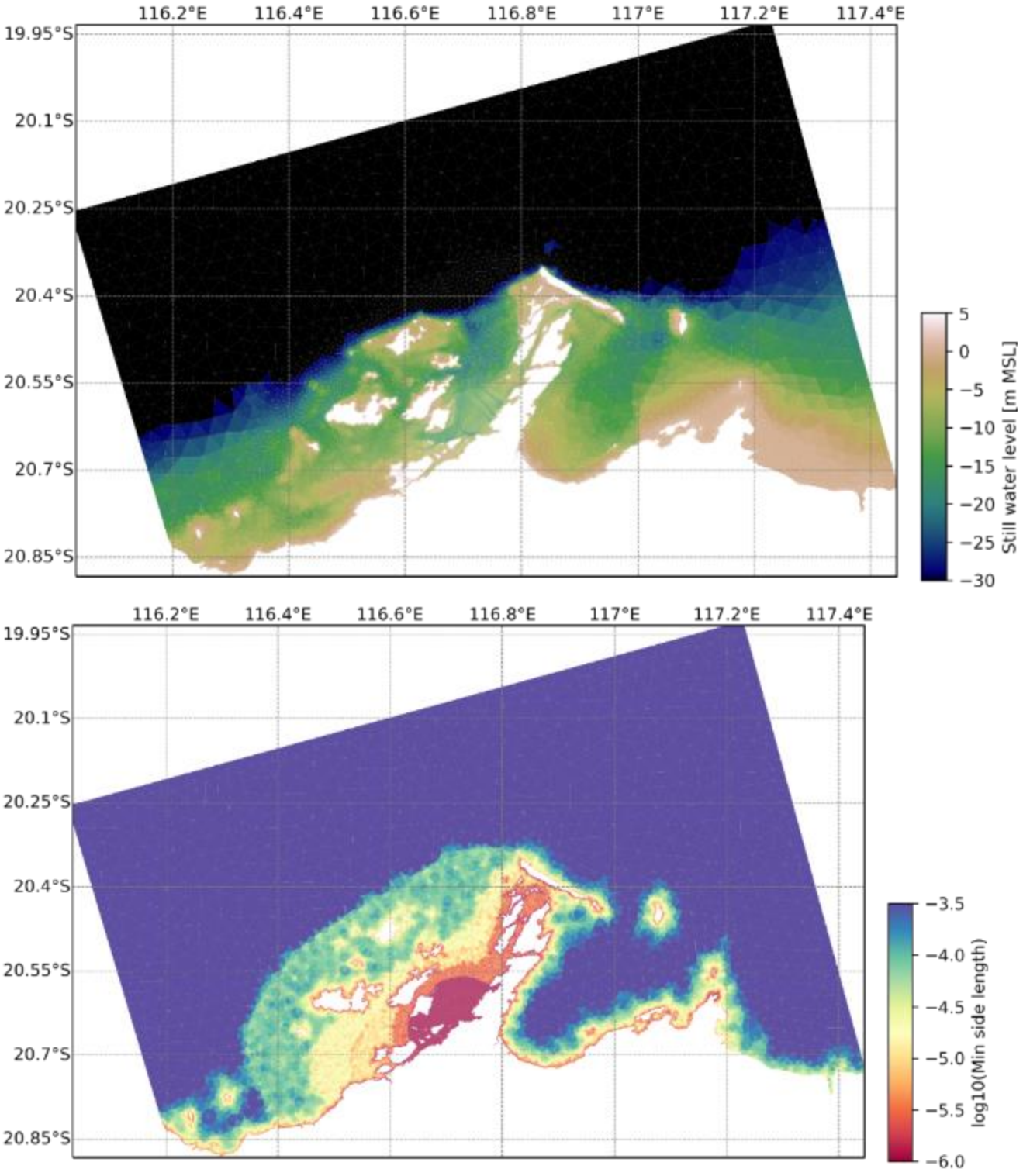

Figure 17 Numerical mesh and model domain. Cell shading in the top panel is the still water depth below mean sea-level with a depth cut-off at 30 m, and clearly shows the resolution of the dredge channels in Mermaid Sound Cell shading in the bottom panel shows indicates the cell size – specifically it shows the base 10 logarithm of the smallest side length in degrees.

Figure 18 High resolution bathymetry data sets against the model domain (pink box). The Lebrec et al. (2021) bathymetry is displayed in black and white shading, and the extent of the PPA aggregated survey dataset is shown in red. Bathymetry for the deeper areas of the domain were taken from the Geosciences Australia 250 m gridded product.

4.2. Sediment transport model

The dredge and disposal program was generated using a sediment transport model, which simulated the far-field plume associated with the proposed dredging. Direct near-field impacts are not assessment in this model. Thus, only far-field source terms are used as input into the model. Therefore, clay, silt and fine sand fractions are modelled (fractions < 125 µm) and it is assumed that all fractions larger than this will settle rapidly within the near-field plume and therefore need not be included in a model for environmental impact assessment.

Two key simplifications were made to the representation of sediments in the model. First, simplistic 'bulk' representation of the dredge material was applied owing to the lack of distinct and geological strata in the dredge material, and the unknown order of dredging. The characteristics of the single representative material were estimated by a weighted average of all the sub geological strata in the geotechnical analysis. Second, erosion of the seabed was excluded from the model, owing to the lack of appropriate validation data for the spatially variable erosion/deposition terms. Background SSC was thus not directly modelled. Rather the background values presented in Section 3.3 were added during post-processing and interpretation of potential environmental impact.

The numerical tool used was DHI's Mike 3 Mud Transport (MT) module (herein the sediment transport module). The sediment transport module handles multiple custom sediment fractions, specified in terms of a particle density, base (i.e. un-flocculated) settling velocity, cohesion characteristics, and critical stresses for erosion or

resuspension. The erosion law used a discrete depth of erosion model, with distinct bed layers of varying density, erosion coefficient, critical shear-stress and roughness. Dredging and dumping of material allows for time varying release of mass for each sediment fraction, at time varying locations (both horizontal and vertical). The model also includes an online near-field model which simulates the rapid fall of dredge spoil released at the sea-surface and associated small-scale processes such as stripping (where shear-driven turbulence erodes the descending gravity current, releasing sediments into the water column).

4.2.1. Simulated Dredge Scenarios

A total of six different scenarios are proposed in the program: two different dredging methods (Backactor and CSD) with three disposal locations. Table 9 lists parameters that were constant across all scenarios, and complements the inputs in Table 1. Table 10 details the parameters that varied between the 6 scenarios.

Table 9 Modelled parameters for the dredge and disposal program common to all scenarios.

Parameter	Value	Notes
Dredge Volume	206,000 m^3	In-situ volume of overburden (i.e. excluding granophyre rock) removed in the model. Note that this is greater than the amount presented in Table 1 due to contingency for dredging past target depth: ¶ An additional 1 m of dredge depth has been accounted for (where the bedrock layer is not reached). ¶ An additional 15% of this total has been included. Note also that the disposed volume is greater owing to expansion during material handling.
Timing of dredging	01/12/2020 – 09/03/2021	Selection of a typical (not extreme ENSO cycle) wet season.
Number of disposal events	294	Number of times a barge travels to the offshore location and disposes of dredged material. Volume of disposal is calculated from the dredge volume, accounts for losses due to spilled material, and bulking due to material handling. Conservatism is applied to account for dredging beyond target depth

Table 10 Scenarios modelled with disposal locations from Figure 3. The latitude and longitude given are the exact point locations of the modelled input.

Scenario	Dredge type	Disposal location / Spoil Ground
1	Backactor	ELI Spoil Ground (20° 36' 44.16" S; 116° 41' 01.39" E)
2		A/B (20° 31' 40.8" S; 116° 45' 3.6" E)
3		2B (20° 22' 58.48" S; 116° 42' 16.41" E)
4	CSD	ELI Spoil Ground (20° 36' 44.16" S; 116° 41' 01.39" E)
5		A/B (20° 31' 40.8" S; 116° 45' 3.6" E)
6		2B (20° 22' 58.48" S; 116° 42' 16.41" E)

4.2.2. Representation of dredge material

Given the large spatial scattering (horizontally as well as vertically) of the distinct layers within the modelled dredge material, the material was simplified into one representative material for each dredging method (one material for Backactor scenarios and another or CSD scenarios).

4.2.2.1. PSD

For Backactor scenarios, coastal limestone and beach deposits are assumed to be broken and lifted without the creation of fines. As such they do not contribute to the dredge source, but the mass is accounted for in disposal.

For CSD scenarios, however, the coastal limestone layer contributes to fines due to greater mechanical disturbance (the CSD is assumed grind the limestone into fine particle sizes). The beach deposits at this site were inadequately characterised to be treated in this level of detail. Instead, gravel and cobble material within the beach deposit geological stratum is assumed to be removed by CSD into the barge without the creation of fines.

As discussed in section 3.7, determination of the particle size of crumbled limestone from a CSD is currently not well understood. As there appears to be a large variation in possible particle size from fine silts to small rocks, the limestone is assumed to be ground into a PSD between silt and coarse sand, with a normal distribution with the mean coinciding with the middle of the fine sand fraction and standard deviation such that one third of the mass falls within this fraction. In reality, very large cobbles may not be removed by the CSD and instead will need to be removed during the blast and removal process, and so the approach here is likely conservative.

An average PSD was calculated for each dredge method (Backactor and CSD), where the PSDs of each geological stratum within the scenarios dredge spill were weighted based on their volumetric percentage within the overburden material. These are presented in Table 11.

Table 11 PSD of representative material for scenarios. Note that this assumes that the swilt has been ground in-situ

Geological Stratum	% Clay (< 2µm)	% Silt (2 µm-75µm)	% Fine Sand (75µm-150 µm)	% Coarse Sand (150µm-2.36 mm)	% Gravel (> 2.36mm)
Backactor (scenario 1 to 3): Weighted Average Material	5.8	35.2	12.5	25.8	20.7
CSD (scenario 4 to 6): Weighted Average Material	4.1	34.7	18.4	27.9	14.8

4.2.2.2. Representative dry bulk density

The mass flux (in kg/h) of dredge material was estimated as the product of the volumetric dredge rate (in m^3/h) and a dry bulk density (kg/m^3). GHD (2020) present dry densities for some samples of coastal limestone, beach deposits the bedrock layers, but none for marine sediments and calcareous gravel. The dry bulk density ($\rho_{dry,mix}$) of the marine sediment and calcareous gravel materials were therefore estimated by van Rijn and Barth (2018). In the absence of organic material, $\rho_{dry,mix}$ is estimated by:

$$\rho_{dry,mix} = \frac{p_{clay}\,\rho_{dry,clay}}{100} + \frac{p_{silt}\,\rho_{dry,silt}}{100} + \frac{p_{sand}\,\rho_{dry,sand}}{100}$$

Here p_{clay}, p_{silt}, p_{sand} are the percentages of clay, silt, and sand based on the particle size distribution of each geological stratum as presented previously in Table 5. Note that in this definition, sand is defined as any material with a particle size greater than the upper limit of silt.

The representative dry density for Backactor dredging was calculated using a weighted average whereby the percentage of each geological stratum that contributes as material for that scenario has been used as the weights. A different dry density was used for CSD to account for mechanical generation of fines. Note that to conserve mass, a greater *effective unconsolidated total volume* must be used for CSD also, which accounts for the volumetric expansion of the limestone layer as it is mechanically altered.

These representative dry densities for each scenario are shown in the last two rows of Table 12.

Table 12 Dry density of model dredge material

Geological Statum	Dry density, $\rho_{dry,mix}$ (kg/m³)
Backactor (Scenarios 1 to 3): Representative Material	1249
CSD (Scenarios 4 to 6): Representative Material	1273

4.2.3. Sediment budget and spill sources

As per Becker et al (2015), a sediment mass budget is required for each sediment fraction at each process stage (i.e. digging, lifting, barge filling, barge overflow, barge transit, barge dumping). The mass of each fraction is generally conserved, except for mechanical fines generation. This section details this modelled sediment

budget, including the proportion of total spill that is assumed to contribute to the far-field (as per Section 4 only the far-field contribution is modelled in this study).

For both Backactor and CSD there are three distinct spill sources. The key assumptions of each source term are noted below and have been made in line with the WAMSI guidelines for source term estimation (Sun et al, 2020 and Becker et al, 2015.

1. Dredging spill: Spill of fine sands, silt and clay, where the nature of this spill is dependent on the dredging equipment used:
    - Backactor dredger: A 4% loss of material from the bucket of the Backactor as it passes through the water volume. This spill is distributed evenly between the top and bottom layer.
    - CSD: For dredging through marine sediment and calcareous gravel, a 5% loss of material from the cutter head at the seabed has been applied. This loss was increased to 8% within the bottom layer when cutting through coastal limestone (see discussion in section 3.7). This results in a weighted average spill percentage of 5.82% applied throughout the simulation using the percentage of each geological stratum within the overburden material (from Table 3) as the weights.
2. Hopper barge overflow: Spill of silt and clay only through overflow.
    - CSD Scenario: Whilst being loaded, the barge overflows for 80% of the time (mainly water and fine sediments). During the time at which the barge is overflowing, 75% of all silt and clay that is added to the barge is said to overflow out of the barge, resulting in a total of 60% of silt and clay overflowing during dredging operations. Of this spill, 85% is assumed to settle quickly in a dynamic plume near the dredge site and the remaining 15% remains suspended and contributes to the far field plume.
    - Backactor Scenario: Whilst being loaded, the barge overflows for 20% of the time (placement of material and not a watered-down slurry). During the time at which the barge is overflowing, 10% of clay and silt is assumed to leave the barge. Resulting in a total of 2% of silt and clay overflowing out of the barge during the dredge program. All overflowing silt and clay is assumed to contribute to the far-field plume
    - It is assumed that silt and clay that settles near the dredge site in a near-field plume (not contributing to the plume), does so outside the dredge footprint and hence it is not re-dredged.
    - All fine sand and other coarse sediments are transported to the disposal ground without any overflow.
    - Overflow contributing to the far-field plume occurs at the water surface.
3. Offshore disposal of silt, clay and fine sand, with the assumed loss of all fractions reduced from the previous spill actions.
    - The disposal plume is assumed to descend to the seabed in the near-field plume disposal before becoming passive at the bottom cell of the model. The spill of fines at the bottom cell differs for each dredging method. This difference in far-field contribution is due to the hydraulic disposal in CSD operation, where the disposal material has a high water-content, compared to mechanical disposal for Backactor.
    - Backactor Disposal: The far field disposal plume is to start in the bottom cell at the disposal location, where 5% of all fine sand sand, silt and clay that was disposed of is assumed to be suspended in this cell (Becker et al, 2015).
    - CSD Disposal: The far field disposal plume is to start in the bottom cell at the disposal location, where 10% of all fine sand sand, silt and clay that was disposed of is assumed to be suspended in this cell (Becker et al, 2015).
    - It is assumed that there is negligible loss of sediment within the water column during the near-field disposal phase.

Sediment budgets for the Backactor and CSD scenarios derived from these assumptions are presented graphically in Figure 19 and Figure 20, respectively. In these figures V_{total} is the volume of all geological layers

that contribute to fines within the dredge volume, $f_{fraction}$ is the percentage of that fraction by mass and ρ_b is the representative bulk density of the insitu material.

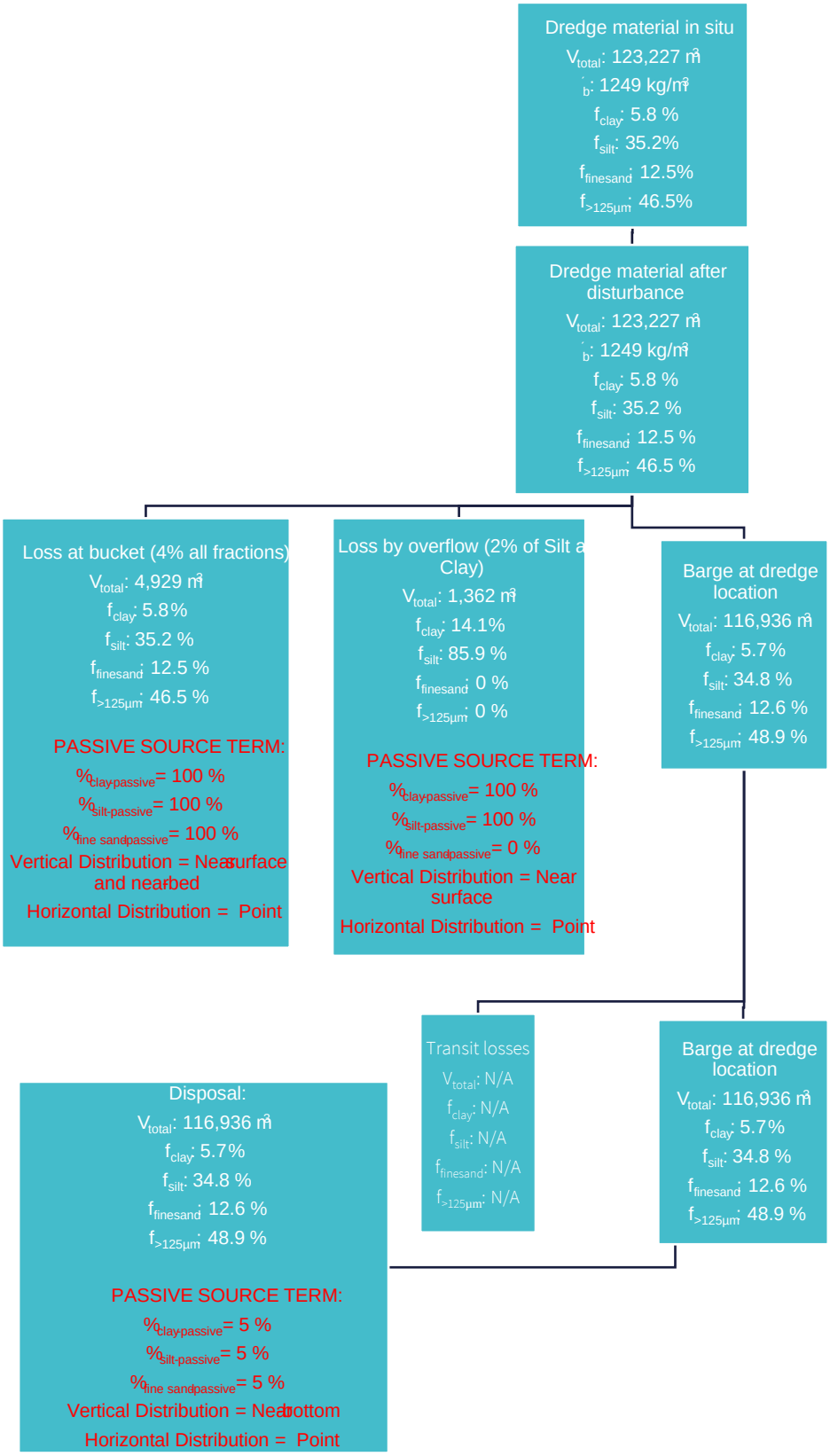

Figure 19 Sediment mass budget for the Backactor scenarios (1, 2 and 3). The passive source terms (red text) are the inputs into the far-field model.

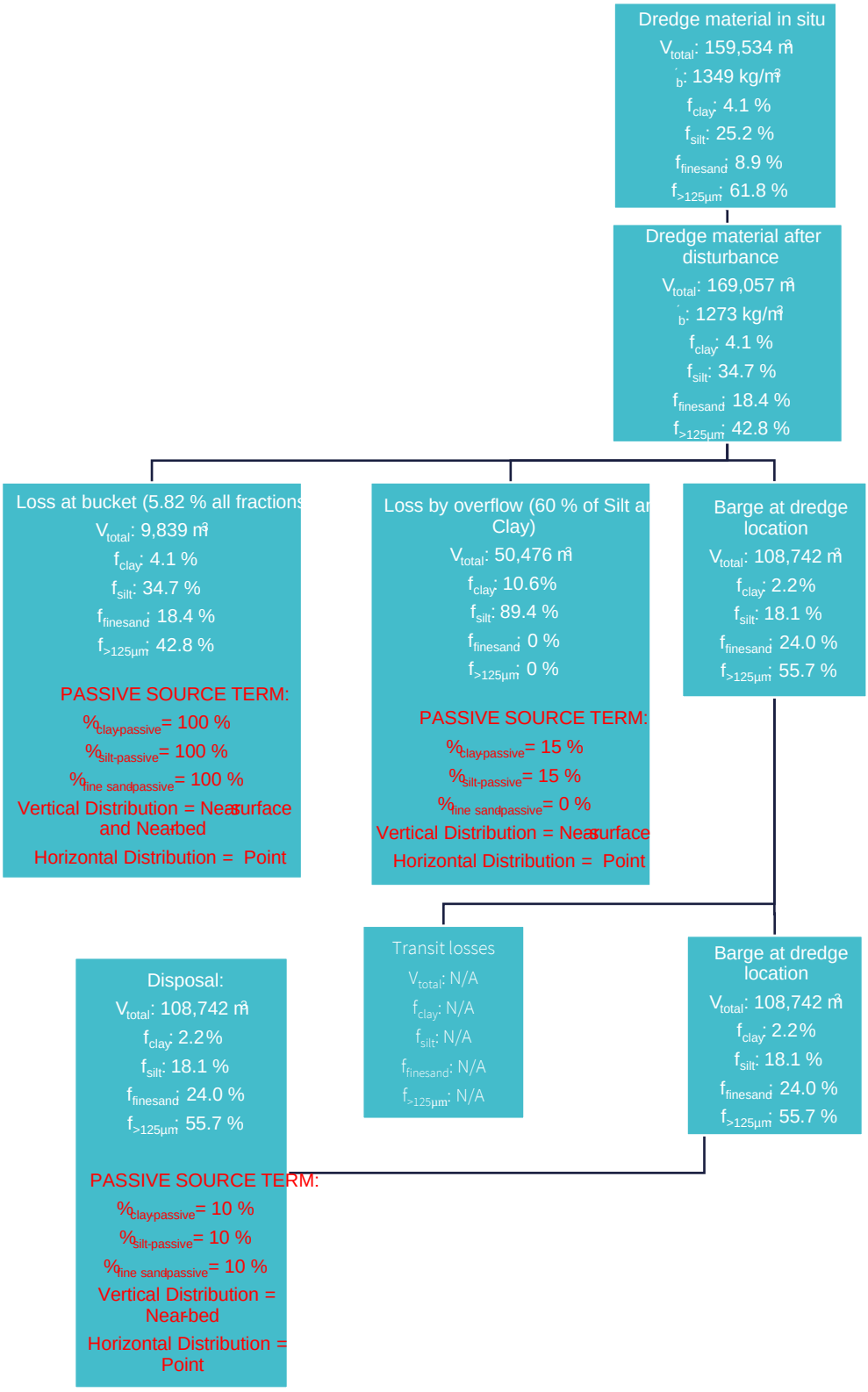

Figure 20 Sediment mass budget for the cutter suction dredger scenarios (4, 5 and 6). The passive source terms (red text) are the inputs into the far-field model.

4.2.4. Settling Velocity

Settling velocities of each sediment fraction was estimated using Stokes' law (Sun et al 2016; DHI 2021b), and are given in Table 13.

Table 13 Settling velocities

Sediment fraction	Settling velocity (m/s)
Gravel	0.210741
Coarse sand	0.153678
Fine sand	0.009350
Silt	0.001281
Clay	0.000004

4.3. Impact Assessment

As described in Section 3.6 , environmental impact was inferred using the EPA (2021) framework. We calculated the extent of the zone of influence (ZoI) by including any region where SSC (at any height in the water column) exceeded background by 5mg/L at any time. This is a highly conservative threshold in which the plume would not likely be visually discernible, where detectible impacts to stable benthic habitat would be highly improbable, and where change with respect to background could be observed in the field with appropriately selected control sites.

Prior to evaluation of EPA (2021) guideline values for SSC and DLI, the modelled SSC was adjusted to account for background levels (see Section 3.3). A conservative implementation of background was applied, with the nearshore background SSC being applied to the entire model domain. As previously mentioned, a factor of 1.5 was applied to the EPA (2021) thresholds (discussed in Section 3.6.2) (i.e., SSC thresholds multiplied by a factor of 1.5, DLI thresholds reduced by a factor of 1.5). For more on this multiplication factor, please refer to Section 3.3 and the references therein.

We also note that there is separate guidance for ZoMI estimation depending on the coral morphology and its inherent ability to clear low amounts of deposited sediment (

Table 8). Here we calculated and present spatial zones according to both methods seperately.

Note that in calculating the ZoMI and ZoHI using combined DLI and SSC thresholds, the deposition constraint to the thresholds was removed. This conservatively assumes that the deposition threshold is breached for all timesteps, and that only DLI and SSC in combination is further required to trigger a ZoMI or ZoHI.

4.3.1. Application of DLI relationship

Following O2 Marine (2022a) and Section 3.5, we used the relationship:

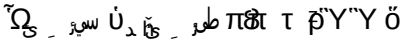

To estimate light attenuation across the PAR band. For depths under 5 m we used Ủ ͘د ኾ ͟ سيز πቒ ά ٩ ๐, as suggested by the local data of MScience (2019) (see Section 3.5). Below 5 m we used Ủ ͘د ኾ ͟ سيز πᏯτ ς ράς٩ ๐ in a rather crude account for loss of long wavelength energy with depth. This piecewise model is a relatively crude compared to a wavelength-dependent attenuation relation, and we return to this point in Section 6.3.

The light attenuation calculation accounted for three-dimensional variation in SSC. DLI was calculated across the model domain and simulation with consideration of:

- Spatially and temporally variable solar elevation;
- Reflection of light at the sea surface;
- Refraction of light at the sea surface;
- Spatially and temporally variable total water depth and mean path length of solar radiation, and;
- Vertically variable SSC and light attenuation coefficient (see Section 3.5);

A 3D approach was taken where light attenuation was calculated separately for each of the 10 model layers. In an attempt to account for the effects of clouds and surface waves, the subsurface PAR was reduced by 15%. It is very difficult to determine this factor robustly, and this is an element of uncertainty in the model. A constant reduction of 15% over the entire simulation is considered a conservative assumption.

Note that the calculation of the zones of moderate impact using the DLI alone thresholds was restricted within the Dampier Archipelago and were not applied offshore. There is no substantial coral habitat in the depths found in the excluded area (Section 3.3).

5. Results

This section presents the results of suspended sediment fate in each dredge and disposal scenario. The interpretation of the model results for the purposes of environmental impact assessment is left for the discussion (Section 6). Sections 5.1 describes the alongshore fate of the dredge plume only, which was much larger than any disposal plume. For this reason, these sections do not contrast the results of the different disposal sites, focus rather on only 2 simulations - Backactor and CSD dredging for disposal at ELI Spoil Ground.

Section 5.2 provides contrast between the disposal scenarios for ELI Spoil Ground and Spoil Ground A/B. The same comparison was not made for Spoil Ground 2B, as the model was quite coarse in this location, and thus the disposal plume was not equally well resolved. Results for Spoil Ground 2B are described in Section 5.3 for completeness.

5.1. Qualitative description of dredge plume trajectory

Snapshots of SSC in the Backactor plume during periods of southwest and northeast coastal drift are presented in Figure 21. Snapshots of the CSD plume are presented in Figure 22 for the same points in time. Similar plume spatial behaviour is observed between the two dredging methods – the northeast plume remains attached to the coast at all times, while the southwest plume detaches from the coast as plume flows into King Bay and towards the Intercourse Islands.

Despite the similar shape, concentrations in the CSD plume are appreciably larger than the Backactor plume. This was expected given the greater quantity of fines due to mechanical disturbance of limestone, and significantly larger overflow of fines.

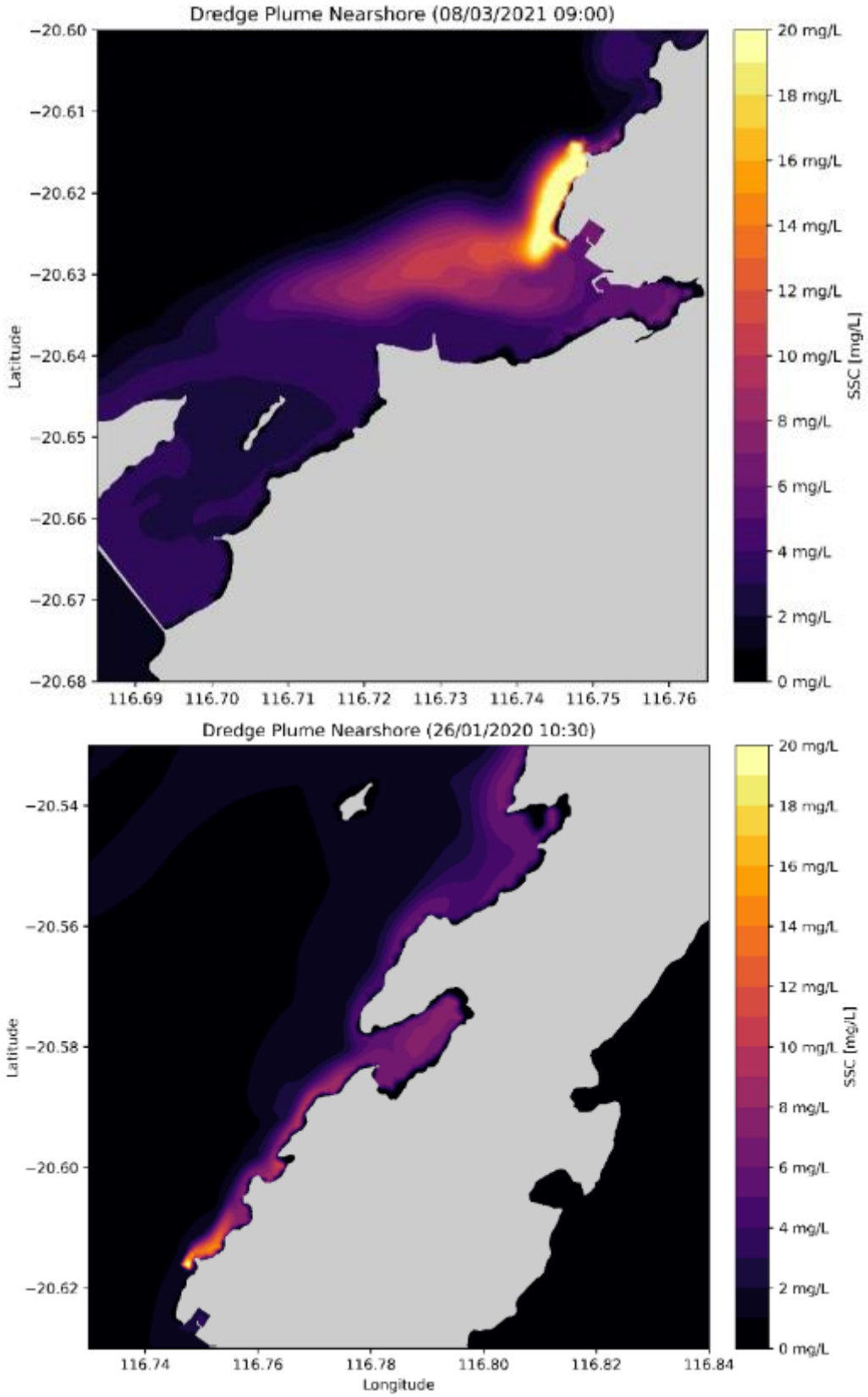

Figure 21 Scenarios 1 to 3: Backactor and barge overflow plume with example of a south westerly (top image) and a north-easterly (bottom image) plume drift (Note: The figure has been developed by extracting the maximum total SSC within all vertical cells for a given location)

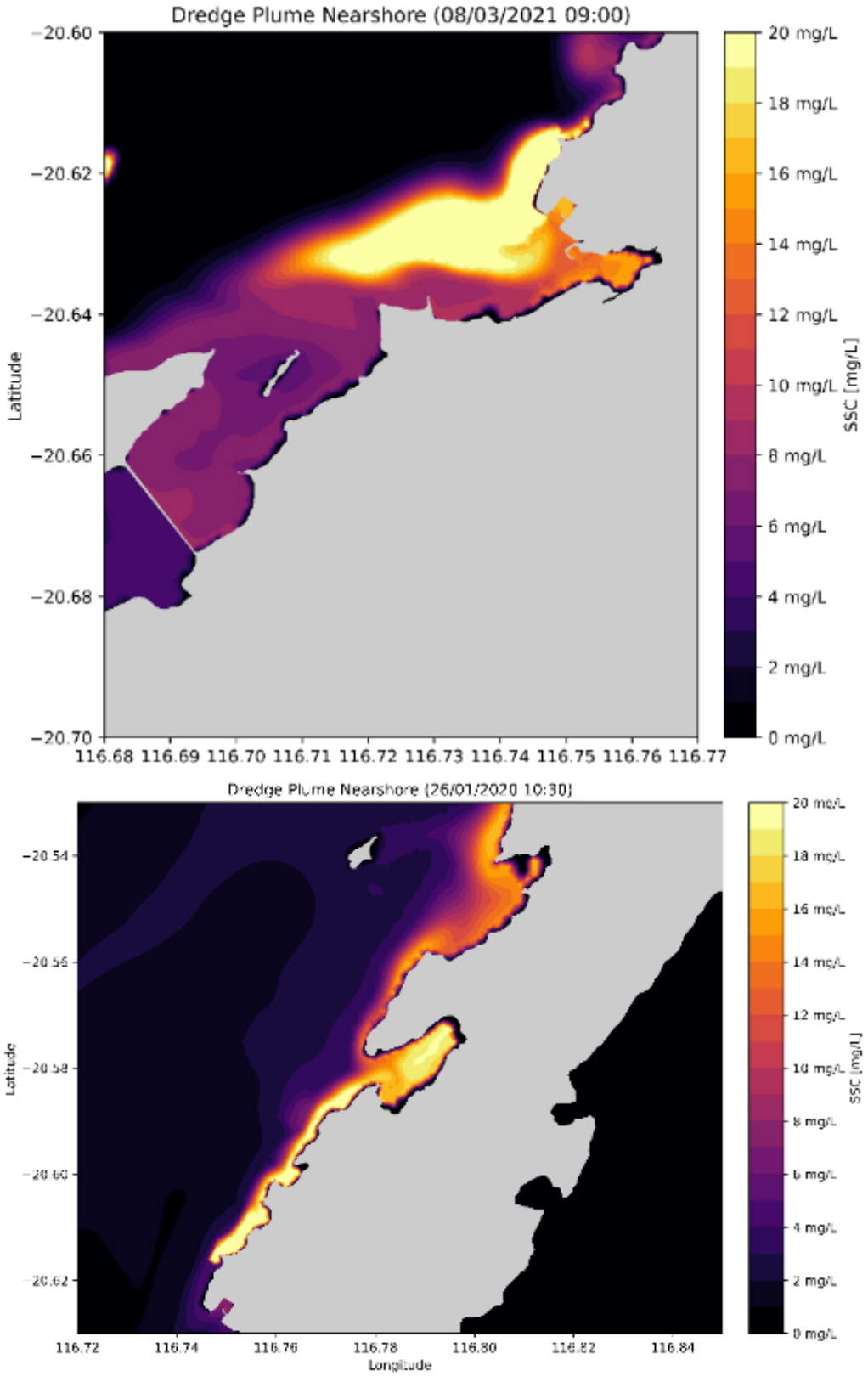

Figure 22 Scenarios 4 to 6: CSD and barge overflow plume with example of a south-westerly (top image) and a north-easterly (bottom image) plume drift (Note: The figure has been developed by extracting the maximum total SSC within all vertical cells for a given location)

To describe the time history of alongshore drift over the entire simulation period, we defined a non-dimensional quantity ***PI*** that describes the relative SSC to the northeast and southwest of the DCW. We did this by comparing total SSC integrated over control volumes (CV) spaced equally eastward and westward of the DCW. Two pairs of CVs were compared - one set approximately one kilometre northeast and southwest of the dredge location (along the coastline), and the second set approximately two-kilometre distances from the dredge location (Figure 23). The integrated SSC was averaged over the total volume of the CV. The analysis is affected somewhat by variable depth between CVs in each set, but nonetheless provides a meaningful quantification of plume trajectory.

We then defined a plume index (***PI***) for each set of CVs:

$$PI = \frac{C_{NE} - C_{SW}}{C_{max}}$$

Here C_{max} represents the maximum CV averaged SSC recorded in either CV over the full simulation. At any time (t) this index, which is bound between +1 and -1, indicates whether the plume is directed towards the northeast ($PI>0$), southwest ($PI<0$), or is in a neutral position ($PI \sim 0$).

PI for the Backactor plume is presented in Figure 24 for each set of CVs (one-kilometre and two-kilometre distances from the dredge footprint) alongside the wind direction. The timeseries of ***PI*** has a strong semidiurnal (tidal) oscillation, over a lower frequency oscillation that qualitatively correlated to the wind direction. Naturally there is a lag between changes in wind direction and changes in ***PI***, which reflects the response time of the tidal currents to changes in wind stress. The low frequency (wind driven) component of ***PI*** is similar for the 1 km CVs (Figure 24a) and the 2 km CVs (Figure 24b), though the semidiurnal response of the 2 km CVs is notably weaker. This is due to a weaker SSC gradient farther from site, which reduces the effect of tidal transport. Also of note is that for the 2 km CVs is, the magnitude of positive ***PI*** values is consistently greater than the magnitude of the negative ***PI*** values.

PI for the CSD plume is presented in Figure 25 for each set of CVs. Despite the higher overall sediment concentrations in the CSD plume (Section 5.1), the results of Figure 24 and Figure 25 are very similar, owing to the normalisation procedure.

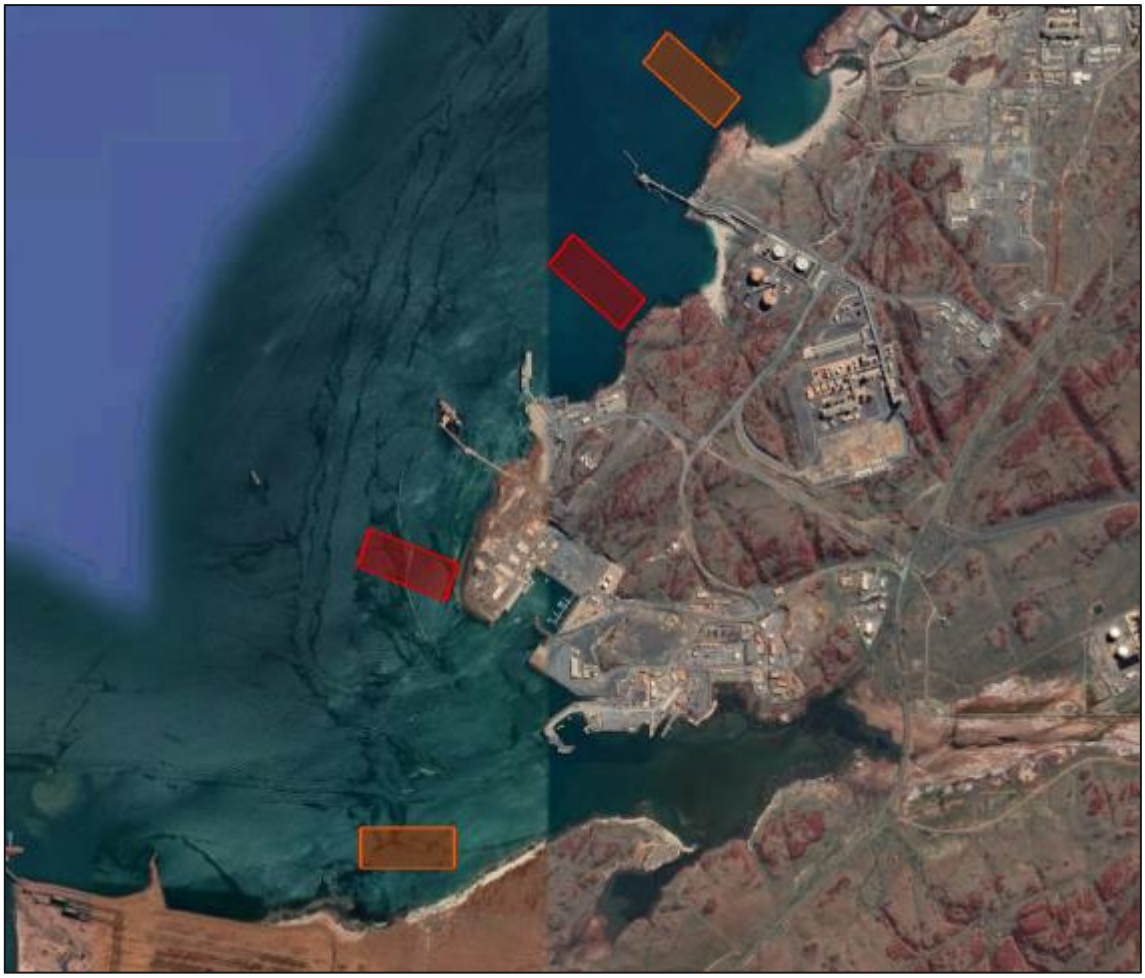

Figure 23 Location of control volumes used to quantify the alongshore plume fate through the index *PI*

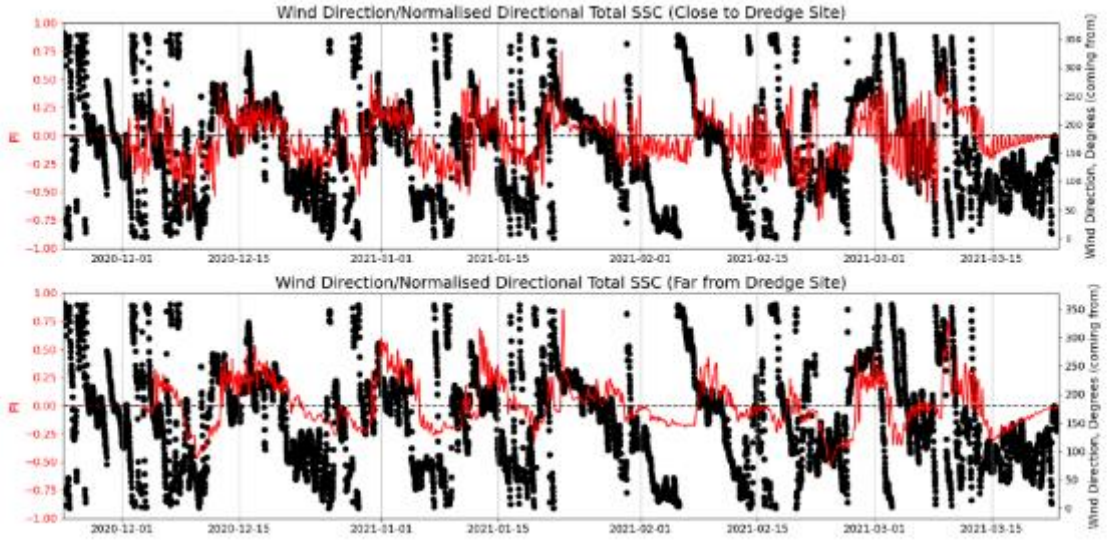

Figure 24 Plume trajectory index (*PI*) for Backactor simulations (red line, right-hand y-axis). *PI* indicates whether the plume is directed towards the northeast (*PI>0*), southwest (*PI<0*), or is in a neutral position (*PI~0*). The wind direction (black dots) is shown on the right-hand y-axis.

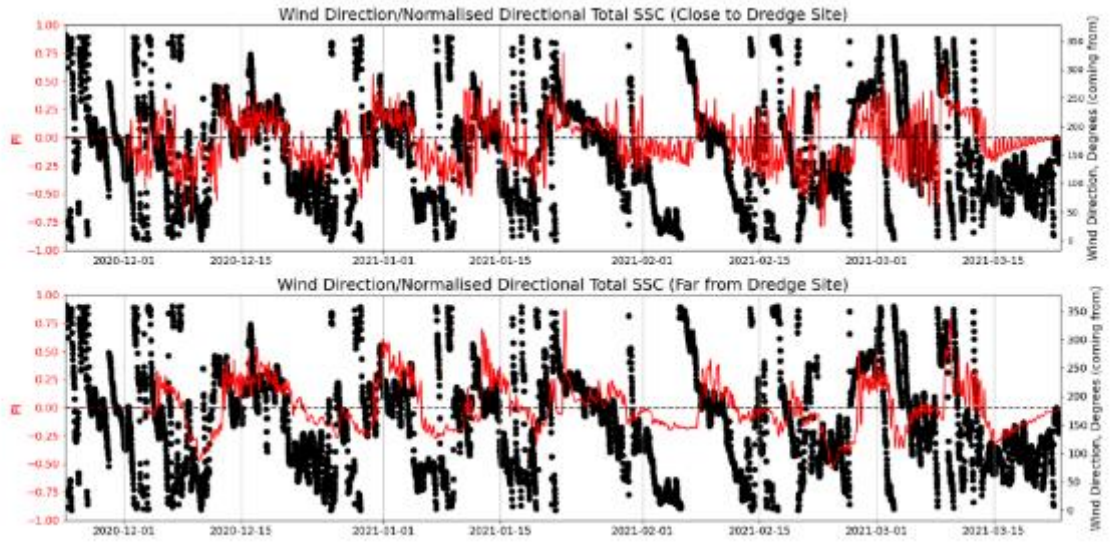

Figure 25 As per Figure 24 but for CSD simulations.

5.2. Dredging and disposal at ELI Spoil Ground vs. Spoil Ground A/B

The contours were presented in this section were generated by first calculating the 99th, 95th and 90th percentile SSC for each model element, and then taking the vertical maximum. Based on these percentage exceedance contours, the spatial extent of the ELI Spoil Ground disposal plume was far greater than the A/B disposal for both Backactor (Figure 26 vs. Figure 27) and CSD (Figure 28 vs. Figure 29) simulations. For Backactor there was little interaction between the dredge and disposal plumes, evident by the very similar plume dredge plume extent between the two scenarios (Figure 26 vs. Figure 27). Disposal plumes were much larger for CSD owing to (1) the larger total quantity of fines due to mechanical disturbance of the limestone, and (2) greater spill rate at disposal due to the different handling methods (hydraulic vs. mechanical dredging). For CSD disposal at A/B the interaction between dredge and disposal plumes was more pronounced. While the contours at the disposal were still confined to a very small spatial extent, the contours at the disposal site were slightly larger for A/B disposal compared to ELI Spoil Ground disposal, as site A/B is on the same side of Mermaid Sound as the DCW.

We note that the difference between 99th percentile exceedance contours for ELI Spoil Ground and A/B disposal may be influenced to some degree by the slightly larger horizontal grid resolution and vertical layer thickness at A/B compared to ELI Spoil Ground, however this extra initial dilution and is commensurate with the additional dilution expected for the descending and collapsing phases of the dynamic disposal plume in the deeper waters of the A/B site. Further, the impact of this initial dilution on the impact assessment of Section 6 is expected to be minor.

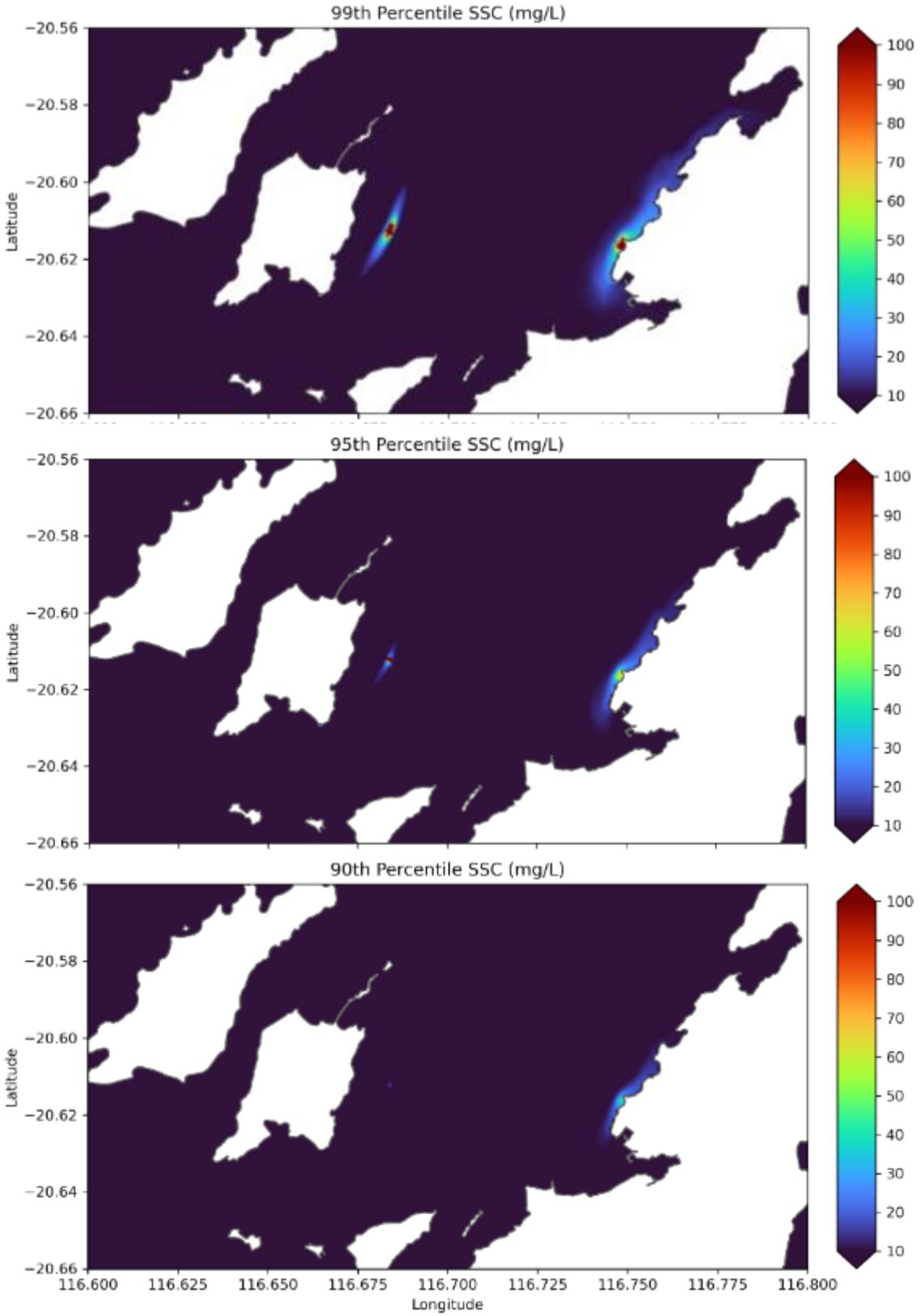

Figure 26 SSC percentile plots percentile for Scenario 1 - Backactor, hopper barge overflow and East Lewis Island Disposal (Note: The figure presents above background SSC, whereby the maximum total SSC within all vertical cells is presented). Top, middle and bottom panels are the 99th, 95th and 90th percentiles, respectively. The contours in these maps cover a much larger area than the plume at any single point in time.

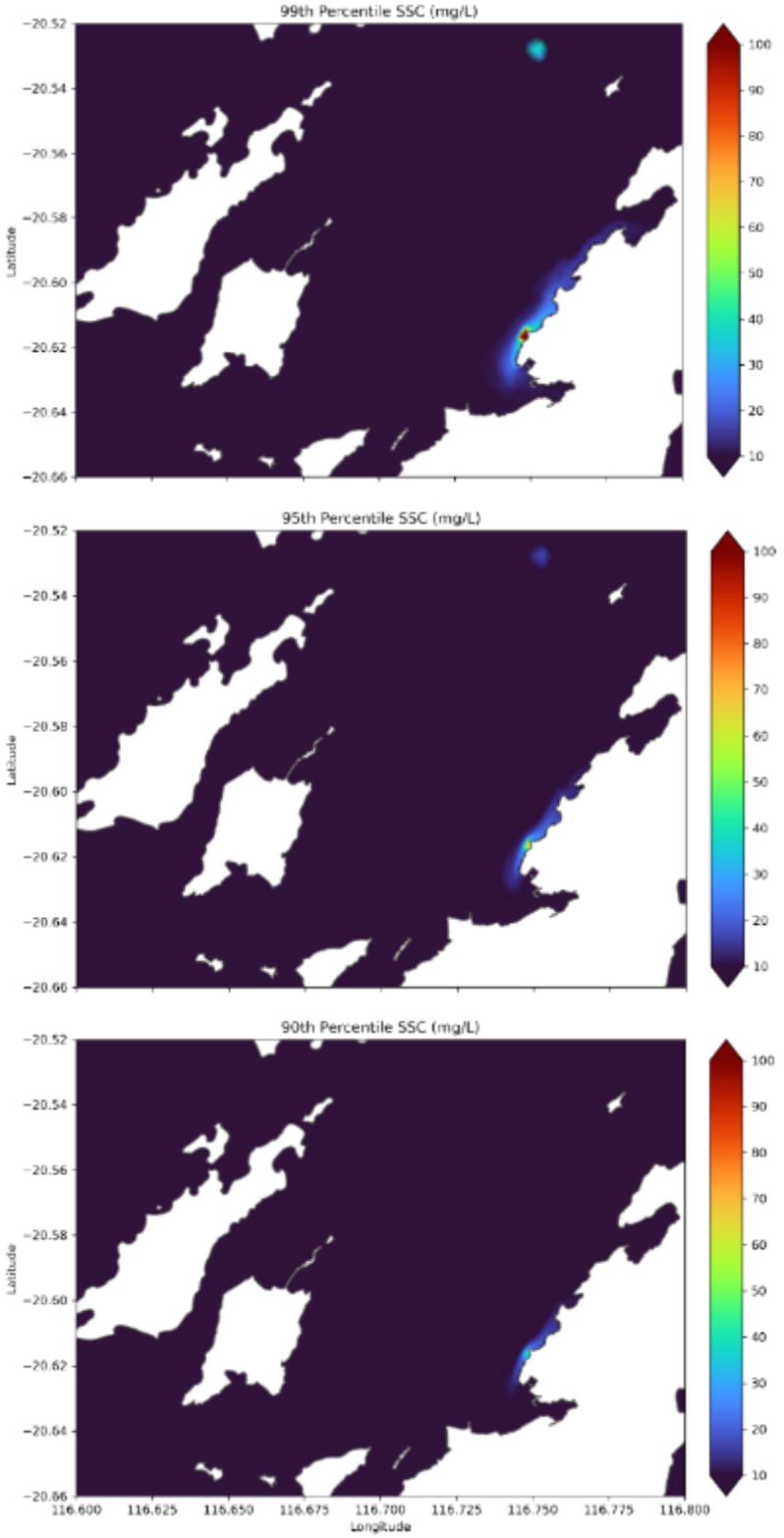

Figure 27 SSC percentile plots percentile for Scenario 2 - Backactor, hopper barge overflow and A/B Disposal (Note: The figure presents above background SSC, whereby the maximum total SSC within all vertical cells is presented). Top, middle and bottom panels are the 99th, 95th and 90th percentiles, respectively. The contours in these maps cover a much larger area than the plume at any single point in time.

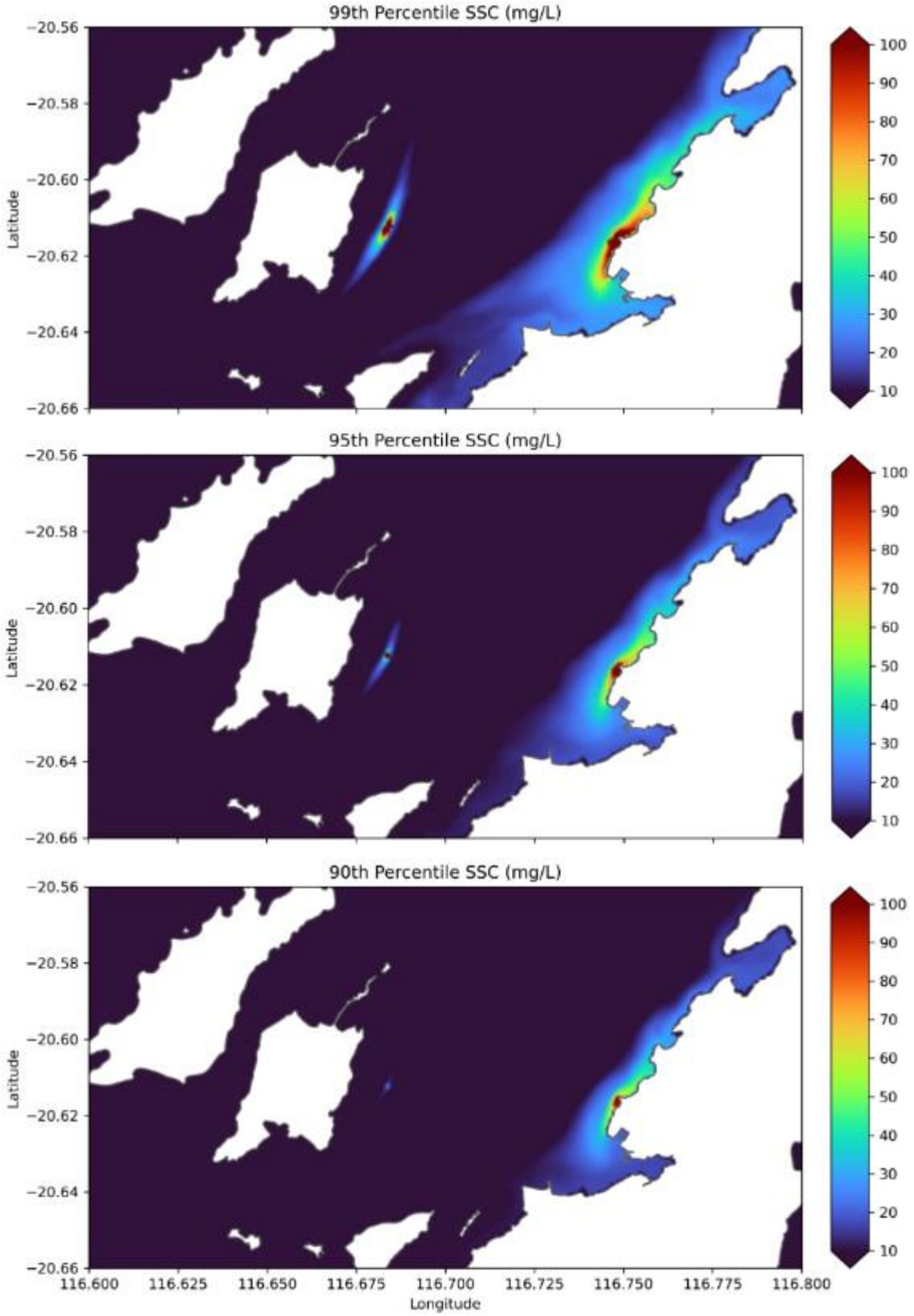

Figure 28 SSC percentile plots percentile for Scenario 4 - CSD, hopper barge overflow and East Lewis Island Disposal (Note: The figure presents above background SSC, whereby the maximum total SSC within all vertical cells is presented). Top, middle and bottom panels are the 99th, 95th and 90th percentiles, respectively. The contours in these maps cover a much larger area than the plume at any single point in time.

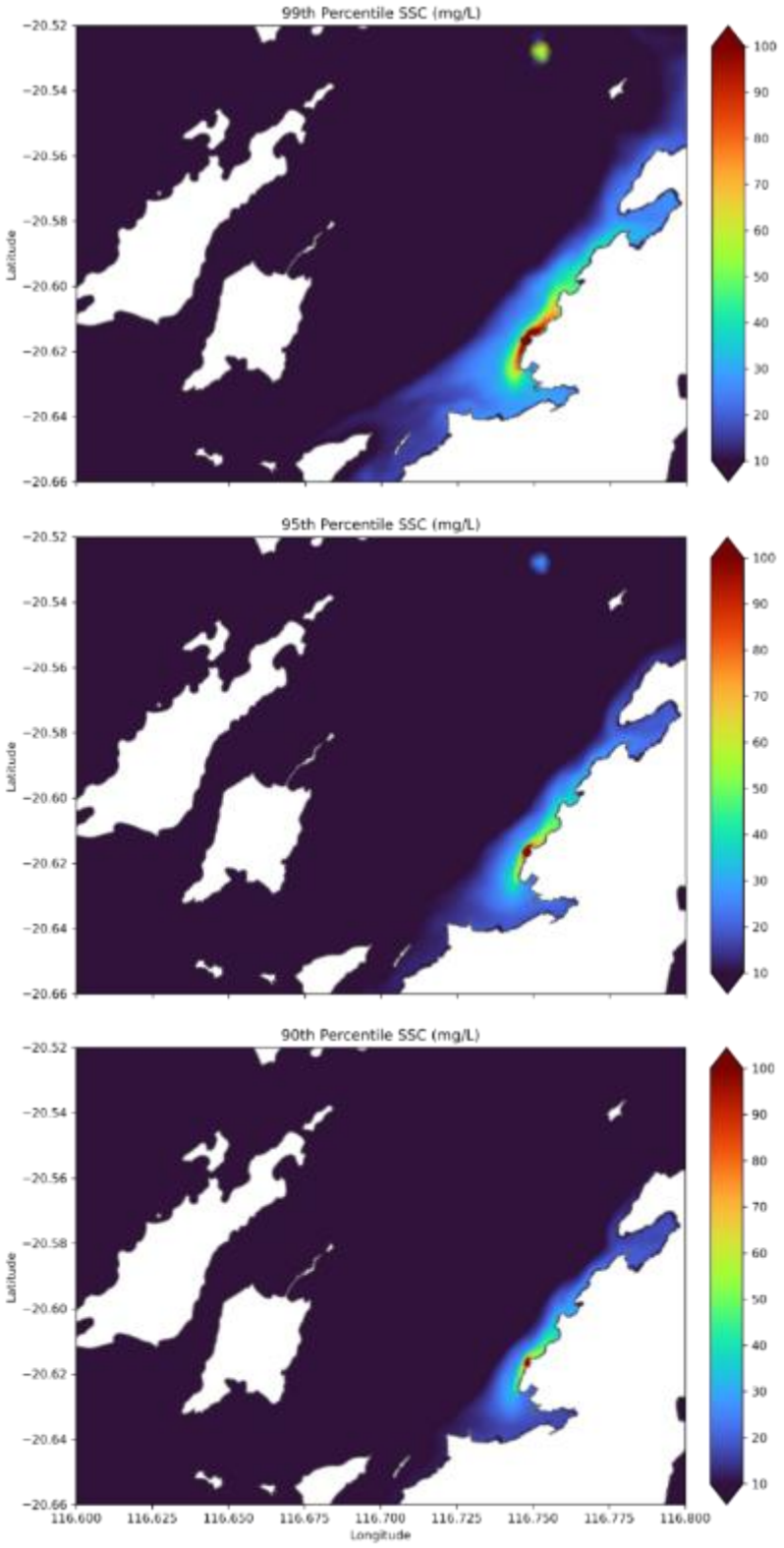

Figure 29 SSC percentile plots percentile for Scenario 5 - CSD, hopper barge overflow and A/B Disposal (Note: The figure presents above background SSC, whereby the maximum total SSC within all vertical cells is presented). Top, middle and bottom panels are the 99th, 95th and 90th percentiles, respectively. The contours in these maps cover a much larger area than the plume at any single point in time.

5.3. Coarsely resolved outputs at Spoil Ground 2B

Disposal of dredged material at Spoil Ground 2B was conducted in scenarios 3 and 6 (Table 10). The model at this site was much less resolved than at the dredge location or either of the other spoil grounds, however. The reason for this was that much greater modelling effort (order 10 to 20 times the cost) would be required to simulate the 2B location to the same level of accuracy owing to its much greater depth. As this location was considered an unlikely location, this additional effort was considered an unnecessary cost, and could not be justified on project timelines. Despite the unlikely use of this spoil ground and reduced model resolution, the disposal at this location was still simulated, processed, and assessed for environmental impact in the same manner as the other spoil grounds. These results give an indication of scale of the impact at this disposal site compared to the other sites.

Spatial maps of the 99th, 95th and 90th percentile in time SSC for Backactor and CSD (scenarios 3 and 6) are presented in Figure 30 and Figure 31. These maps have been created in the same manner described in Section 5.2, with the following two changes:

- The colour scale has been reduced to a maximum of 2 mg/l (previous maps in Section 5.2 show a maximum of 100 mg/l); and
- No contouring has been conducted and rather the percentile results for each element are displayed (as emphasised by the inclusion of the mesh).

For both Backactor and CSD scenarios, the modelled SSC at the 2B disposal location was very low in comparison to the other two disposal grounds (ELI Spoil Ground and A/B).

The change in colour scale (compared to maps in Section 5.2), emphasises the lower concentrations observed at 2B disposal. Unlike disposal at ELI Spoil Ground and A/B, the concentrations at 2B are within a similar magnitude to the dredge related concentrations that reach the end of Mermaid Sound.

Disposal at 2B differ in magnitude between Backactor and CSD scenarios, with CSD providing higher concentrations and covering a larger area than what was observed in the Backactor scenarios.

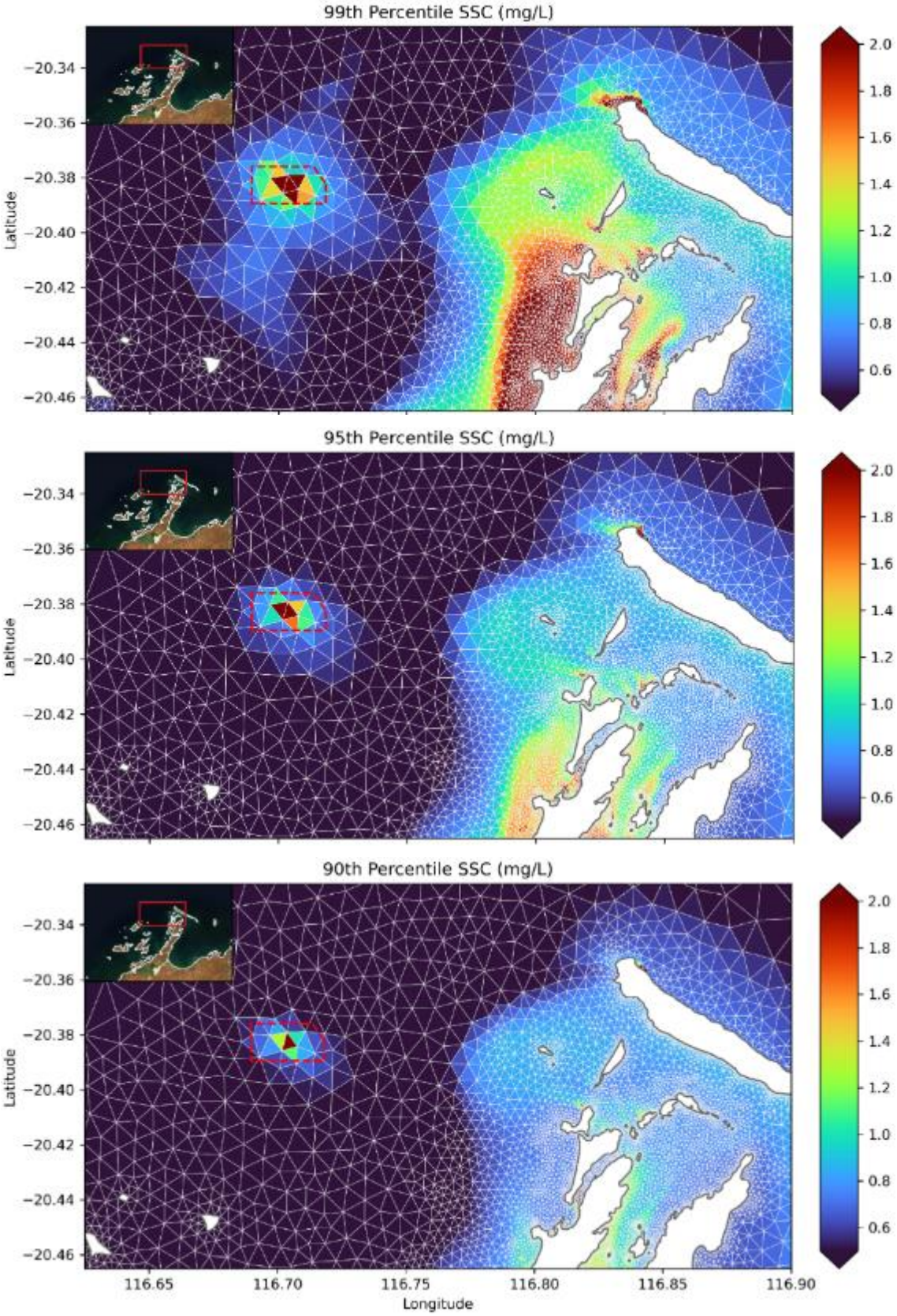

Figure 30 SSC percentile plots for Scenario 3 - Backactor, hopper barge overflow and 2B disposal (Note: The figure presents above background SSC, whereby the maximum total SSC within all vertical cells is presented). Top, middle and bottom panels are the 99th, 95th and 90th percentiles, respectively.

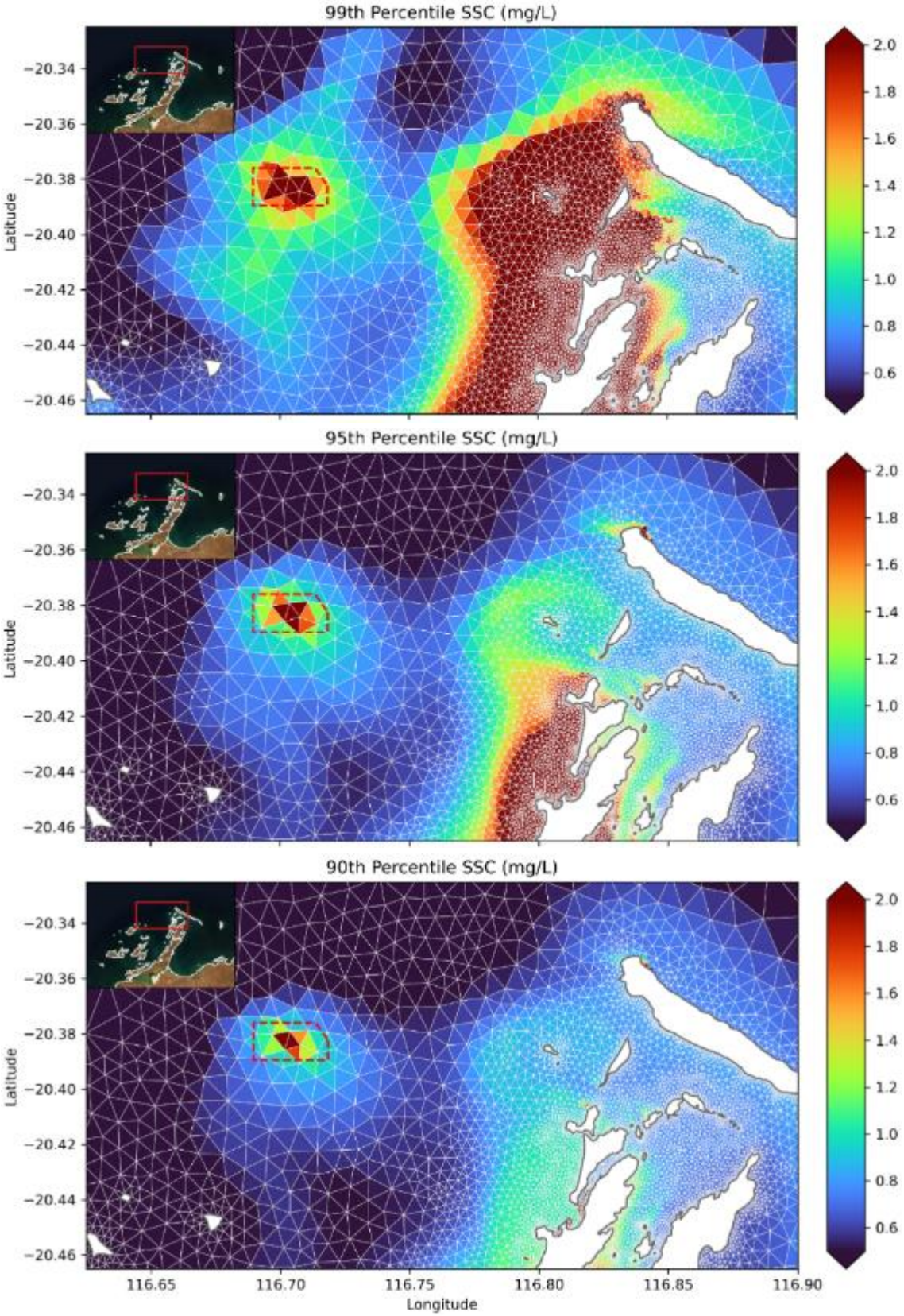

Figure 31 SSC percentile plots for Scenario 6 - CSD, hopper barge overflow and 2B disposal (Note: The figure presents above background SSC, whereby the maximum total SSC within all vertical cells is presented). Top, middle and bottom panels are the 99th, 95th and 90th percentiles, respectively.

6. Discussion: environmental impact assessment

6.1. Zone of Influence

The ZoI has been calculated for each scenario using the assessment method defined in Section 4.3. For Backactor scenarios (1, 2 and 3), these zones have been overlaid to create one ***all-inclusive*** ZoI of Backactor operations (i.e. all three disposal sites included Figure 32). This process was repeated for CSD scenarios (4, 5 and 6; see Figure 33). Due to the coarseness of the grid in the vicinity of the 2B disposal site, the ZoI here may be slightly underrepresented. Given the depth of this site and the distance from any coral receptors, the added numerical cost of mesh refinement at this deep-water site (discussed in Section 5.3), refinement was not justifiable within the project constraints. We return to this in Section 6.3.

Figure 32 Zone of Influence: Scenario 1, 2 and 3 (Backactor, barge overflow and disposal at East Lewis Island, A/B and 2B.

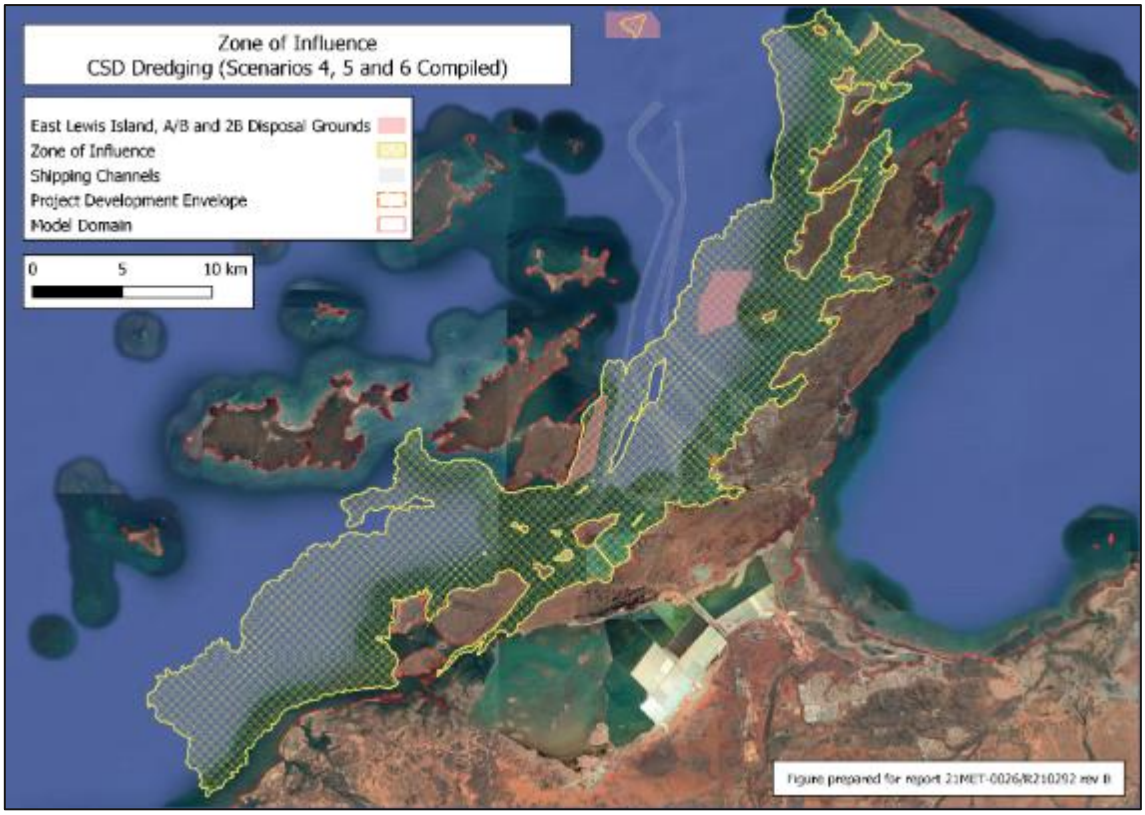

Figure 33 Zone of Influence: Scenario 4, 5 and 6 (CSD dredging, barge overflow and disposal at East Lewis Island, A/B and 2B.

6.2. Zones of Impact

Zones of impact have been calculated using the assessment method defined in section 4.3. There are no zones of impact (moderate or high) within any of the disposal ground footprints in any of the six scenarios. However, disposal plumes at A/B (scenarios 2 and 5) do interact with the dredge plume throughout the simulation, leading to slightly larger sized zones when compared to disposal at ELI Spoil Ground (scenarios 1 and 3) and 2B (scenarios 3 and 6). Interaction leading to larger zones of impact does not occur with disposal at ELI Spoil Ground and 2B. Hence, the zones of impact in scenario 1 are the same as those in scenario 3 for Backactor operations and similarly the zones of impact in scenario 4 are the same as those in scenario 6 for CSD operations. Thus, zones from scenarios 3 and 6 are not presented as they would be repetition of those from scenarios 1 and 4 respectively.

Figure 34, Figure 36, Figure 38 and Figure 40 present the zones of impact for corals, with moderate impact being determined using the combined DLI and SSC thresholds. Figure 35, Figure 37, Figure 39 and Figure 41 present the zones of impact for corals with moderate zones being determined using the DLI alone thresholds.

In all scenarios, the ZoMI determined using the DLI alone thresholds are larger than the ZoMIs determined using the combination of DLI&SSC thresholds. This is primarily due to the 10+ m CD depths surrounding the project site, which experience low light conditions even at background SSC (i.e. prior to commencement of dredging). As such only even small deviations of SSC above background are required to reduce benthic light below the threshold levels. This provides an explanation as to why these '*DLI only*' ZoMIs are 'patchy' (i.e. not

always connected to the dredge source), as the zones are controlled by bathymetry and not SSC alone. These 'patches', align with isolated pockets of relatively deep bathymetry. We note also that these deep patches align with areas of low BCH cover (Section 3.3), which adds context to the interpreted output.

The ZoMIs determined using the combination of DLI and SSC thresholds were smaller, and more closely linked to the actual plume shape (see results Section 5) owing to the additional control of high SSC. The ZoMIs are larger using CSD operation when compared to the Backactor operation. This is expected owing to much greater spill for CSD and the extra generation of fines by mechanical disturbance of the limestone by the cutter head.

ZoHIs exist only for CSD simulations (scenarios 4, 5 and 6) and do not extend beyond the development envelope. Unlike the case for the ZoMIs interaction between the A/B disposal plume and dredge plume had no practicably measurable impact on the ZoHI.

Given the results for ELI Spoil Ground disposal, and the relative depths of the three disposal sites, it is unlikely that grid refinement around zone 2B would have resulted in any change to the zones of impact. Given the depth of this site and the distance from any coral receptors, the added numerical cost of mesh refinement at this deep-water site (discussed in Section 5.3), refinement was not justifiable within the project constraints. We return to this in Section 6.3.

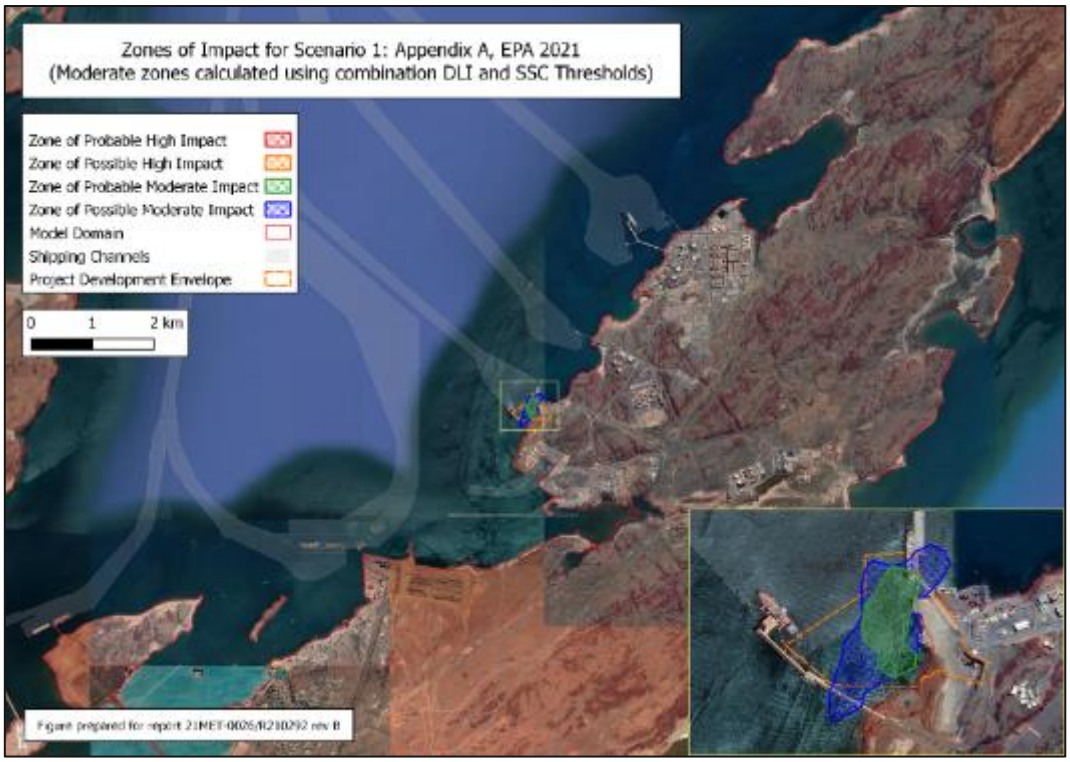

Figure 34 Zones of impact for Scenario 1: Backactor, barge overflow and ELI Spoil Ground disposal. Note that moderate impact zones have been determined using combined DLI and SSC thresholds.

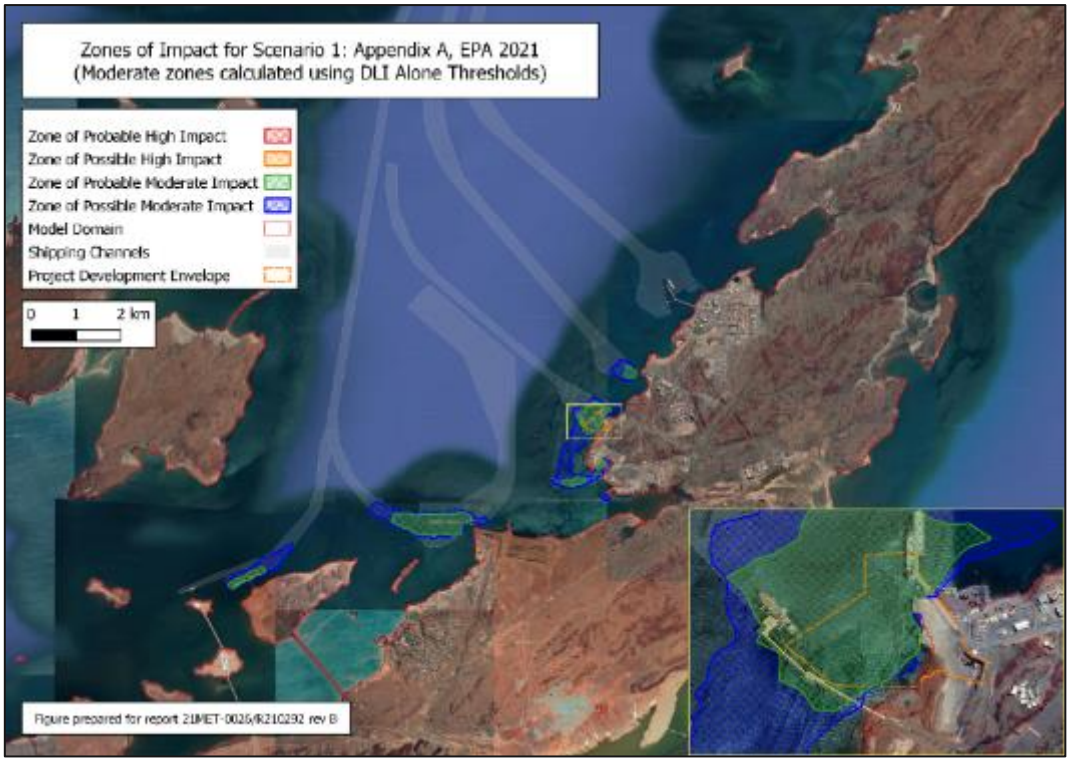

Figure 35 Zones of impact for Scenario 1: Backactor, barge overflow and ELI Spoil Ground disposal. Note that moderate impact zones have been determined using DLI alone thresholds. Note also that the DLI alone thresholds for moderate imapct zones have only been applied within the Dampier Archipelligo (not applied offshore, where water depths are deep enough to attenuate light below thresholds without the presence of dredging acitivity).

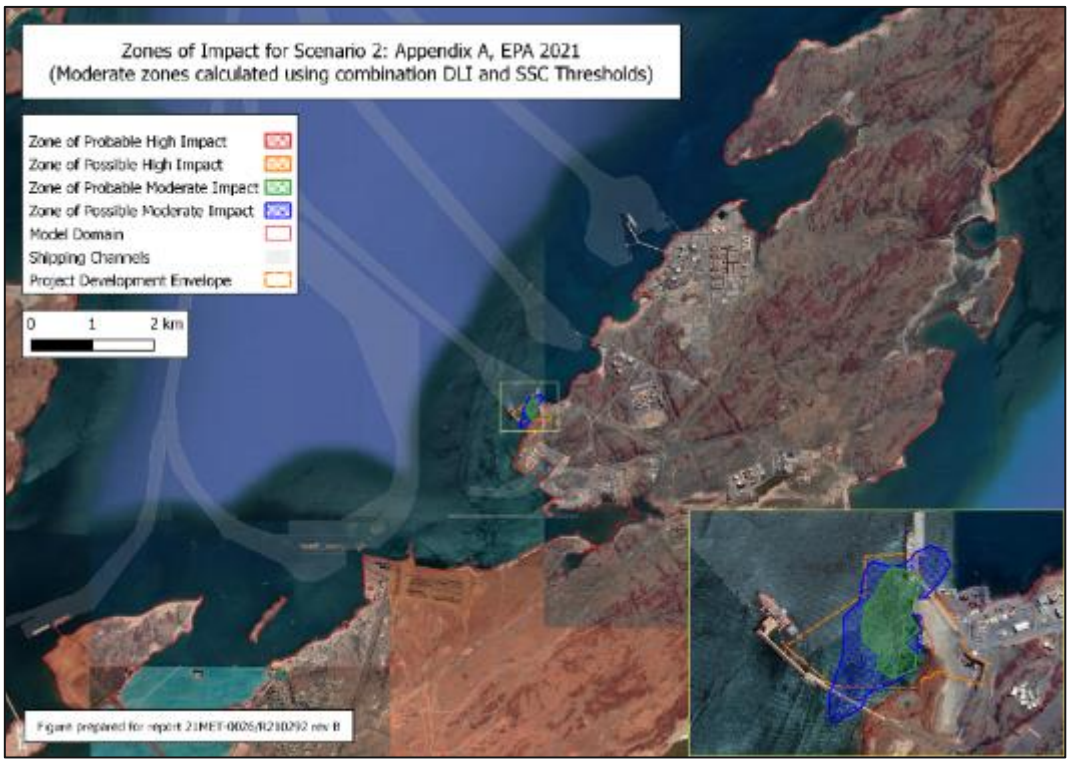

Figure 36 Zones of impact for Scenario 2: Backactor, barge overflow and A/B disposal. Note that moderate impact zones have been determined using combined DLI and SSC thresholds.

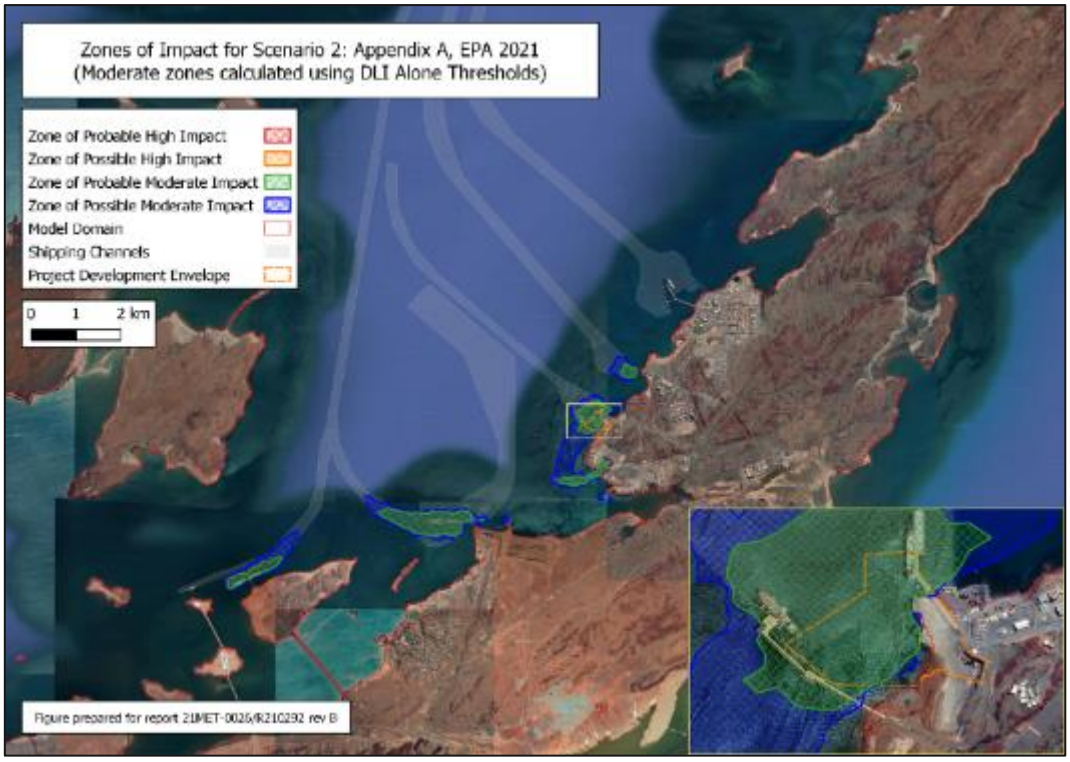

Figure 37 Zones of impact for Scenario 2: Backactor, barge overflow and A/B disposal. Note that moderate impact zones have been determined using DLI alone thresholds. Note also that the DLI alone thresholds for moderate imapct zones have only been applied within the Dampier Archipelligo (not applied offshore, where water depths are deep enough to attenuate light below thresholds without the presence of dredging acitivity).

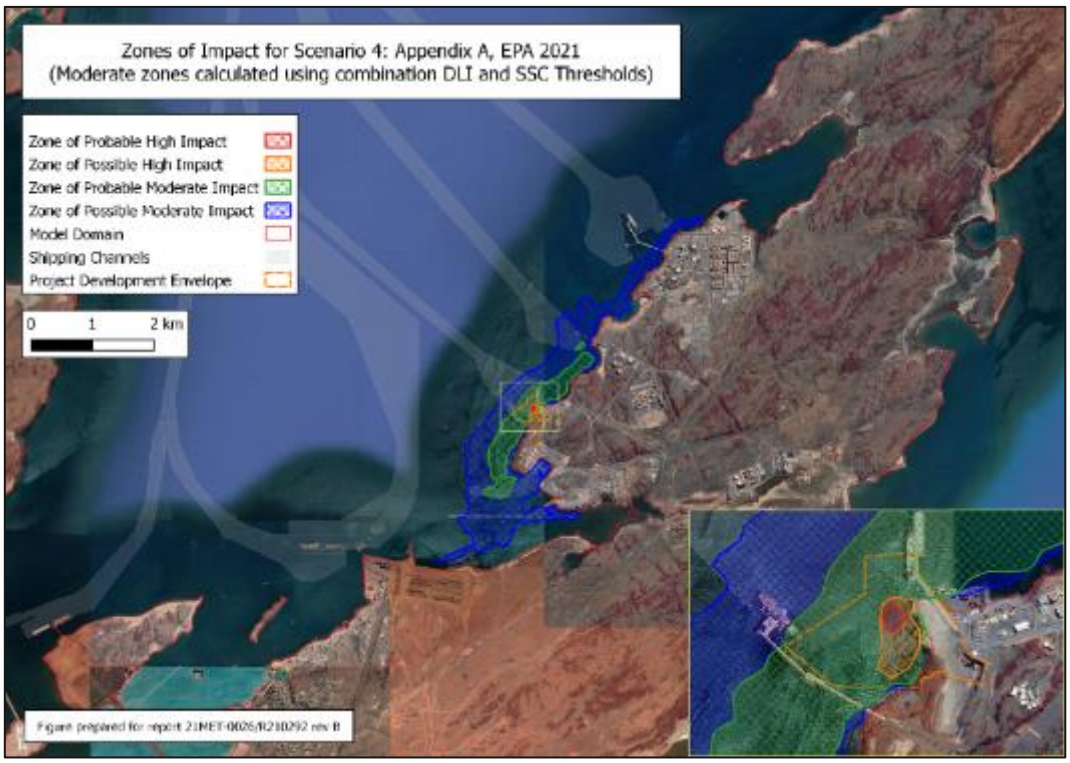

Figure 38 Zones of impact for Scenario 4 CSD, barge overflow and East Lewis Island disposal. Note that moderate impact zones have been determined using combined DLI and SSC thresholds.

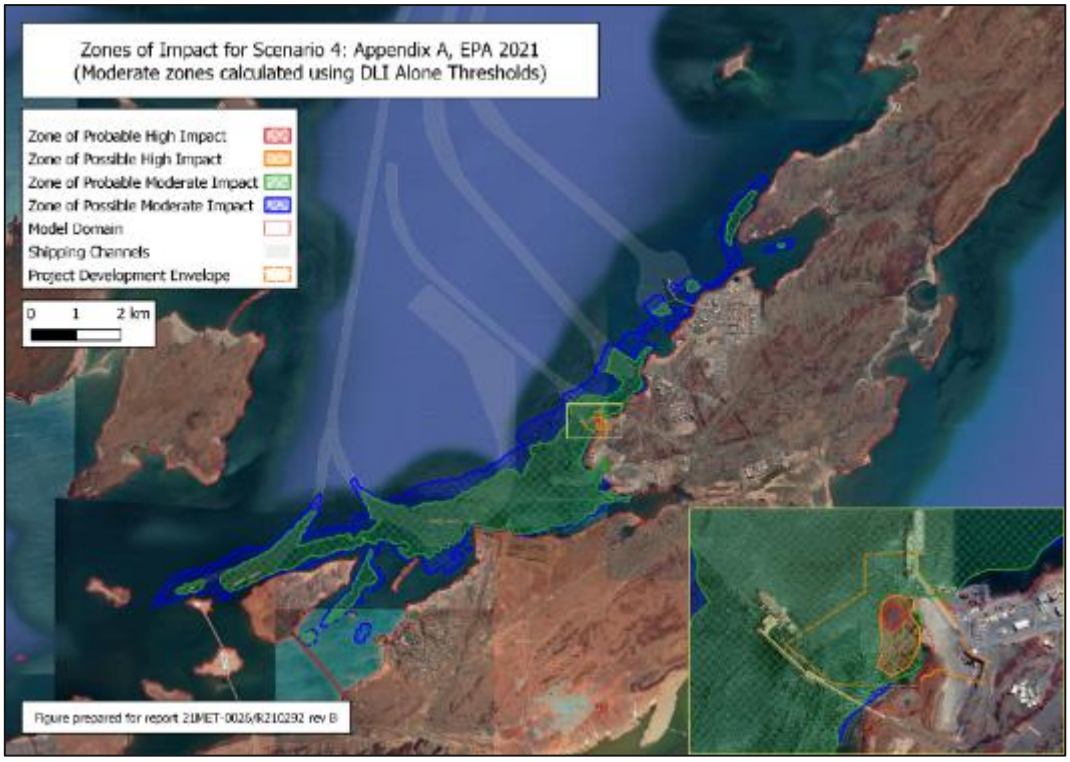

Figure 39 Zones of impact for Scenario 4: CSD, barge overflow and ELI Spoil Ground disposal. Note that moderate impact zones have been determined using DLI alone thresholds. Note also that the DLI alone thresholds for moderate imapct zones have only been applied within the Dampier Archipelligo (not applied offshore, where water depths are deep enough to attenuate light below thresholds without the presence of dredging acitivity).

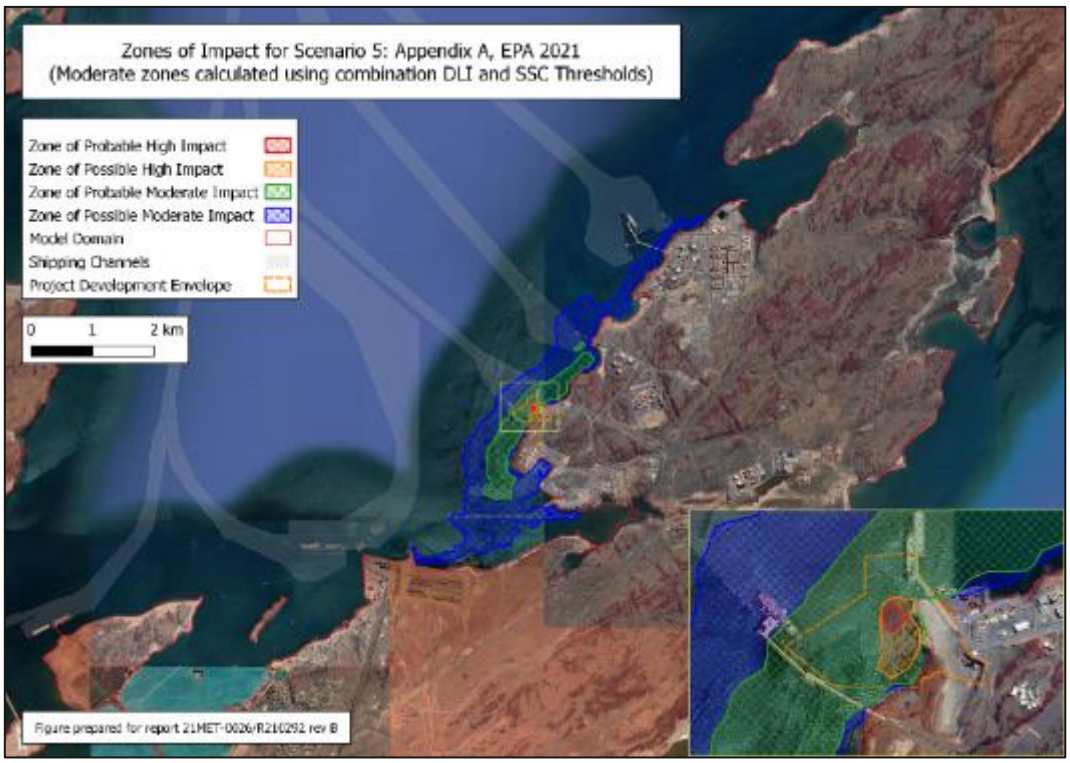

Figure 40 Zones of impact for Scenario 5: CSD, barge overflow A/B disposal. Note that moderate impact zones have been determined using combined DLI and SSC thresholds.

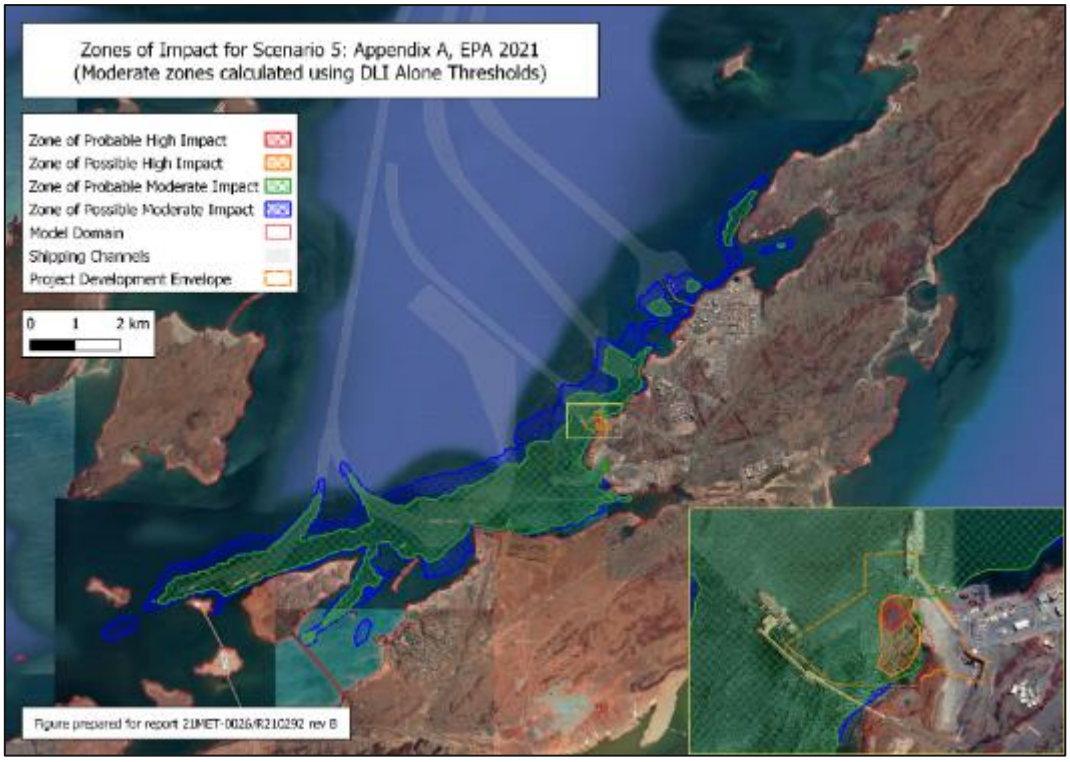

Figure 41 Zones of impact for Scenario 5: CSD, barge overflow A/B disposal. Note that moderate impact zones have been determined using DLI alone thresholds. Note also that the DLI alone thresholds for moderate imapct zones have only been applied within the Dampier Archipelligo (not applied offshore, where water depths are deep enough to attenuate light below thresholds without the presence of dredging acitivity).

6.3. Key areas of uncertainty

This section highlights the key areas of uncertainty in this assessment. Areas of uncertainty affecting the actual model TSS estimates are given in Table 15, while those affecting the estimated zones of impact are given in Table 16. These tables also include suggestions for monitoring that may be useful for either a hindcast the dredge plume model, or to contribute to national state and local dredge databases, such that these areas of uncertainty be reduced in future studies. Uncertainties associated with source term estimation, which are common to all dredging EIA studies are not included below. The approach to management of these uncertainties was consistent with, described in see Sections 3.7 and 4.2.3, was consistent with the guidance of the WAMSI DSN (Sun and Branson, 2018).

Table 14 Key areas of uncertainty affecting the actual SSC estimates and their estimated level of significance to the results

Factor	Relative importance	Description/recommendation
Spill rates for each process and contribution to the passive plume.	High	This is a key area of uncertainty in any dredge plume assessment. Logging of dredge parameters (i.e. dredge locations, dredge rates and dredge depths), source term flux estimates (e.g. ADCP backscatter calibrated against in-situ water samples near the spill sources), and near-source deposition estimates would be greatly beneficial for these public databases
The PSD resulting from mechanical fracturing of limestone by cutter-suction dredging	Moderate	This will be a function of the limestone strength, cutter suction head, cutter suction power and the mode of operation. As such, this is not possible to predict with any certainty at this earlier EIA phase. If possible, sediment sampling from barges should target areas with significant limestone concentration (see Figure 15), such that this may be estimated.
Nature of the 'beach deposit' matrix	Low	While the geotechnical sampling in this study was comprehensive, it was not able to resolve the quantity of fines in the beach deposit matrix with a high degree of certainty (GHD 2020).
Spatio-temporal progression of the dredger	Low	The exact spatial progression of the dredger is unknown. This is expected to be a relatively minor area of uncertainty as the dredging is confined to a relatively small area directly adjacent to the coastline, and the layering of deposits within the dredge material is relatively incoherent.
Low resolution at 2B	Low	As discussed throughout, the disposal 2B disposal site was relatively coarsely resolved in the model, and thus the initial dilution is likely overestimated. The modelling nonetheless shows very little accumulation at these depths, and no impact is expected given the depth (~30 m CD) compared to the deepest light sensitive benthic habitat (~12 m CD). Given the (vertical) distance from sensitive receptors, and the modelled result that very little appreciable SSC was detected beyond the disposal site footprint, the high modelling effort required to resolve this deep-water site with the same accuracy as the ELI Spoil Ground and Spoil Ground A/B was not justified.

Table 15 Key areas of uncertainty affecting the estimated stress on benthic habitats

Factor	Relative importance	Description/recommendation
TSS/SSC to attenuation relationship.	High	This a key area of uncertainty for the present study. The baseline data for TSS vs. light attenuation were very limited. Further, in the absence of a more suitable model, the analysis here (rather unrealistically) treats only a single attenuation coefficient for the entire PAR spectrum. Given that the relation used here was developed in shallow waters (~4-5 m), the relation used would be biased high by the presence of highly attenuated (red) wavelengths. The attenuation coefficient should rather reduce with depth as the in-situ spectrum is skewed towards blue-green light. We recommend sampling of dredge material from the barges for use in laboratory testing of the relation between TSS and light attenuation. Such testing should include high SSC values commensurate with the expectation of dredge plumes, not be constrained to low ? : 9 ; C ? J G M F < D = N as baseline monitoring studies typically are. We note the following comment from Sun and Branson (2021): *U 2 @ = J = D 9 L A G F K @ A H that of TSS and light attenuati utilised during the EIA process should be confirmed during the dr campaign and published for use in future EIA studies where geote ; G F < A L A G F K 9 J = K A E A D 9 J J Λ*
Reflection of light at the sea surface	Low to moderate	While clear-sky solar intensity at the water's surface is straightforward to model, so too reflection and refraction at a still water-interface, predicting the impact of clouds and the modulation of reflection and reflection by surface waves is more complex. In lieu of a better model, we have adopted a constant reduction of 15% for this wet-season assessment. This area of uncertainty is judged as low to moderate, as it would be dwarfed by the contribution of in-water attenuation described in the row above.
No significant coral BCH below 15 m	Low	We have limited the assessment of DLI thresholds to 15 m based on the observation coral is rarely found beyond 12 m (Section 3.3). There is uncertainty around this observation, and hence around this depth cut-off. Deeper corals are expected to be tolerant to low-light conditions, and hence the application of guideline thresholds is likely overconservative. As such the relative importance of this uncertainty has been judged to be low.

7. References

Becker J, Eekelen E, Van Wiechen J, De Lange W, Damsa T, Smolders T and Van Koningsveld M. (2015). Estimating Source Terms for Far Field Dredge Plume Modelling. *Journal of Environmental* Management, 149, 282-293.

BOM (2022); http://www.bom.gov.au/jsp/ncc/cdio/cvg/av?p_stn_num=004083&p_prim_element_index=0&p_comp_element_index=0&redraw=null&p_display_type=full_statistics_table&normals_years=1991-2020&tablesizebutt=normal. Accessed 22/02/2022

Condie, S. A., & Andrewartha, J. R. (2008). Circulation and connectivity on the Australian North West shelf. Continental Shelf Research, 28(14), 1724-1739.

Eliot, I., Gozzard, B., Eliot, M., Stul, T., & McCormack, G. (2013). Geology, Geomorphology & Vulnerability of the Pilbara Coast, In the Shires of Ashburton, East Pilbara and Roebourne, and the Town of Port Hedland, Western Australia. Damara WA Pty Ltd and Geological Survey of Western Australia, Innaloo, Western Australia.

Godfrey, J. S., & Mansbridge, J. V. (2000). Ekman transports, tidal mixing, and the control of temperature structure in Australia's northwest waters. Journal of Geophysical Research: Oceans, 105(C10), 24021-24044.

GHD (2020). Dampier Cargo Wharf Landside Extension and Redevelopment Geotechnical Investigation – Factual Report. Prepared for Pilbara Ports Authority. Report No. 12523649-PRP-001.

Lebrec, U., Paumard, V., O'Leary, M. J., & Lang, S. C. (2021). Towards a regional high-resolution bathymetry of the North West Shelf of Australia based on Sentinel-2 satellite images, 3D seismic surveys, and historical datasets. Earth System Science Data, 13(11), 5191-5212.Lorenz R. 1999. Spill from dredging activities. *Proc Oresund Link Dredging and Reclamation Conference*, Copenhagen.

Mills D, Kemps H. (2016). Generation and release of sediment by hydraulic dredging: a review. Report of Theme 2 – Project 2.1 prepared for the Dredging Science Node (DSN), Western Australian Marine Science Institution (WAMSI), Perth, Western Australia. 97 pp.

MScience (2009). Wheatstone LNG Development: Baseline Water Quality Assessment Report November 2009. Prepared for URS Corporation, Report No. MSA134R3

MScience (2014). Dampier Port Authority Marine Environment: Distribution of Benthic Primary Producer Habitats within Port Waters. Report prepared for Dampier Port Authority.

MScience, (2019). Woodside Scarborough Dredging Threshold Levels for Model Interrogation,

MScience (2022). Dampier Cargo Wharf Extension Project – Capital Dredging Sampling and Analysis Plan Impementation Report. Prepared for Pilbara Ports Authority. Report No. MSA313R01.

O2 Marine (2019). *Marine Environmental Quality Sampling and Analysis Plan: Port of Dampier*. O2M Report R1800118, Revision 1, 23 September 2019.

O2 Marine (2022a). *Dampier Cargo Wharf Extension Project: Marine Water Quality Baseline Report*. O2M Report R210203.

O2 Marine (2022b). *Dampier Cargo Wharf Extension Project: Benthic Communities and Habitat Cumulative Loss Assessment*. O2M Report R210276.

Pearce, A., Buchan, S., Chiffings, T., D'Adamo, N., Fandry, C., Fearns, P., ... & Simpson, C. (2003). A review of the oceanography of the Dampier Archipelago, Western Australia. The Marine Flora and Fauna of Dampier, Western Australia. Western Australian Museum, Perth, 13-50.

Ridgway, K. R., & Godfrey, J. S. (2015). The source of the Leeuwin Current seasonality. Journal of Geophysical Research: Oceans, 120(10), 6843-6864.

Smith, R. C., & Baker, K. S. (1981). Optical properties of the clearest natural waters (200–800 nm). Applied optics, 20(2), 177-184.

Sun C, Branson P, Mills D. (2020). Guideline on dredge plume modelling for environmental impact assessment. Perth, Western Australia. Western Australian Marine Science Institution (WAMSI).

Sun C, Shimizu K and Symonds G. (2016). Numerical Modelling of Dredge Plumes: A Review. Perth, Western Australia. Western Australian Marine Science Institution (WAMSI) and CSIRO Oceans and Atmosphere Flagship.

Sun C Branson PM. (2018). Numerical modelling of dredge plumes. Report of Theme 3 - Project 3.4 prepared for the Dredging Science Node, Western Australian Marine Science Institution, Perth, Western Australia. 81pp

Woodside, (2019). Scarborough Dredging and Spoil Disposal Management Plan. Report number SA0006AH0000002 rev 0, June 2019.

Van Rijn L and Barth R. (2018). Settling and Consolidation of Soft Mud Layers. *Journal of Waterway, Port, Coastal and Ocean Engineering (ASCE)*, 144, 27-45.

IMOS (2022). *Australia's Integrated Marine Observing System (IMOS) is enabled by the National Collaborative Research Infrastructure Strategy (NCRIS). It is operated by a consortium of institutions as an unincorporated joint venture, with the University of Tasmania as Lead Agent.*

Appendix A. Hydrodynamic and Wave model Setup and Validation

Appendix A.1. Oceanographic data availability

There are many observations available for boundary-condition establishment and establishment of boundary conditions for Pilbara coastal models:

- Pilbara Ports Data Network: PPA host a network of telemetered loggers near their ports that include tide weather stations, pressure sensors (tide gauges), ADCPs, acoustic wave sensors and wave buoys. The water level data are generally of high quality, though care must be taken with the wave and current observations as many sensors are prone to interference (physical or magnetic). The data are proprietary, and cannot be used without the approval of PPA;
- National tide centre: long-term water-level records are available at many sites across the coast as part of the national tide centre, accessible through the Integrated Marine Observing System (IMOS).
- IMOS national mooring network: The Australian Institute of Marine Science (AIMS) maintain a network of moorings, the data from which are also accessible through IMOS.
- Observations made by O2 Marine: O2 Marine have operated numerous oceanographic data collection campaigns across the Australian coast which have been used to validate previous iterations of our coastal models.
- Bureau of Meteorology: BOM maintain a national network of weather stations and for which
- Satellite based observations: Numerous satellite-based observations are available for ocean model development and validation. Data are available in a number of process levels from raw 'along-track' observations to derived products – e.g. tidal inversions, geostrophic currents, sub mesoscale eddy currents. For coastal models, altimetry satellites (e.g. JASON-3, 2, 1 and TOPEX/Poseidon) are particularly useful. Altimetry data has been used to map the global ocean tides through inversion of the Laplace equation.

This Pilbara data network is shown graphically in Figure 42. In addition to these observations there are:

- Third party numerical model products: The quality of commercially available global numerical reanalysis models is continually improving through improved compute power and assimilation techniques, as well as the quality and availability of both conventional (moorings/buoys/autonomous vehicle-based/ship-based) and satellite-based meteorological and oceanographic observations. The European Centre for Medium-range Weather Forecasts and Mercator Ocean International organisations providing such products.
- O2 Marine numerical model products: O2 Marine have numerous validated 3D Pilbara coastal models that in some instances may be appropriate for nesting smaller model domains.

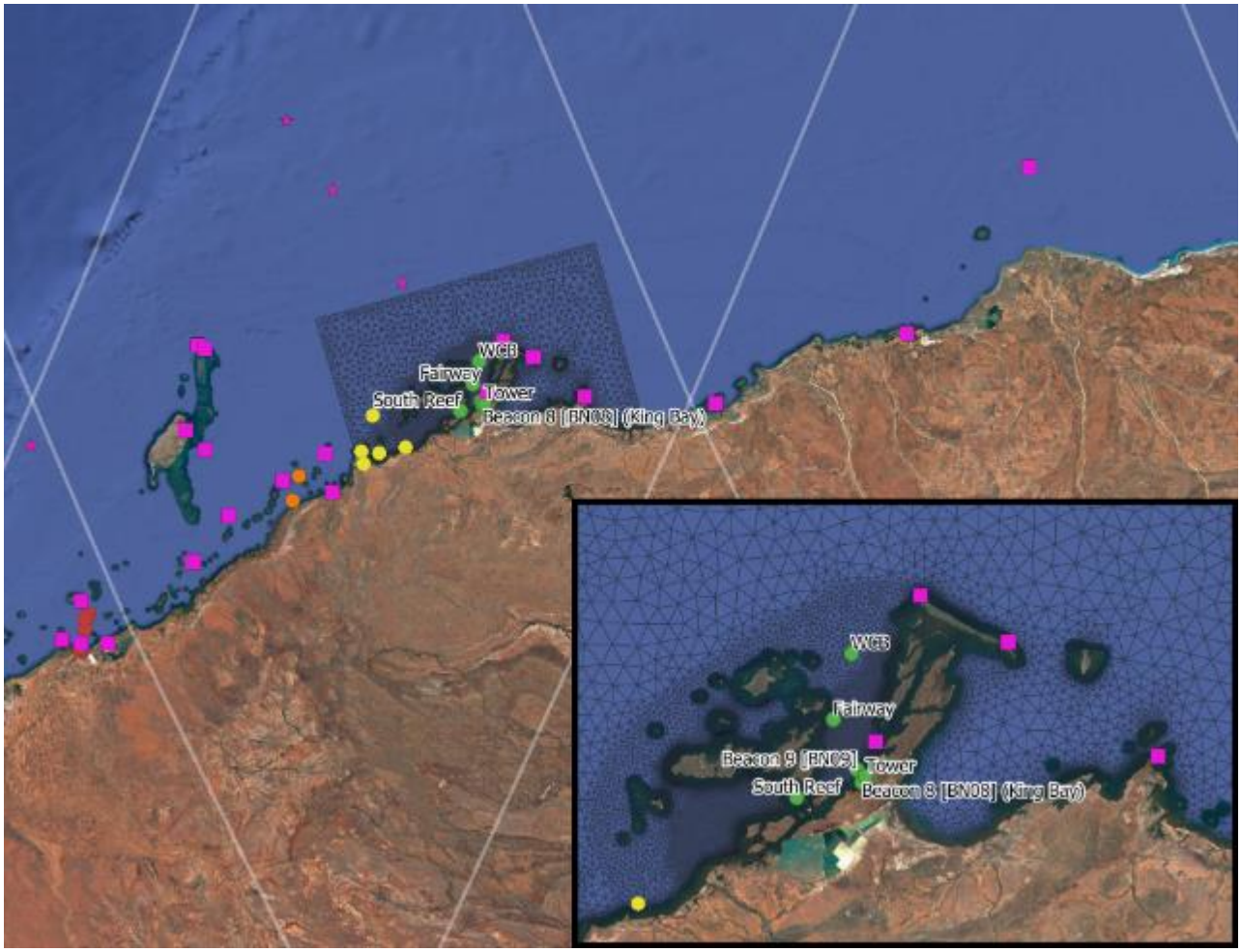

Figure 42 Data available for optimisation of boundary conditions and validation of Western Pilbara Coastal models with the numerical mesh used in this study overlaid for reference. Green Circles: PPA Port of Dampier observations – mixed wave current and water level. Red Circles: PPA Port of Ashburton – mixed wave current and water level. Yellow Circles: data collected by O2 Marine near Regnard Bay – 12 montshs of waves currents and water levels. Orange Circles: data collected by O2 Marine near Mardie – 12 montshs of waves currents and water levels. Pink Squares: national tide centre data available through IMOS. Pink Stars: deepwater (>50 m) IMOS moorings. White diagonal lines: flight path of the JASON-3 satellite.

Table 16 PPA Port of Dampier monitoring sites. For this study all data from the start of 2018 through to 19th of November 2021 (the day in which the download was conducted) were accessed and reviewed.

Site	Latitude	Longitude	Site Depth [m LAT]	Data type
BN09	-20.608	116.739	8.5[1]	Waves and current (AWAC)
				Meteorological station
				Tide station
Fairway	-20.534	116.704	15.7	Meteorological station
				Tide station
BN08 [King Bay]	-20.627	116.746	5.6	Tide station
South Reef	-20.649	116.650	8.1	Tide station
Tower	-20.618	116.752	N/A	Meteorological station
WCB	-20.436	116.731	15.5	Waves (WRB)
				Meteorological station
				Tide station

Appendix A.2. Model Setup

O2 Marine use all available data when optimising open boundary-locations and boundary conditions for Pilbara coastal models. For the present application a reasonable resolution of the dominant tidal and wind-driven currents was achieved using a relatively small model domain centred around the archipelago. The open boundaries were forced with predicted tides and hindcast waves from ECMWF's ERA5. Surface stress was too derived from ECMWF's ERA5 hindcast winds.

PPA survey data was used for bathymetry in port area, which covers most of Mermaid Sound and Mermaid Strait. This was supplemented by the Lebrec et al. (2021) satellite derived bathymetry product, which extends to around 30 m (MSL). Beyond this we used the Geosciences Australia 250 m gridded bathymetry product.

[1] As this site is on a channel marker beacon, exact depth will vary as a result of maintenance dredging. The depth shown is for the 'undisturbed depth' just outside the dredge channel.

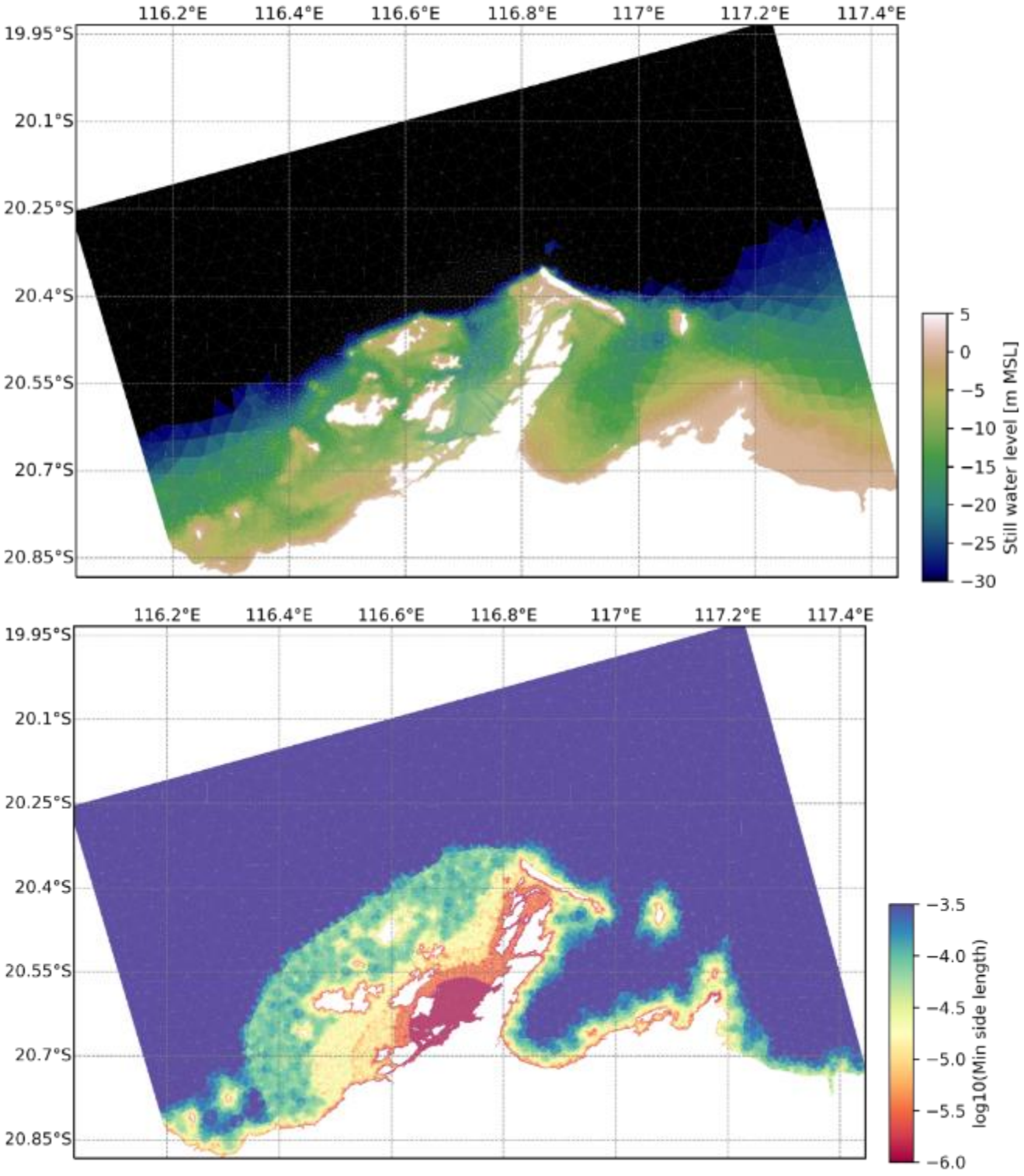

Figure 43 Numerical mesh and model domain. Both images show the same mesh and bathymetry with different rendering. The top image highlights the unstructured mesh and change in mesh resolution throughout the model domain (where depth<30m). The bottom image removes the mesh outline to better present the bathymetry near the dredge location.

Appendix A.3. Model Validation

As this model was adapted from an existing model, a full validation is beyond the scope of this report. Presented below are example hydrodynamic and wave validation plots for data PPA data measured within the archipelago. The model performs favourably compared to recent models used in EIA of dredge plumes in Western Australia in resolution of the major tidal constituents and low-frequency currents driven by local wind stress. We note also that the validation and skill scores below use the raw (heading corrected only) operational PPA current measurements, which are noisy by compared to typical modern measurements for EIA or design criteria of new capital works.

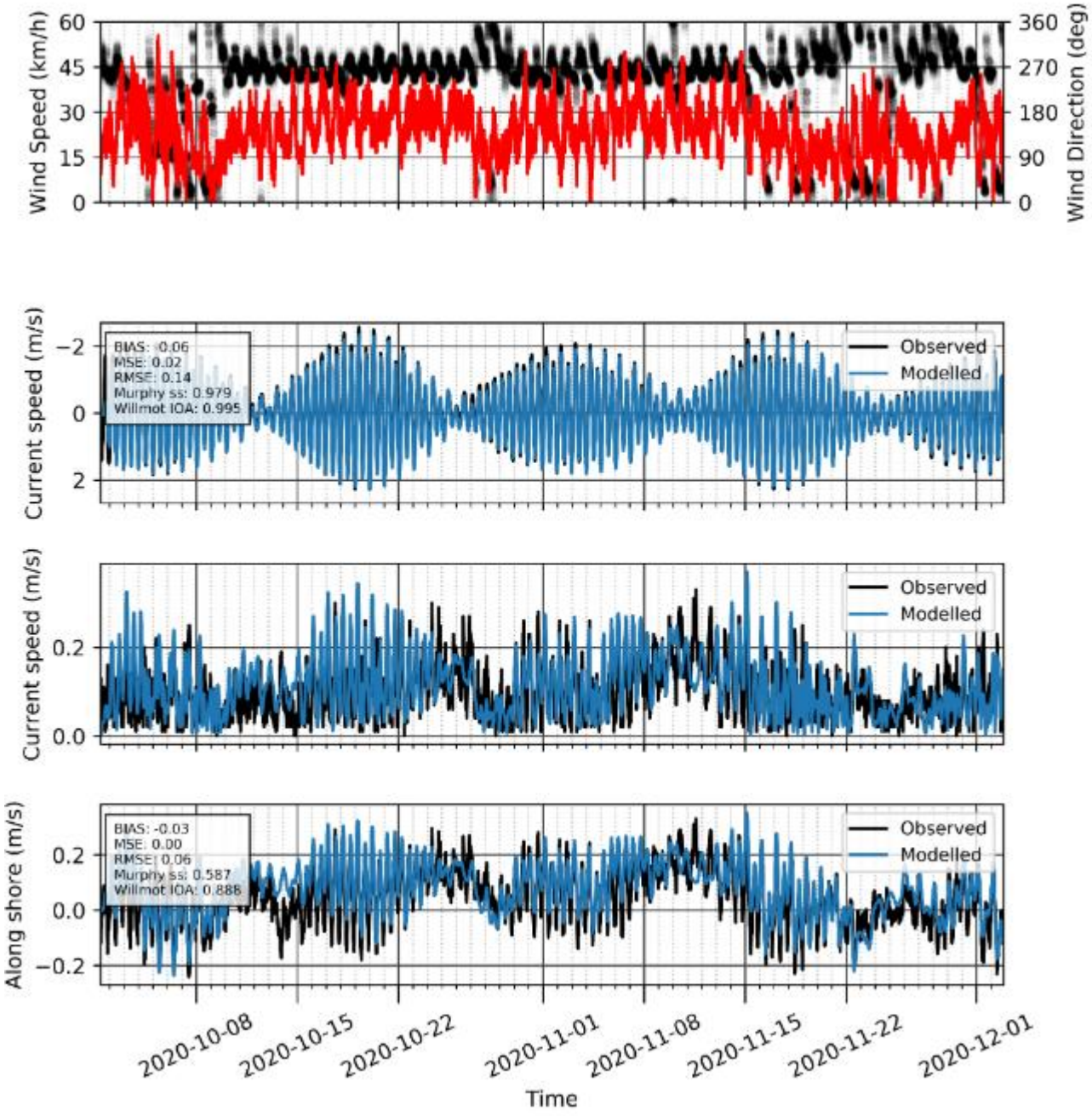

Figure 44 Sample hydrodynamic validation plot at the BN09 location

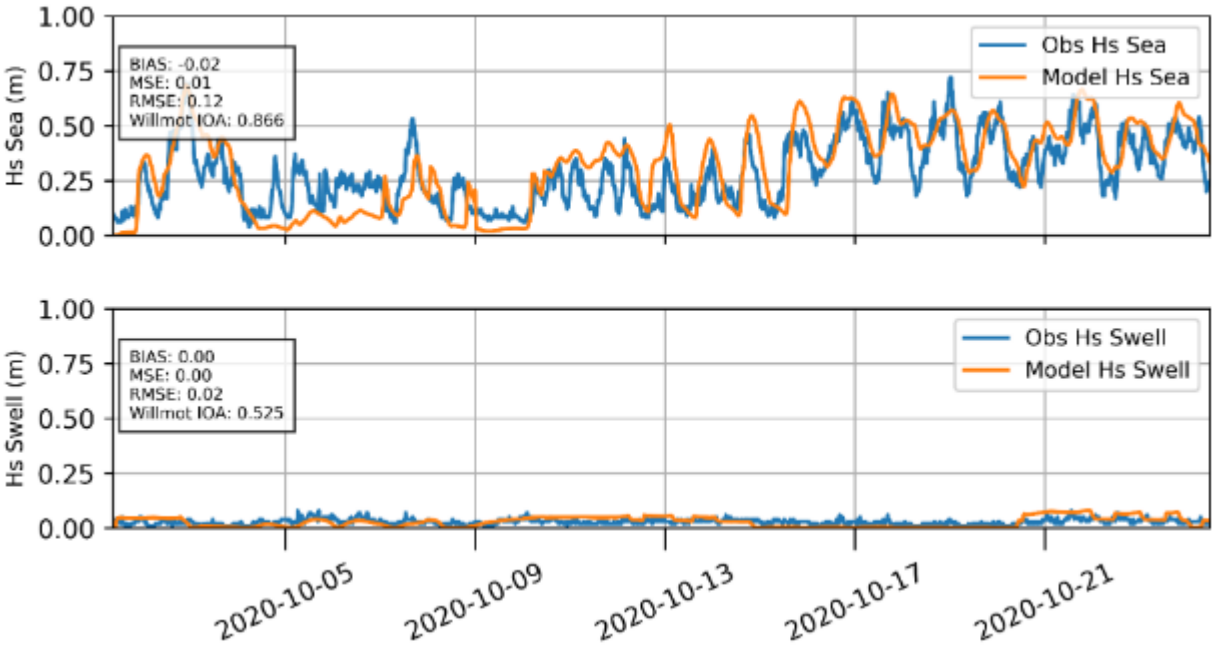

Figure 45 Sample spectral wave validation plot at the BN09 location